U. S. Army Corps of Engineers

DEVELOPMENT OF A SUSPENSION FEEDING AND DEPOSIT FEEDING BENTHOS MODEL FOR CHESAPEAKE BAY

July, 2000

Project No. USCE0410

CONTENTS

CONTENTS (Continued)

LIST OF FIGURES

LIST OF FIGURES (Continued)

LIST OF FIGURES (Continued)

LIST OF FIGURES (Continued)

LIST OF TABLES

ACKNOWLEDGMENTS

This project was conducted in support of the Chesapeake Bay Program's Modeling Subcommittee, and sponsored by the U.S. Army Corps of Engineers under contract DACW39-96-D-0001.

We gratefully acknowledge the support, guidance, and assistance provided by the many dedicated scientists, engineers, and managers involved in the Chesapeake Bay Program, notably, Dr. Carl Cerco (WES/USACE), Mr. Lewis Linker (US EPA CBPO), Mr. Richard Batiuk (US EPA CBPO), Dr. Walter Boynton (U.Md.), Dr. Eric Powell (Rutgers Univ./Haskin Shellfish Laboratory), Ms. Jacqueline Johnson (ICPRB/CBPO), Dr. Ananda Ranasinghe (Versar), Dr. Robert Diaz (VIMS), and Dr. Daniel Dauer (ODU).

SUMMARY AND CONCLUSIONS

The coupled water quality-sediment diagenesis model for Chesapeake Bay has been enhanced with the addition of dynamically-computed benthic biomass. The benthos was divided into two functional components, deposit-feeding polychaetes and suspension-feeding bivalves. Analysis of the Chesapeake Bay Benthic Monitoring Program database indicated that these two components comprised most of the benthic biomass, categorized by taxon and feeding group. These groups have significant and distinct roles in the coupling of production and decay cycles in the water column and the sediments. Deposit feeding benthos enhance sediment mixing rates and the decay of sediment organic matter. Suspension feeders directly influence both organic and inorganic particulate matter concentrations in the overlying water column, enhancing particle fluxes to the sediments. As a result, filtration by suspension feeders can increase light penetration and control water column algal biomass. This can affect the sources of primary production, enhancing the productivity of both sediment algae and submersed aquatic vegetation Respiration by benthic infauna enhances the recycling of nutrients back to the water column and increases the sediment oxygen demand. However, the benthos is sensitive to hypoxia and anoxia induced by eutrophication. Loss of benthos as a result of hypoxia/anoxia alters the nature of benthic-water column coupling, for example, by the reductions of benthic filtration controls on water column processes and of food resources for waterfowl, fish, and crustaceans. Thus, the inclusion of benthic infauna within the eutrophication modeling package provides an important link between water quality processes and the estuarine food web.

The direct impact of suspension feeders on particulate concentrations in shallow estuarine waters has been well-noted. However, estimates of filtration and respiration rate are strongly dependent upon species and individual size. An empirical relationship was derived based on monitoring data for the dominant species inhabiting the major salinity regimes of Chesapeake Bay that related modeled areal biomass to characteristic individual size, so that filtration and respiration rates varying dynamically over time and space. This allowed for a more precise representation of suspension feeder impact than would be obtained through the use a set of constant specific rates.

Hypoxic and anoxic conditions are observed in deep holes and channels along the mainstem Chesapeake Bay and its tributaries. While estuarine benthos have adaptations for surviving occasional hypoxic conditions, prolonged hypoxia or anoxia is inimical to most organisms. Laboratory studies show death of estuarine species after one to thirty days of anoxic exposure. Instantaneous observations in the field are confounded by uncertainties in the time of exposure; some observations show high biomass at moderate or even severe hypoxia. In the model, bivalves are somewhat less sensitive to hypoxia than are polychaetes.

The modeled benthos reproduces major temporal and spatial patterns found in the monitoring data. Predicted and observed benthic biomass are higher in the oligo- to mesohaline portions of the bay. Seasonal hypoxia/anoxia captured by the water quality model leads to severely diminished benthic biomass in the lower reaches of impacted tributaries (e.g., the Potomac River) and at the head end of mainstem bay channels.

The benthos model is very sensitive to the food supply and to the severity and duration of hypoxia predicted by the water quality model. Modeled suspension feeding bivalve biomass does not attain the peak levels seen in highly productive areas of the bay. This may be the result of several factors. One factor is a function of the eutrophication model's scale of resolution. Based on the model's grid size, the model computes spatially averaged values for regions on the order of square kilometers to tens of kilometers. Environmental factors operating on smaller scales, including non-modeled parameters such as sediment grain size, will result in spatial patchiness scales smaller than the model can resolve. While this could be mitigated by comparing large-scale spatial aggregates of both modeled and observed biomass, such comparisons tended to obscure the impacts of modeled forcing functions, such as organic matter flux, total suspended solids, and hypoxia/anoxia.

A second factor leading to undersimulation of benthic biomass was the potential undersimulation of food resources at locations within the bay. At present, the water quality model's predicted gross and net primary production are under review. It is likely that net primary production is too low and water column respiration is too high. As a result, particulate organic matter in the bottom layer of the model (i.e., food accessible to suspension feeders) and particulate organic matter

flux to the sediments is low. With regard to the suspension feeders, it is possible that resuspended sediment organic matter contributes significantly to their diet. This process is not included in the present water quality model, nor is sediment organic matter included as a food source for suspension feeding bivalves in the present benthos model.

Other poorly resolved or unresolved ecological factors affected the ability to calibrate the benthic model. The predation term was poorly resolved in both time and space. This term had no spatial variability and limited temporal variability in that its magnitude was tied to seasonal temperature variations. Again, patchiness of benthic predators may have contributed to high variability in the observations, but was not simulated in the model, adding to difficulties in model-data comparisons of benthic biomass. Also, slow recovery of benthic biomass in the simulation following periodic hypoxia, particularly in the case of the deposit feeders, may be the result of a lack of a recruitment signal in the model.

Analysis of the dynamics of the benthos in response to the water quality prediction suggests that the present model contains many of the essential elements of benthic-pelagic coupling. Improvement in water quality prediction and refinements in the sources and sinks for benthos (recruitment and predation) should yield more accurate results. Further insights regarding the impact of habitat variability on spatial scales below that of the model will improve our interpretation of living resource monitoring databases as well as our methods for comparing observations and predictions.

SECTION 1

INTRODUCTION

During the period 1992-1993, final evaluation, summarization, and conclusions were being made from the previous phase of eutrophication modeling in Chesapeake Bay (e.g., Cerco and Cole, 1993; Thomann et al., 1994). During the summer of 1993, three workshops were held to determine the future direction of Chesapeake Bay modeling (HydroQual, 1993). One workshop, "Living Resource Processes and Ecosystem Modeling," was devoted to the exploration of the linkages between eutrophication and living resources, and modeling paradigms which would enable simulation of such linkages. Increasingly, estuaries are being examined not only from a water quality perspective, but also from the point of view of habitat and living resource quality. Until recently, management-oriented simulation models addressed only the eutrophication aspect. With this latest phase of Chesapeake Bay modeling, important connections to living resources have been included. These are (1) benthic algae, (2) submersed aquatic vegetation (SAV), (3) zooplankton, and (4) benthos. This report describes the new submodels for two classes of benthos: deposit feeding polychaete worms and suspension feeding bivalve mollusks.

In defining benthic-pelagic coupling, both deposit and suspension feeding benthos have been shown to play important roles in sediment processes, nutrient cycles, and trophic transfer within shallow water environments such as Chesapeake Bay (Diaz and Schaffner, 1990; Kemp and Boynton, 1992). Examination of some shallow, eutrophic estuaries suggests that observed algal biomass is lower than expected based on the available nutrients and light. Based on analyses of filtration rates, abundance, and environmental factors such as average water column depth, vertical mixing, nutrient and light inputs across estuaries, it has been shown that suspension-feeding benthos can control phytoplankton biomass (Cloern, 1982; Officer et al., 1982). The critical environmental factors favoring benthic control are shallow depths and a well-mixed water column. Under these conditions, removal of algae by filtering benthos can keep pace with algal growth rates, keeping algae biomass low. These sorts of analyses, however, are either based on steady-state assumptions, or are spatially

aggregrated with little resolution of bivalve species-specific phenomena, physiological processes, or small-scale hydrodynamics. For example, Cloern's (1982) analysis of South San Francisco Bay suggested that suspension feeding induced particulate losses from the water column were equivalent to settling velocities of 7-10 m d^{-1}. With an average depth of 3 m, and absent resuspension events, such rates, continuously applied, would rapidly clear the water column, which is not observed. Nevertheless, even after inclusion of benthic boundary layer effects and a probabilistic treatment of overfiltration (repeated filtering of the same volume of water), Gerritsen et al. (1994) have shown that suspension feeders in the shallow zones of the Potomac River and upper Chesapeake Bay could crop 50% of the annual primary production. Furthermore, analysis of phytoplankton biomass and suspended matter in the tidal freshwater Potomac River showed ca. 50% declines in chlorophyll concentration, a tripling of water clarity and increases in coverage of SAV associated with high abundance of the invasive asiatic clam, *Corbicula fluminea* (Cohen et al., 1984; Phelps, 1994). However, in deeper zones of the bay, factors such as vertical stratification and seasonal oxygen depletion (hypoxia and anoxia) limit benthic biomass and the amount of primary production consumed by the benthos (Gerritsen et al., 1994).

Almost all metazoan life requires oxygen in order to respire and sustain metabolic processes. Estuarine benthic invertebrates are able to sustain themselves at low dissolved oxygen concentrations. A critical dissolved oxygen level, defined as hypoxia, based on changes in benthic species composition and biomass appears to occur at concentrations at 2.0-2.5 mg L^{-1} (Pearson and Rosenberg, 1978; Diaz and Rosenberg, 1995). Some benthic fauna can survive for extended periods of time under hypoxia. The polychaete fauna shifts from larger, deep-dwelling species to small, surface dwelling ones (Dauer et al., 1992; Diaz and Rosenberg, 1995). Some estuarine bivalve species also appear to survive mild hypoxia. Sustained dissolved oxygen concentration below 1.0 mg L^{-1}, however, leads to complete loss of metazoan benthos (Diaz and Rosenberg, 1995). Experimental work has been performed on individual invertebrate species, but usually these involve highly artificial environments (no sediments, altered pH due to N_2-gas purging of dissolved oxygen) with uncertain ecological consequences (Diaz and Rosenberg, 1995). These experiments show a range of tolerance to anoxia varying on the order of days to weeks, with bivalves showing higher capacity to withstand anoxia than polychaetes (Figure 1-1), which formed the basis for the time-to-death parameters described

below in the present models. It is difficult to quantify sensitivity to hypoxia/anoxia in the estuarine environment for the diverse suite of benthic fauna beyond these generalized thresholds.

Benthic production and eutrophication processes are tightly coupled. Increased food yields increased benthic biomass, while intense suspension feeding may limit water column phytoplankton production. Increasing levels of nutrient enrichment together with vertical stratification, however, can lead to hypoxia, which alters benthic community structure and eventually leads to severe degradation of the benthos. Within complex estuarine environments, benthic production is affected by physical and biological processes across a broad range of temporal and spatial scales. Advanced eutrophication models still only simulate limited aspects of the estuarine ecosystem, with respect to both spatio-temporal scale and important biological processes.

The model presented here contains many of the biogeochemical interactions associated with the coupling of water quality and sediment-benthos processes (Figure 1-2). Benthic biota impact particulate matter concentrations in the water column, affecting both the level of water column primary production and the penetration of light to stimulate benthic primary production (by benthic algae and SAV). Both deposit and suspension feeders convert organic matter derived from the water column into benthic biomass, while their respiration contributes to sediment-water fluxes of inorganic nutrients and dissolved oxygen. The coupling of water column and benthic production allows for a dynamic feedback between these two habitats, as they both are influenced by environmental factors.

As with any simulation, in this first step towards linking an advanced eutrophication model with living benthic resources, some population-level and individual-level processes had to be parameterized or left out. The benthic model retains the spatially normalized mass units used in eutrophication mass balance modeling rather than modeling individuals. Bivalves are non-motile

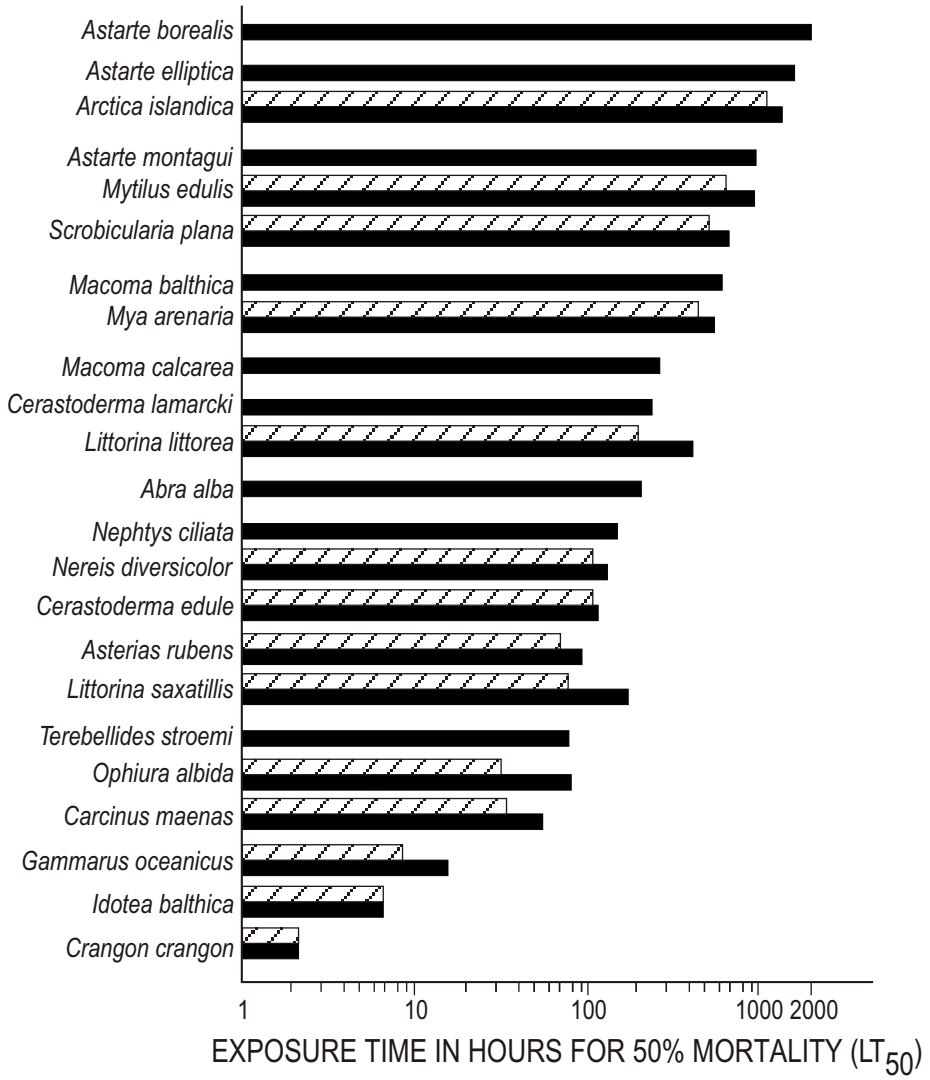

Figure 1-1. Time to death (50% mortality) for various invertebrates held under anoxia (solid bars) and anoxia + hydrogen sulfide (hatched bars) (from Diaz and Rosenberg 1995)

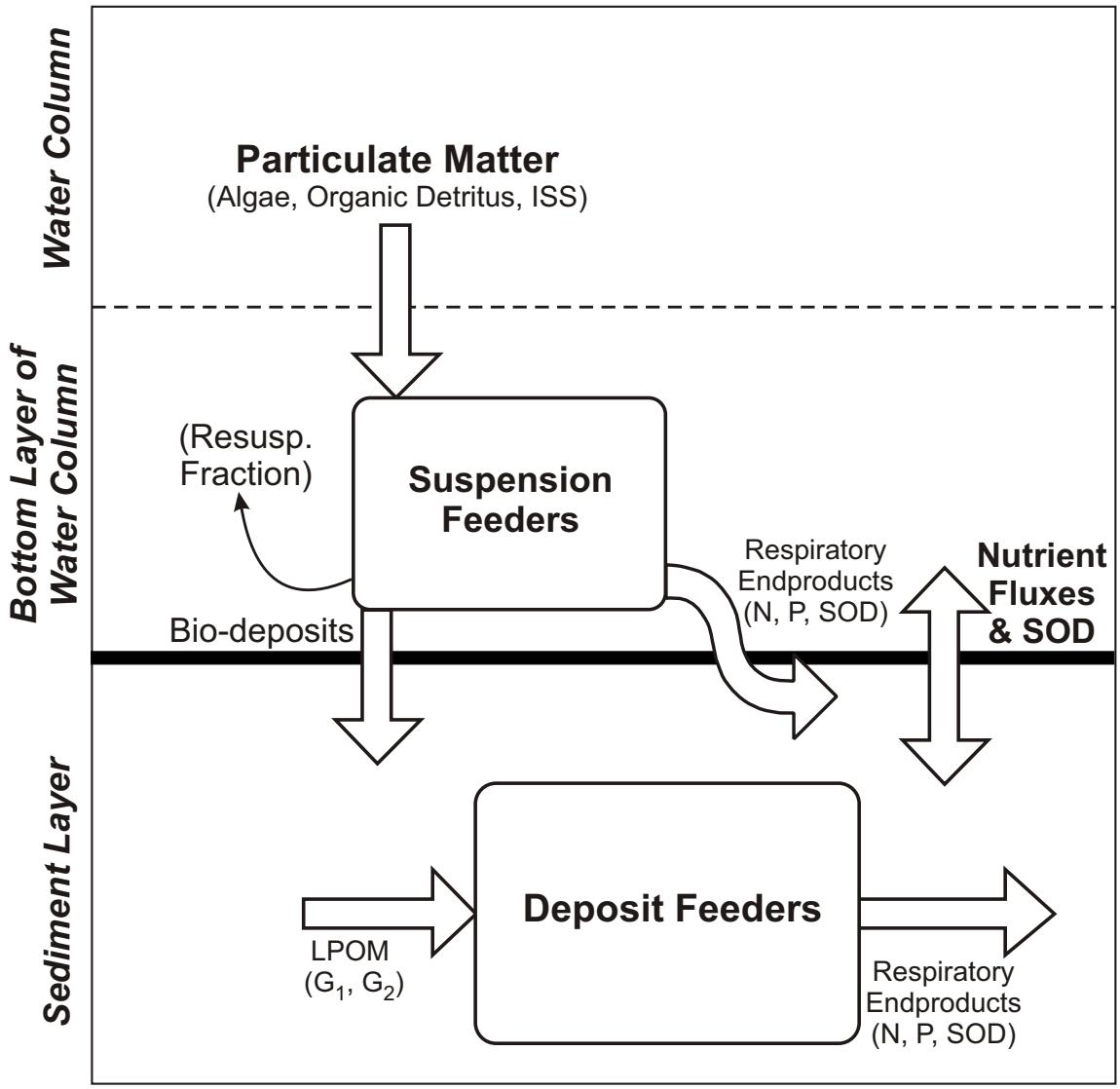

Figure 1-2. Schematic of water quality-sediment model coupling with active benthos.

and polychaetes only weakly so; once settled from pelagic larvae, they do not escape the confines of a modeled grid cell of approximately 2-4 km^2 in surface area. The interactions of these benthic fauna and the overlying water column properties of food, nutrients for algal growth, and oxygen cycles are readily included. The populations are modeled as biomass per unit surface area of sediment, dM/dt. The normalized mass, M, can be represented by the sum of the number of individuals per unit area, N, and their individual weights, w, i.e., M = Nw. Thus, dM/dt can be expressed as:

$$\frac{dM}{dt} = N \frac{dw}{dt} + w \frac{dN}{dt} \qquad (1\text{-}1)$$

The variation in individual weight, dw/dt, is typically neglected for phytoplankton, with relatively uniform size within taxa or for given functional groups. For higher trophic levels, certain biological processes involving growth, reproductive status, and predation losses, are coupled to size and numbers. Thus, variations in weight become important.

Population models, resolving either individuals or size classes using an energy and/or mass balance approach, are used to analyze these processes. However, population models are designed for one, or at most, a few species, and require multiple age classes. Modeling higher trophic levels at the spatial resolution of the eutrophication model would require too many state variables. This requires that the benthic models retain the normalized biomass approach. Nonetheless, as will be shown below, size dependent processes were empirically developed for the suspension feeder model. Future efforts in modeling will need to further consider new ways to couple processes at the individual level with water quality modeling.

In the sections that follow, the data from the long-term Chesapeake Bay Benthic Monitoring Program will be discussed, followed by descriptions of the sub-models for suspension feeding bivalves and deposit-feeding polychaetes. Lastly, the application and calibration of the models coupled to the Chesapeake Bay Water Quality Model will be presented.

SECTION 2

THE DATA: THE CHESAPEAKE BAY BENTHIC MONITORING PROGRAM

2.1 INTRODUCTION

Ongoing environmental monitoring programs within the Chesapeake Bay watershed include extensive benthic monitoring principally performed by the states of Maryland and Virginia in cooperation with the US EPA's Chesapeake Bay Program (CBP). Maryland's program began in July 1984 (Ranasinghe et al., 1996). Virginia's program began in March 1985 (Dauer and Alden, 1995). During the first five years, the Maryland program sampled up to 70 fixed-location stations eight to ten times per year (through June 1989). Since July 1989, monitoring has been performed at 29 fixed-location sites (23 of which were from the original 70 locations with additional samples from sites randomly selected within 25 km^2 of the fixed locations using a stratified random design (strata defined by salinity, sediment type, and bottom depth). Four to six samples per station or stratum were collected each year. An additional sampling component was added in summer 1994; based on EMAP-style probabilistic sampling, the Maryland portion of the bay was divided into a few large geographic strata, with 11-28 samples randomly taken in each region. Replicate sampling (usually 2-3 samples, sometimes 1 or >3) was performed at fixed-location stations. Single cores were taken from randomly chosen sites. Virginia's program collects triplicate samples from among 26 fixed sites quarterly through 1995 and semi-annually since then. In 1996, a probabilistic sampling design was added, covering 25 sites randomly chosen in each of five geographic strata within the Virginia portion of the Bay. In all, through 1996, the data base consists of approximately 7,500 station occupations and 16,000 samples (cores) taken (Figure 2-1).

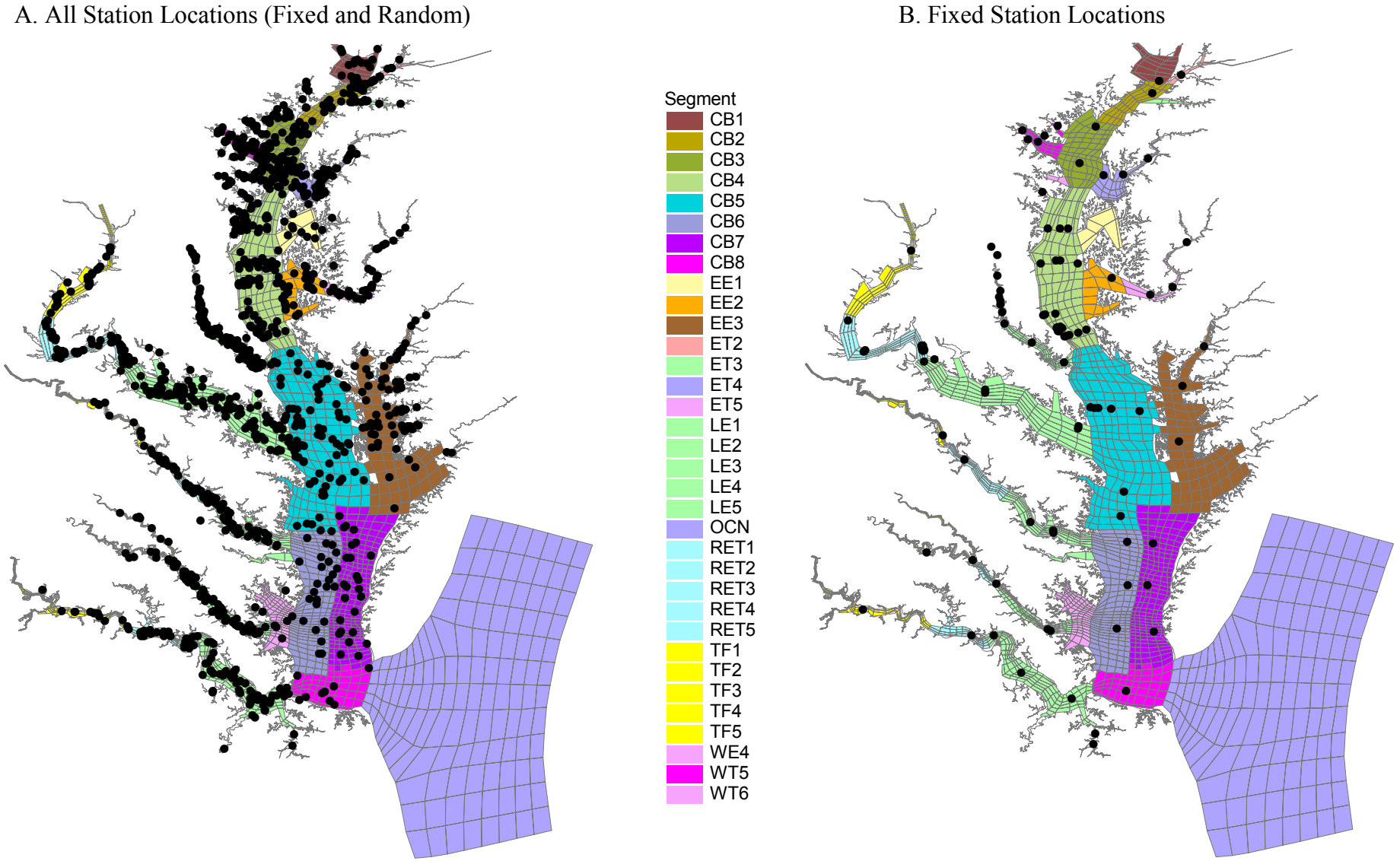

Figure 2-1. Chesapeake Bay Benthic Monitoring Program Station Locations (1984-1998), with the 1998 Hydrodynamic/Water Quality Model Grid and the 1985 Segmentation Scheme.

It should be noted that these programs sample soft-bottom benthic *infauna*, organisms living within the sediment column, but not on top of it, thus excluding, for example, oyster reefs. Detailed information on these programs is available from the EPA Chesapeake Bay Program Office (CBPO), Annapolis, MD, and at the "Data Hub" located at the CBP's web site (http://www.chesapeakebay.net/data/index.htm).

Collection methods are slightly different between the Maryland and Virginia programs (Table 2-1). The Maryland program has made use of various sampling gear, depending on station water - column depth and time in the program. A post hole digger was used in shallow ($\leq$5 m), near shore sites. At deeper locations, either a hydraulic grab, Young-modified Van Veen grab, or Wildco box corer was used. The Virginia program has consistently used a rectangular spade-type box corer; for consistency with EMAP samples, a Young-modified Van Veen grab (0.04 m^2) has been used more recently at some mainstem bay sites. Besides surface area, these devices vary in their depth of penetration. Both area and penetration depth may influence the quantity and kinds of organisms captured.

Table 2-1. Sampling gear used in the Chesapeake Bay Benthic Monitoring Program (CBBMP)

Program	Gear	Area (m^2)	Penetration Depth (cm)
Maryland	Hand-operated corer	0.0225	25
	Wildco box corer	0.0225	23
	Van Veen grab	0.10	?
	Young-Modified Van Veen grab	0.044	10
Virginia	Box corer	0.0184	25

The data are made available as either flat text files or as a Microsoft Access (version 97) relational database from the Living Resources Data Manager at the CBPO. The data consist of taxonomic identifications to the lowest possible level with abundance and biomass (as ash-free dry weight (AFDW) for each taxon. Reported biomass was either measured or estimated based on morphometric (length, width) relationships to individual mass (e.g., Ranasinghe et al., 1996). The database also contains water quality observations (e.g., temperature salinity, and dissolved oxygen) collected contemporaneously with benthic sampling. In particular, the bottom water dissolved

oxygen (DO) data were compared with observed benthic biomass. The relational database was used in order to extract and analyze data for dominant individual species and in the reductionist, lumped categories employed by the benthic modeling framework.

In the model, with which these data were compared, infaunal benthos have been divided into two general feeding components, deposit and suspension feeding. While both feeding types are found among the broad suite of benthic taxa, the physiological-based design used by the model divided the benthos into deposit-feeding annelid worms (polychaetes and oligochaetes) and suspension-feeding bivalve mollusks. In this reductionist mode, the benthic biomass data used in model calibration was derived in the following manner. For deposit feeders, ash-free dry weight biomass of all polychaete and/or oligochaete taxa in a given sample was summed and normalized to a unit square meter. For bivalve mollusks, taxa identified as suspension and/or surface deposit feeding were aggregated in similar fashion as "suspension feeding biomass." Individual bivalve species were also examined for both abundance and biomass, related to determinations of average individual size in a given sample and their response to bottom water DO. For calibration purposes, benthic biomass time series were derived from data at the fixed sampling stations, which were then matched to model grid cells from the latest 10,196-cell water quality model grid (2,100 bottom layer cells) (Figure 2-2).

In the early stages of model development, the database was examined for patterns and empirical results reflective of the interaction of benthos in the ecosystem. Benthic biomass was aggregated by the dominant taxa of interest in this project (oligochaetes, polychaetes, and bivalves) and within groups was pooled by feeding group. For this project, polychaete taxa classified as deep deposit or interfacial feeders were pooled together as deposit feeders, while bivalves classified as suspension feeding were aggregated. The tellinid bivalve *Macoma baltica* was included as a suspension feeder in this project; evidence has shown that this bivalve exhibits both interfacial and suspension feeding modes (Hummel, 1985; Olafsson, 1986). Deposit feeding polychaetes and suspension feeding bivalves together comprised most of the benthic biomass. Suspension feeding polychaetes (primarily *Chaetopterus*) are found in the Virginian lower mainstem bay. Deposit

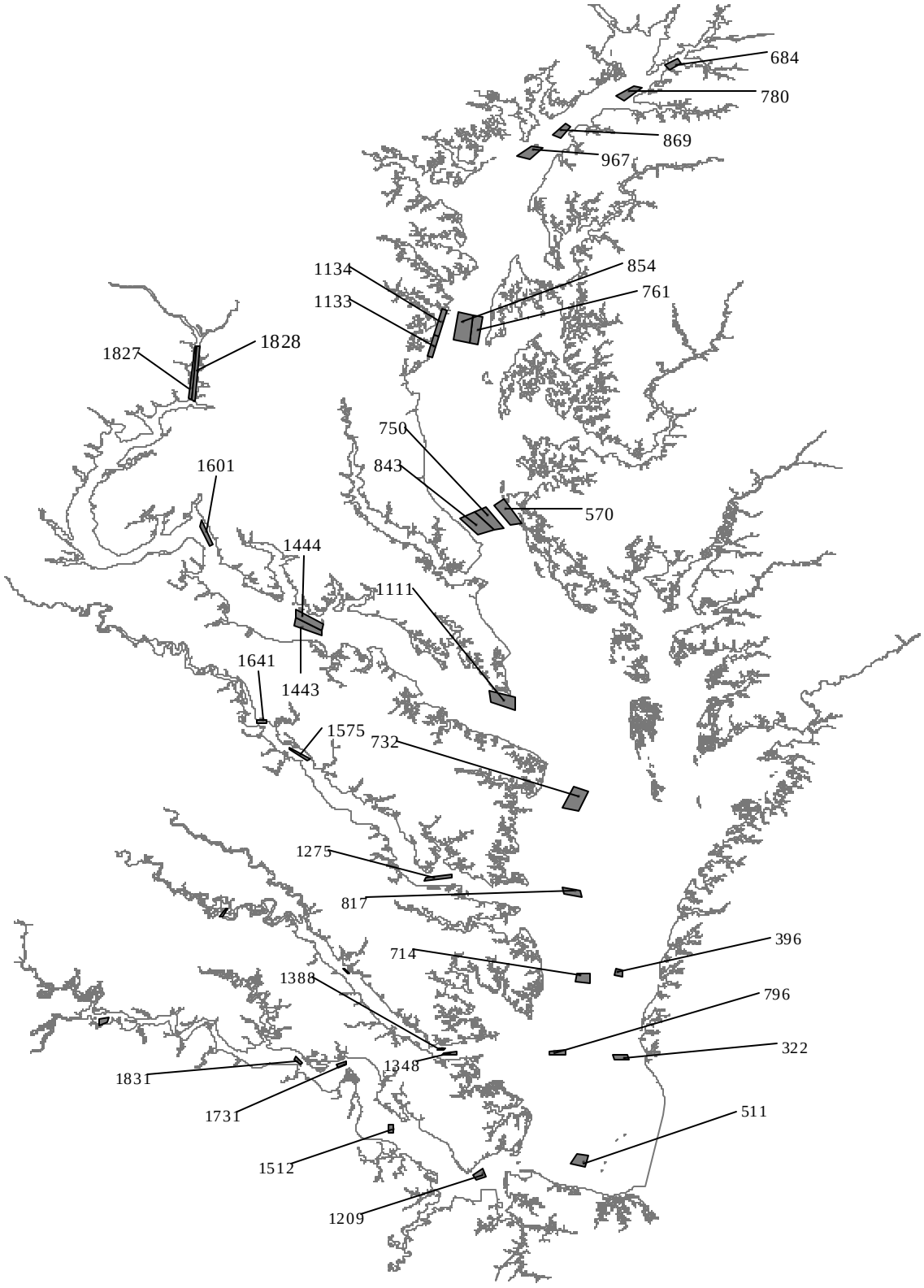

Figure 2-2. Location of fixed monitoring sites used for benthos calibration, referenced by their corresponding Chesapeake Bay Water Quality Model grid-cell number.

feeding bivalves comprised less than one percent of the bivalve biomass sampled by the BMP, although relatively large, deep-dwelling bivalves were likely missed, given the sampling methods. Lastly, the suspension feeding bivalve biomass does not include oyster biomass as a result of the design of the BMP.

2.2 GENERAL PATTERNS

Deposit feeding polychaete biomass was in the range of 0.1 - 1.0 g AFDW m^{-2} with higher biomass in shallow waters extending from lower mesohaline to polyhaline salinity regimes (Figure 2-3). In the Virginia program, fixed stations tended to be taken in or near the middle of the tributaries, in deeper waters. Biomass along the nearshore shoals tended to be higher as is shown in the paired deep and shallow stations in the Potomac River.

Suspension-feeding bivalve biomass was in the range of 1 - 50 g AFDW m^{-2} with high biomass in the lower mesohaline and mesohaline portions of the bay (Figure 2-4). Two exceptions to this were a population of the freshwater invasive clam, *Corbicula fluminea* in the tidal freshwater of the Potomac River near Washington, D.C. and a population of the hard clam, *Mercenaria mercenaria* in the polyhaline lower James River.

Because of the size-dependent nature of filtration rates in bivalves (see Suspension Feeder Model section below), a closer examination of individual species biomass was made by considering average biomass and abundance by species for all cores taken across all fixed sites (Figure 2-5). This would tend to produce low species biomass for taxa which are not broadly distributed. It is apparent that a few suspension-feeding species dominate the biomass of the bay. Five species have baywide average biomasses greater than 0.5 g AFDW m^{-2}: *Rangia cuneata*, *M. baltica*, *C. fluminea*, *Mya arenaria*, and *M. mercenaria*. As described above, *C. fluminea* and *M. mercenaria* have rather restricted habitats within the bay, such that their presence in this list, averaging across the entire bay, reflects the high biomass these species attain in their localized habitats. Figure 2-5 also shows abundance, with the same biomass dominants ranking high. Very small-sized species (*Gemma*

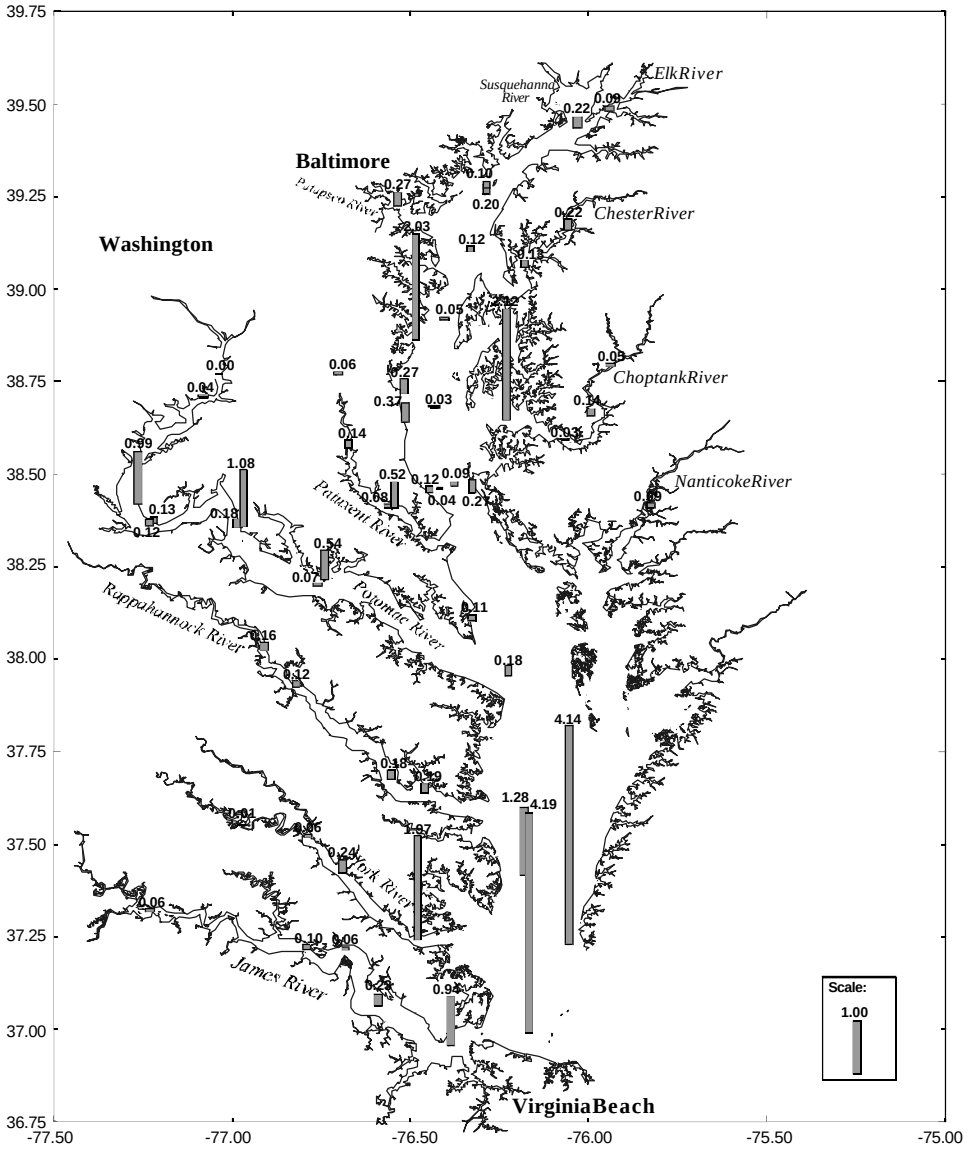

Figure 2-3. Average deposit feeding polychaete biomass (g AFDW m^{-2}; 1984-1995) at fixed survey sites from the Chesapeake Bay Benthic Monitoring Program.

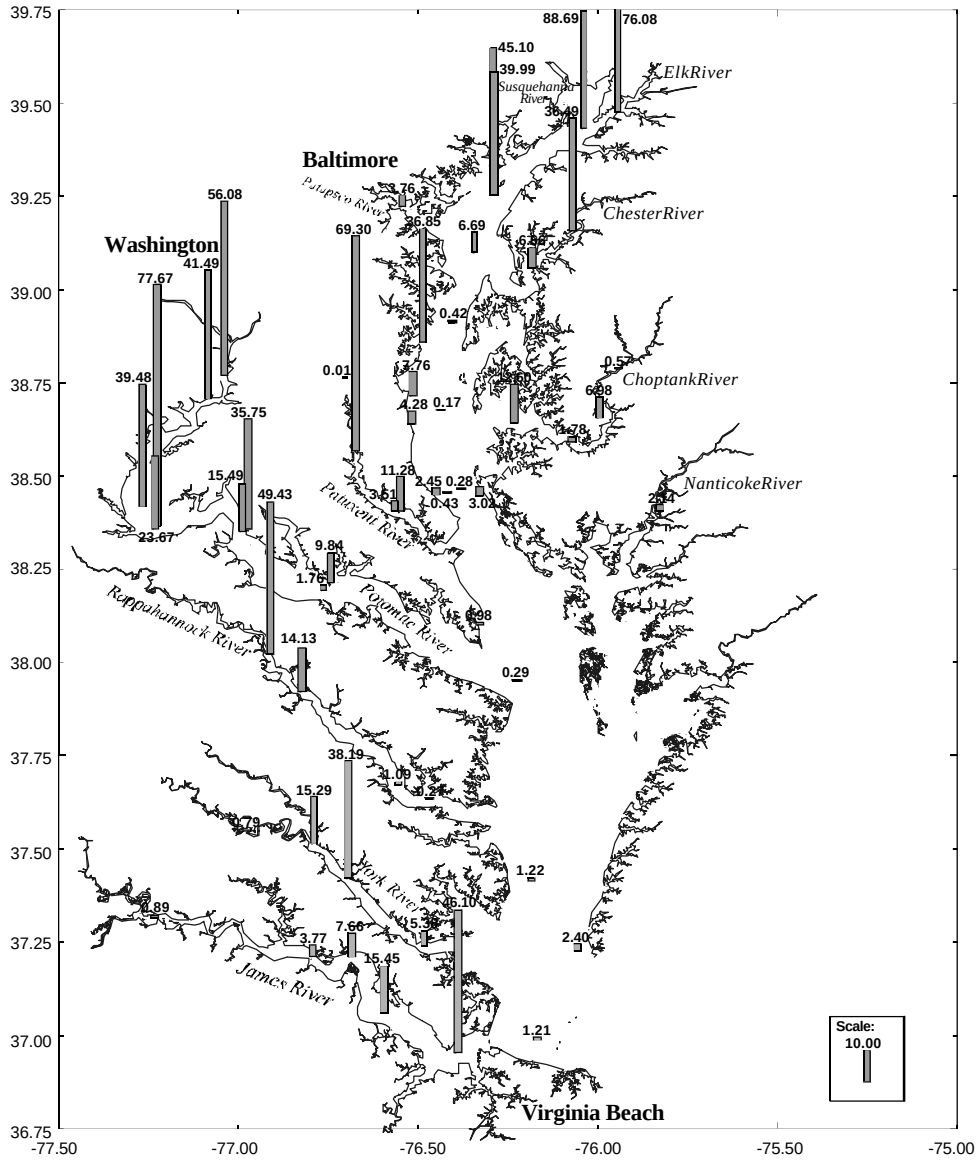

Figure 2-4. Average suspension feeding bivalve biomass (g AFDW m^{-2}; 1984-1995) at fixed survey sites from the Chesapeake Bay Benthic Monitoring Program.

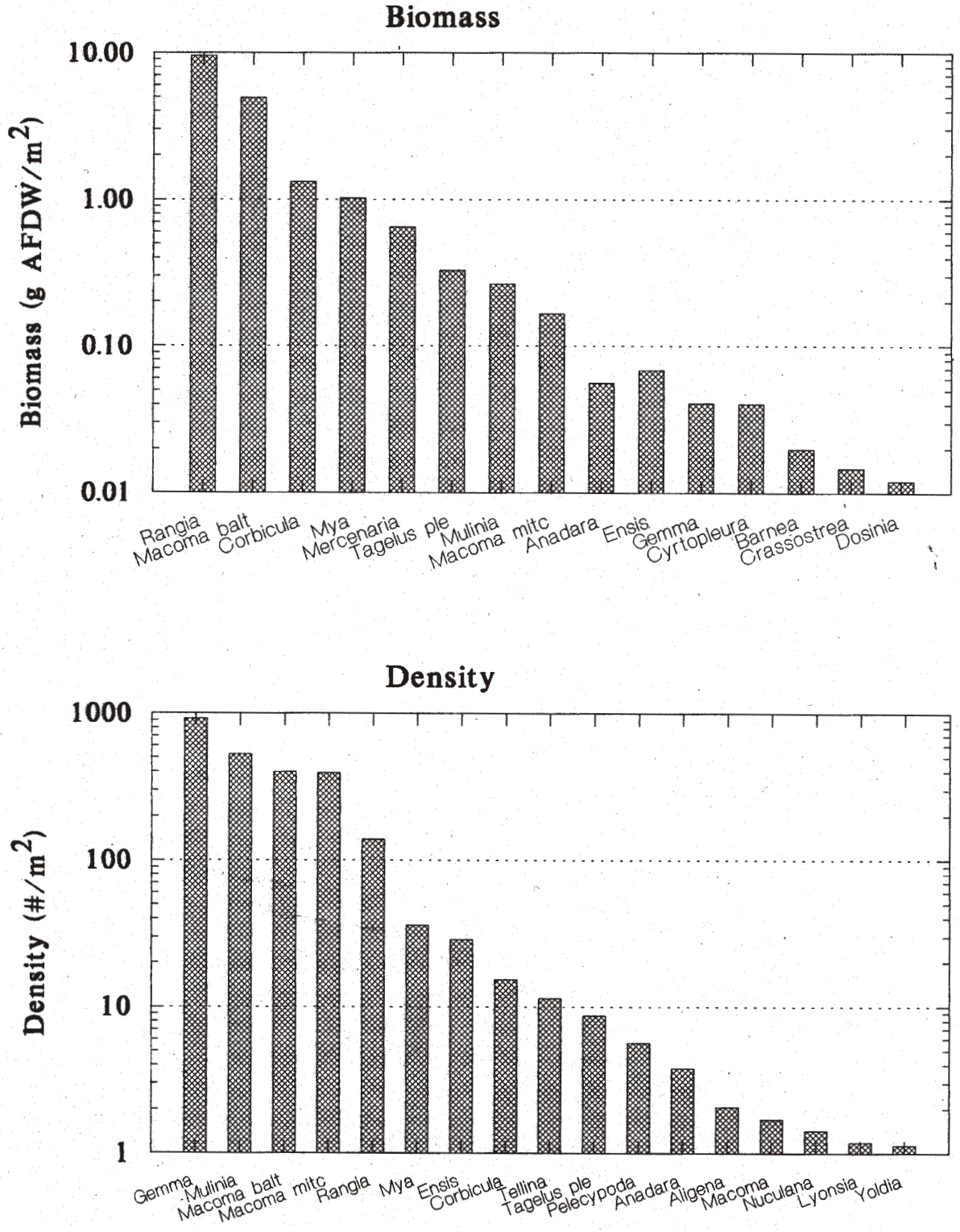

Figure 2-5. Overall average (1984-1995) biomass (g AFDW m^{-2}) and abundance (# m^{-2}) for the dominant bivalve species across all fixed survey sites from the Chesapeake Bay Benthic Monitoring Program.

gemma; *Macoma mitchelli*) and small, opportunistic species (*Mulinia lateralis*) rank highest in abundance, but contribute little biomass. The bivalve density shown in Figure 2-5 includes that of a few deposit feeding species (e.g., *Yoldia, Nuculana*) with relatively low abundance. Further examination of individual species' biomass and abundance data will made below in the discussion of the development of filtration and respiration rate relationships and computed biomass.

2.3 DISSOLVED OXYGEN

As will be seen in the description of the suspension and deposit feeder model frameworks, the principal controls on simulated benthic biomass are food (organic matter produced and transported by the water quality model), temperature, and bottom water dissolved oxygen. High algal biomass and low bottom water dissolved oxygen are major indicators of eutrophication. High quantities of the former, however, provides food to the benthos, while hypoxia and anoxia are detrimental to benthic infauna. Indeed, an early sign of incipient eutrophication in estuaries is an enhanced benthic fauna (Pearson and Rosenberg, 1978). However, once persistent, extremely low levels of DO occur in bottom water, benthic populations die off. The critical point at which this occurs depends on the fauna, and is highly dependent on individual species' tolerance for anoxia, ability to survive using facultative anaerobic pathways for energy metabolism, and the presence or absence of free sulfide in bottom waters. With respect to polychaetes, species shifts from larger, deeper dwelling or tube-building species to smaller, surficial or near-surface dwelling species occurs under both hypoxic as well as physically disturbed conditions. Estuarine bivalve species tend to show significant anaerobic capacity and may be less sensitive to short-term hypoxic events than other fauna.

Thus, a fundamental question that can be posed with respect to the monitoring program data is: what relationships are there between periodic hypoxia/anoxia and benthic biomass in the data record. It should first be noted, however, that site selection in the monitoring program is not random; zones deeper than 20 m in the bay were outright excluded from sampling, as persistent summertime anoxia was expected in these zones. This does not represent a significant fraction of the total bottom

area, though. Nonetheless, potential habitat in the mouth of the Potomac River was excluded from fixed station monitoring because of persistent anoxia. In the probability-based sampling schemes, sample depths within the same region varied from cruise to cruise, so that depending on the region, time of year, and station depth, effects of hypoxia may or may not be represented in the data set.

The relationship between bottom water DO and benthic biomass is examined in Figures 2-6 and 2-7. Time series of bottom water DO, suspension feeding bivalve biomass, and deposit feeding polychaete biomass are shown from fixed-location stations deeper than 5 meters, where periodic hypoxia is likely to be found. The stations are grouped by CBP segments (see Figure 2-8). The symbols are coded for hypoxic conditions: values at DO concentrations greater than 2.0 mg/L are shown as "0", less than 2 mg/L as "2", less than 1.0 mg/L are shown as "1", and values were DO was not recorded are shown as "<". Note that sampling frequency declined following 1989, and some fixed stations were replaced with probability-based stations, not shown here. In the mesohaline bay proper (Figure 2-7), BMP data regularly captured summertime hypoxia at some sites within CB4, to a lesser extent in CB5, and rarely in CB3. The observations of hypoxia in the lower Potomac River (Figure 2-6) appear to be less regular, but changes in sampling frequency during the program as well as avoidance of regularly hypoxic deep zones in the mouth of the Potomac may be responsible for this pattern.

Benthic biomass under normoxic conditions (open circles) varied with time over several orders of magnitude, particularly for suspension feeding bivalves (Figures 2-6 and 2-7). Observations with little or no suspension feeding bivalve biomass were frequent under both normoxic and hypoxic conditions (true zeros do occur in the data record and were plotted along the x-axis in the semi-logarithmic plots). Given the variation in biomass of both deposit and suspension feeders under normoxic conditions, no obvious distinctions in biomass patterns in normoxic versus hypoxic conditions are apparent for either deposit or suspension feeders. This is a somewhat surprising result in view of the sensitivity of benthic organisms to anoxia (Figure 1-1). Perhaps spatial patchiness, well-known in benthic distributions and especially important in highly aggregated

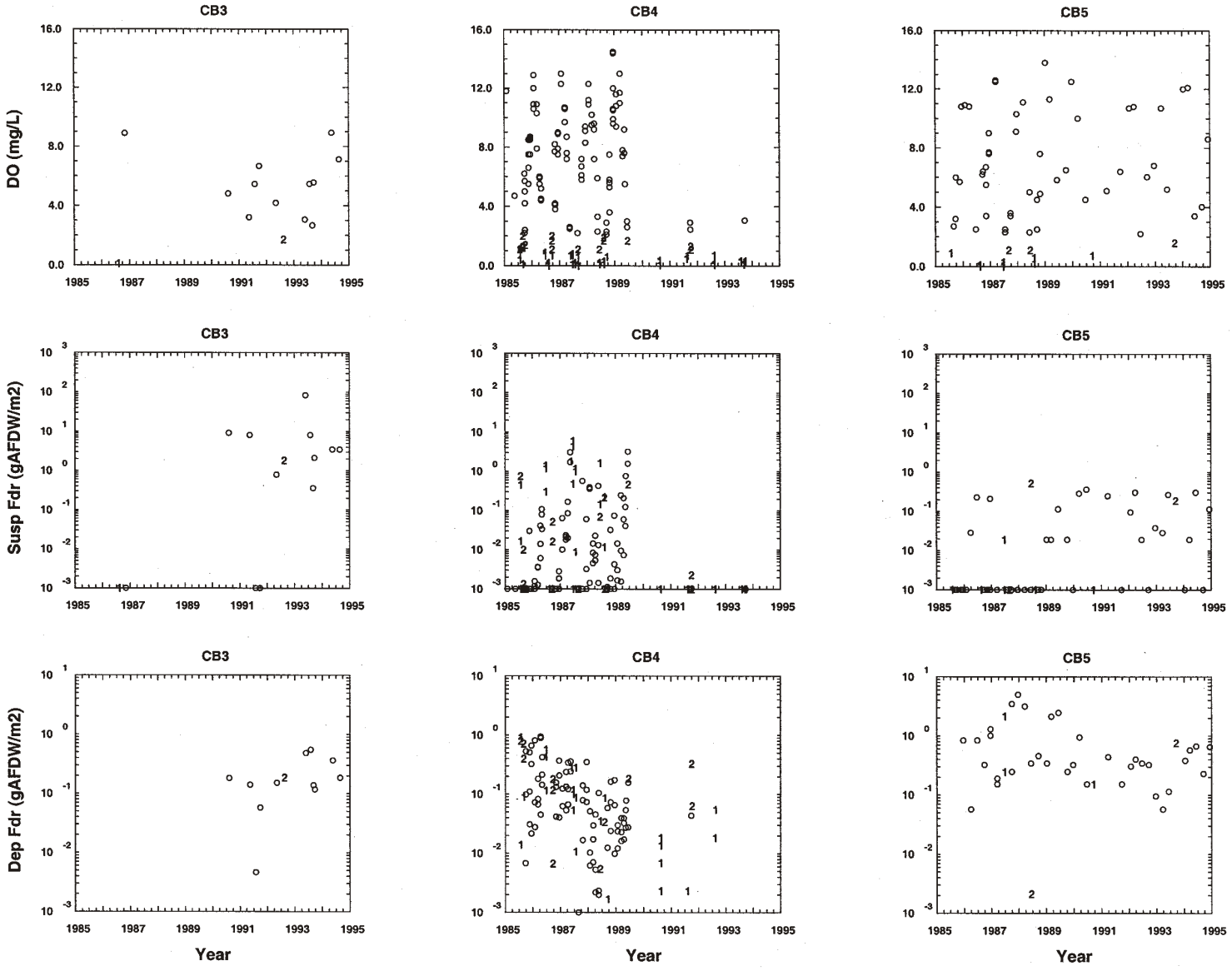

Figure 2-6. Time series of bottom water dissolved oxygen (DO; mg L-1), suspension feeding bivalve biomass (Susp Fdr; g AFDW m^{-2}) and deposit feeding polychaetes (Dep Fdr; g AFDW m^{-2}) within mesohaline Chesapeake Bay Program segments (stations deeper than 5m). Values are coded by DO: ->2 mg L^{-1}; 2- < 2 mg L^{-1}; 1 - < 1mg L^{-1}.

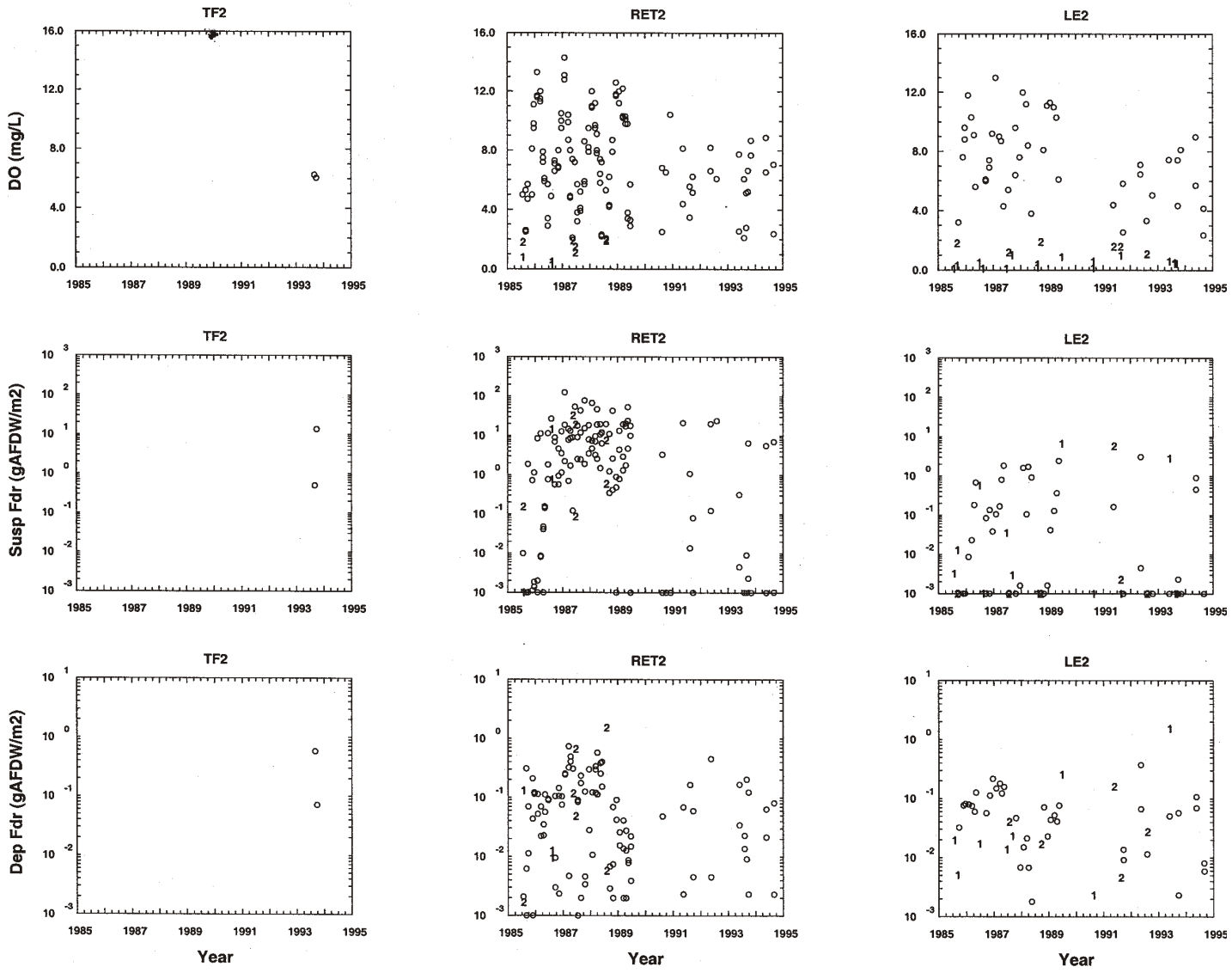

Figure 2-7. Time series of bottom water dissolved oxygen (DO; mg L-1), suspension feeding bivalve biomass (Susp Fdr; g AFDW m^{-2}) and deposit feeding polychaetes (Dep Fdr; g AFDW m^{-2}) within the Potomac River (stations deeper than 5m). Values are coded by DO: -> 2 mg L^{-1}; 2- < 2 mg L^{-1}; 1 - < 1mg L^{-1}.

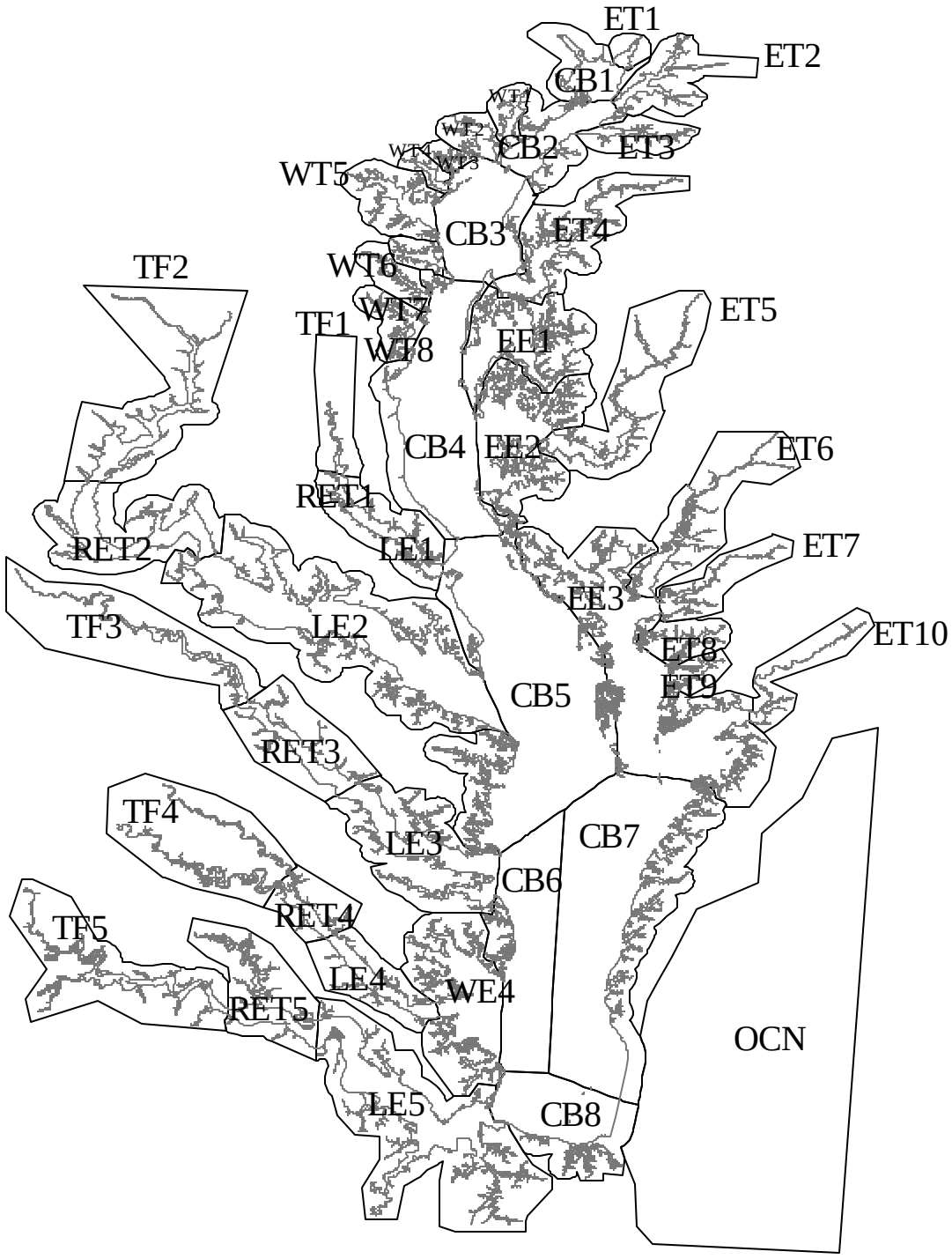

Figure 2-8. Chesapeake Bay Program Segmentation Scheme (1985), primarily based on salinity regime.

bivalve spatial distributions, may account for as much of the observed variation in regions susceptible to hypoxia as DO itself in these time series as a result of variation in station position from cruise to cruise.

The high degree of variability exhibited by the data suggest how these data can be used to calibrate the benthos models. There are large-scale features in the distributions of both suspension and deposit feeders, associated with productivity and the supply of food to the benthos, bottom water oxygen, depth, and habitat defined by salinity and sediment regimes (e.g., Diaz and Schaffner, 1990). The coupled water quality model can simulate much of the determining factors over spatial scales of square kilometers. However, spatial patchiness on scales of hundreds of square meters is evident in the fixed survey sites; coefficients of variation from replicate cores yielded values of 3 for suspension feeders and 1 for deposit feeders. Because of its scale, the model cannot resolve factors affecting the benthos at this resolution. However, gross lumping of model and data by region, such as by Chesapeake Bay Program segment, would mask many of the local factors affecting both model and data, such lack of food supply or of dissolved oxygen in deeper versus shallow zones. Thus, comparisons will be made between model and data at the station/grid cell scale, together with an evaluation of the model's ability to capture regional trends and processes affecting benthic distributions and biomass.

SECTION 3

SUSPENSION FEEDER MODEL

3.1 INTRODUCTION

Benthic fauna are critical links within biogeochemical and trophic processes, coupling traditionally distinct views of water quality and trophic dynamics within estuarine ecosystems. It has been well recognized that benthic suspension feeders, especially bivalve mollusks (e.g., clams, oysters, and mussels), can have significant impacts on algal biomass and productivity and on overall water quality within shallow estuarine environments. Similarly, poor water quality associated with eutrophication can have devastating impacts on benthic infauna, including bivalves. The benthos are important links between water column primary production and food for higher trophic levels, including commercially important species of fish and crabs. Described in this section is the development and calibration of a suspension-feeding bivalve model as one aspect of a practical application of benthic-pelagic coupling employed in the CE-QUAL-ICM water quality model of Chesapeake Bay.

Within the framework of the coupled water quality-sediment diagenesis model, suspension feeders occupy a position at the sediment-water interface (Figure 3-1). They filter organic and inorganic particles directly from the bottom-most water quality model layer (in the Chesapeake Bay application, the bottom layer thickness is two meters). Food availability may be limited by transport (advection, turbulent mixing, particle settling) of material from the penultimate model layer. Unassimilated material is added to the appropriate organic and inorganic particle fluxes delivered to the sediment, with the possibility of resuspension. Respiratory endproducts are returned to the water column as components of the inorganic nutrient fluxes computed by the sediment model at the sediment-water interface. Oxygen consumption, likewise, is represented as an additional component of the sediment model's sediment oxygen demand (SOD). Thus, this addition still preserves the

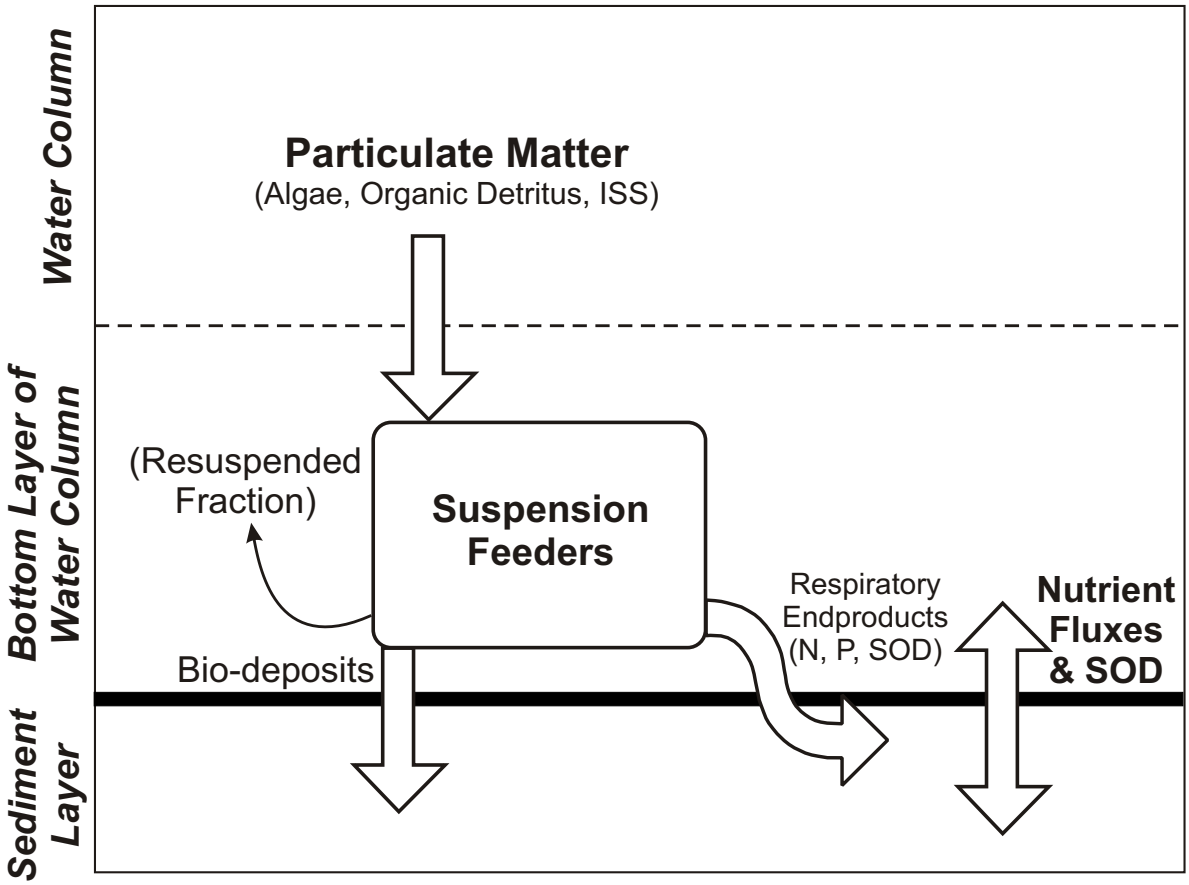

Figure 3-1. Schematic of suspension feeding bivalve submodel interactions with the water quality and sediment diagenesis models.

framework of the previous version of the coupled models, and the predicted nutrient fluxes and SOD are still comparable with core- and dome-based measurements of these exchanges.

In this section, the development and implementation of the suspension feeder model is described. The mass balance for suspension feeder biomass is presented, along with supporting equations and rates, as well as the model's computational framework and its interactions with other components of the coupled water quality-sediment model. Of particular note, in this development is the treatment of suspension feeder growth and respiration rates. In eutrophication modeling, specified maximum growth rates for algae and zooplankton are typically based on the functional group considered, allowing for faster and slower growing taxa, and are modified by environmental factors. Individual size, while well-recognized to affect the maximum growth rates of all organisms (e.g., Banse, 1979; Banse and Moser, 1980; Peters, 1983) is rarely considered as a factor when modeling algal growth. In bivalves, however, filtration and respiration rates are highly sensitive to individual size (length or mass). As the present model does not explicitly simulate size- or age-dependent classes, empirical relationships between individual mass and areal biomass were developed to include individual size as a factor influencing filtration and respiration rates. The development of these relationships is described below, as well.

3.2 THE MODEL FRAMEWORK

The state equation for the suspension feeder model is shown in Equation 3-1.

$$\frac{dS}{dt} = gS - rS - \beta S^2 - mS \qquad \textbf{(3-1)}$$

where:

S = suspension feeder biomass, mg C m^{-2}

g = growth rate, d^{-1}

r = respiration rate, d^{-1}

β = predation rate, m^2 mg^{-1} d^{-1}

m = hypoxia mortality rate, d^{-1}

This equation represents the time rate of change of suspension feeder biomass as a balance between growth processes, denoted as gS, and loss processes. The loss processes considered in this model are respiration, rS, predation, βS^2 , and mortality caused by anoxia, mS. The use of the quadratic form for the predation closure term reflects the fact that, while not explicitly modeled, predators are known to exert a significant control on benthic biomass (e.g., Virnstein, 1977). The model is formulated as a mass balance on carbon with working units of mg C/m^2 . This represents the areal biomass of suspension feeders on the bottom. To compare model results expressed in terms of carbon with data, commonly expressed in terms of ash free dry weight (AFDW), the model results, upon output, were multiplied by 2 (ash free dry weight is *very approximately* 50% carbon). Note that suspension feeding and filter feeding may be used alternately, and while such terms may be generally applied to many different aquatic organisms, the model has been specifically derived to simulate suspension feeding bivalve mollusks.

3.2.1 Growth and Filtration Rate

Growth occurs as a result of the assimilation of organic matter ingested during the filtration process (Equation 3-2):

$$g = I_f \sum_{i}^{n} (\alpha_i \, POC_i) \qquad \textbf{(3-2)}$$

where

I_f = Ingestion rate, as a function of biomass, temperature, dissolved oxygen and suspended solids, L mg^{-1} d^{-1}

α = assimilation efficiency of particulate organic carbon pool i, where i represents the three algal carbon pools as well as the refractory and labile particulate detrital carbon pools, (mg mg^{-1})

POC = particulate organic carbon, as algae or detrital POC, mg L^{-1}

The ingestion rate, I_f was computed from a filtration rate which was scaled for the average individual size of a population of suspension-feeding bivalves, and was further modified by bottom water temperature and dissolved oxygen concentration, and by total suspended solids (Equation 3-3).

$$I_f = f \cdot Z_{DO} \cdot \left[1 - 0.01\left(a_{tss} + b_{tsss} \cdot \log_{10} TSS\right)\right] \quad \textbf{(3-3)}$$

where

f = filtration rate, L mg^{-1} d^{-1}

Z_{DO} = a logistical shaping function reflecting the effects of low dissolved oxygen

a_{tss}, b_{tss} = constants reflecting the effects of total suspended solids (TSS)

The filtration rate, f defined in this model is not a simple constant. In nature, bivalve filtration rate is dependent on physiological as well as environmental factors (Griffiths and Griffiths, 1987; Dame, 1996). Filtration occurs as the result of ciliary movements along molluscan gill filaments. Individual size (relating to gill surface area), temperature, suspended matter concentration, and food quality can affect filtration and ingestion rates. Particle trapping occurs on cilia, on mucus strands and by direction of laminar flow into oral palps, leading to the organism's "mouth". Food and non-food particles can be sorted to varying degrees with the former passing into the gut and the latter being passed directly out the excurrent siphon. At high particle concentrations, filtration rate can decline, while ingestion rate can remain constant. In situations with low particle concentration or with sluggish hydrodynamic conditions, over-filtration can occur as recently filtered water, stripped of its particulate matter, is reprocessed. Under these circumstances, the water in a boundary layer accessible to filtration has particle concentrations significant less than those of the surrounding bulk fluid. Thus, in the natural environment, hydrodynamics in concert with filtration rate and the abundance of individuals in a unit area of bottom can influence the food available to an individual organism (Dame, 1996). Overarching all of these complexities, though, is the relationship between individual size and the individual's intrinsic rate of filtration.

While fundamental, the exact relationship of individual size to filtration rate does not have a universally accepted equation. Even the interpretation of meaningful measurements of rates is open to question (Powell et al, 1992; Dame, 1996). Powell et al. (1992) have extensively reviewed laboratory-based size-specific estimates of bivalve filtration rates. For a twenty-fold variation in individual length, filtration rate (volume per individual per day) varied over 400-fold (Figure 3-2A). Also evident in their review was an apparent bimodal distribution in the nature of the size-rate relationship, which they referred to as high-gear and low-gear filtration rates (the filled and open symbols, respectively). They suggested that the high-gear rate observed in laboratory studies, while physiologically possible and perhaps functional, is unlikely to be the rate at which bivalves regularly filter. Annual growth estimates using these high rates in an oyster population model, assuming sufficient food supply, were much higher than observed rates while the low-gear rate yielded realistic annual growth values. We re-analyzed Powell's data by linear regression of log-transformed data to obtain suitable power functions for filtration rate per individual based on individual length.

The impact of Powell's analysis can be placed into context by plotting a few of the published size-filtration relationships (Figure 3-3). Filtration rate here is expressed in two ways, as volume filtered per individual (as frequently reported), and as normalized by individual mass. Conversion from length to mass, depending on the original form of the published equation, was done using a length-weight relationship for *Mercenaria mercenaria* (Hibbert, 1976). Equations were taken from Coughlan (1969), Doering and Oviatt (1986), and Gerritsen, et al. (1994). Officer et al. (1982) and Cloern (1982) used similar relationships in their analysis of benthic filter feeder impacts on water quality. These relationships yield filtration rates which may differ by a factor of 10 for a given size. For example, assuming an areal biomass of 1.0 g C m^{-2} of 10 mg AFDW individuals, the total filtration would be equivalent to a particle settling rate of 0.4 to 3 m d^{-1}, depending on the choice of equation (Figure 3-3). Powell's high-gear and low-gear equations roughly bracket other relationships used to define filtration rates over the range of individual sizes for bivalves. After conversion from length to individual mass, Powell's low-gear rate equation was used as the basis of the size-specific filtration rate relationship.

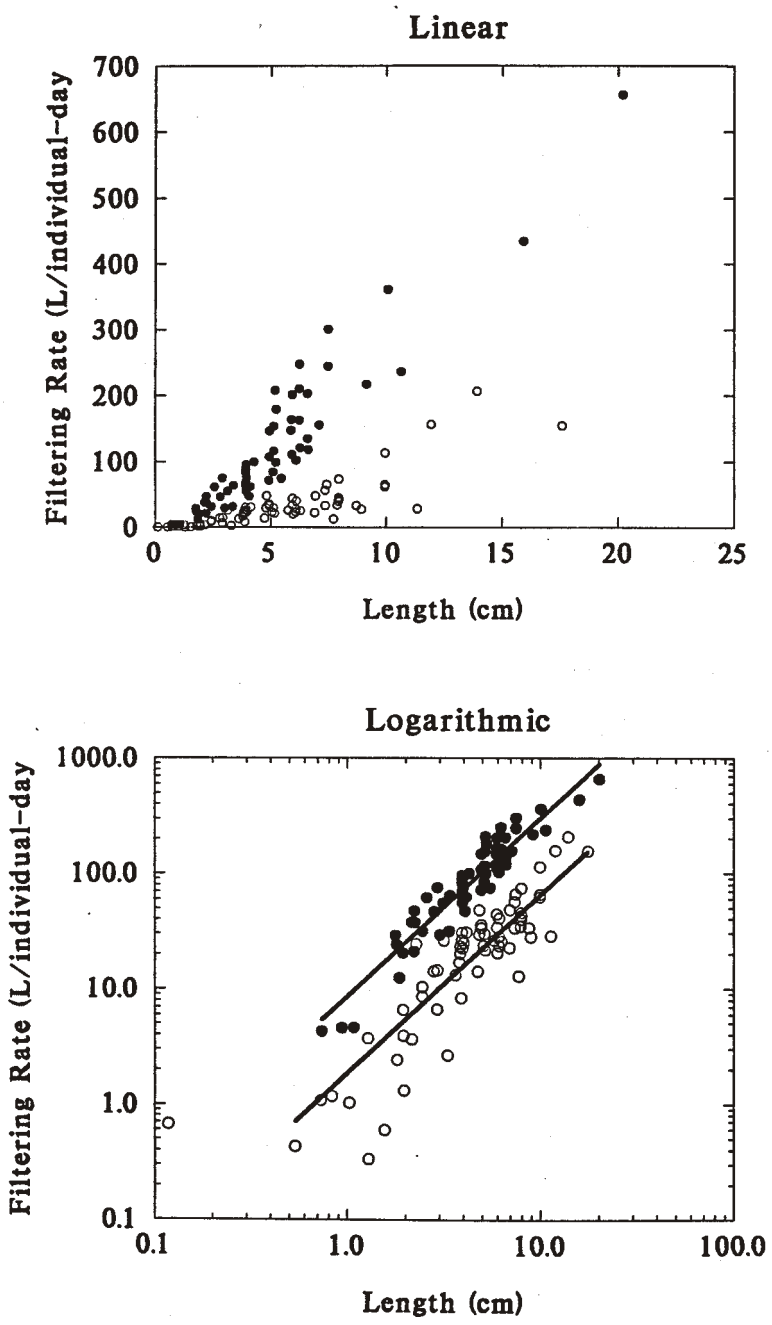

Figure 3-2. Bivalve filtration rate with individual size (from Powell et al., 1992).
A. The data suggest separate "high gear" (filled symbols) and "low gear" (open symbols) modes of filtration (Powell et al., 1992).
B. Power functions were fitted with linear regression on log-transformed data.

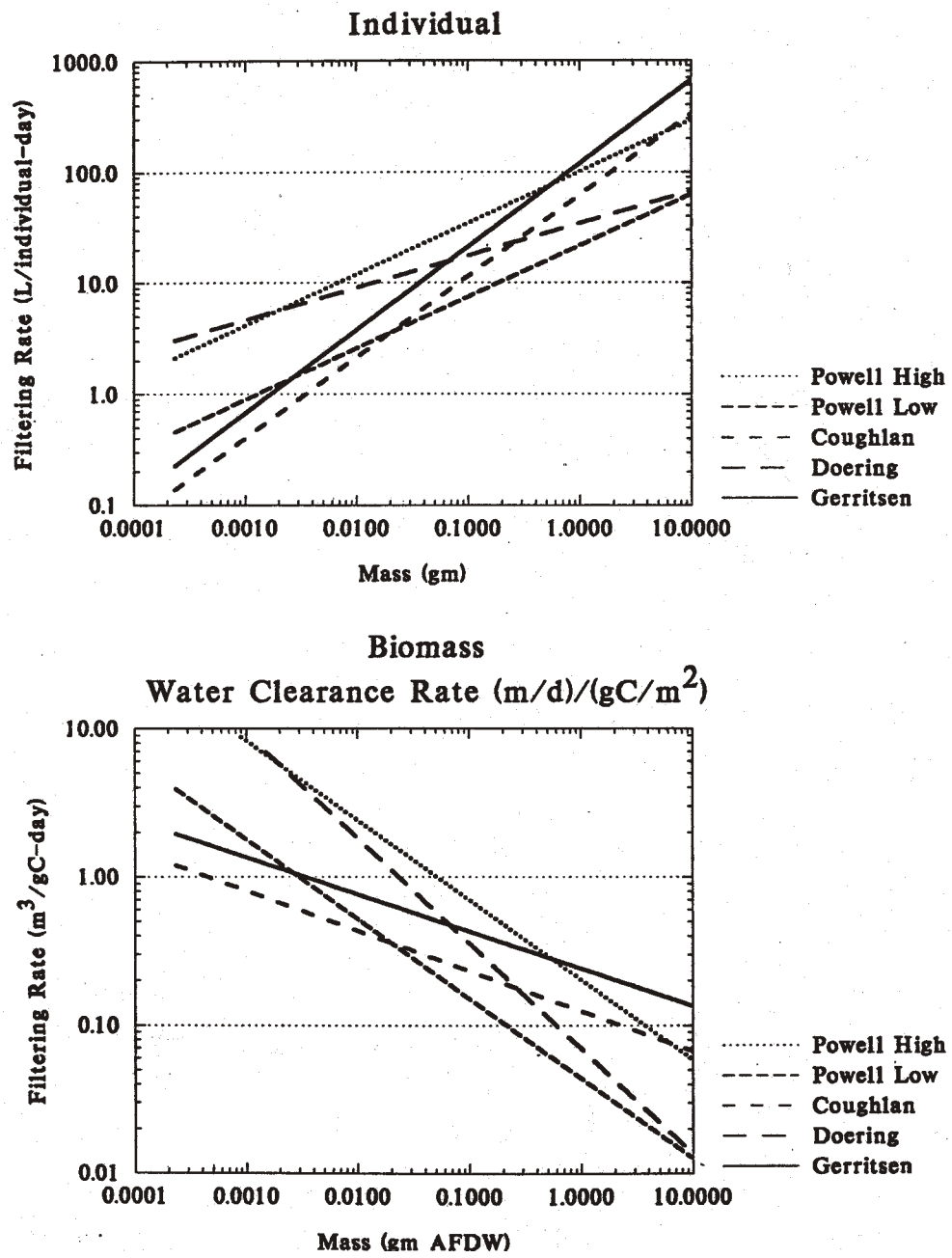

Figure 3-3. Estimates of bivalve filtration and clearance rates with individual mass using equations of Powell et al., 1992; Coughlan, 1969; Doering and Oviatt, 1986; and Gerritsen et al., 1994.

3.2.1.1 Individual Weight and Biomass

In models of individuals or populations with defined size classes, the variation of filtration rate with individual size can be handled explicitly. However, the framework used here, in concert with traditional water quality models, uses mass per unit area as the state variable, rather than tracking individuals or size classes. A relationship between individual size and biomass is required. Average individual mass was derived from contemporaneous abundance and biomass data in the BMP database for the dominant bivalve species. Interestingly, larger areal biomass tended to occur with higher abundance (Figure 3-4). Abundance, though, was not a predictor of individual size (Figure 3-5). However, individual mass was found to systematically increase with areal biomass for all species examined (Figure 3-6). Individual mass, W, could thus be estimated from areal biomass, such as computed by the model, as a power function, $W = aB^b$. An independent database, from the US EPA R-EMAP study of the New York-New Jersey Harbor region, yielded a strikingly similar result (Figure 3-7). While highly empirical, this is a vital and necessary link for estimating size-dependent rate processes.

Given the dominance of suspension-feeding bivalve fauna by a few species in the bay and the importance of the size-biomass relationship, four species were used as the basis of this relationship, *Corbicula fluminea, Rangia cuneata*, *Macoma baltica*, and *Mercenaria mercenaria*. These species occupy, respectively, tidal fresh, oligohaline-lower mesohaline, mesohaline, and polyhaline habitats within the bay. *C. fluminea* is exclusively found in the upper Potomac River (ignoring small, isolated populations in the upper James River). *M. mercenaria* is found almost exclusively in the lower James River, and its derived empirical mass-biomass coefficients were very similar to those of *M. baltica*. Filtration and rate biomass relationships for the three suspension feeding categories are shown in Figure 3-8. These relationships were derived using the low gear Powell filtration rate function and the species-specific weight-biomass relationship (Figure 3-6). Thus, three classes of suspension feeding bivalves were tracked in the model, a tidal freshwater class restricted to the Potomac River based on *C. fluminea*, an oligohaline-mesohaline class based on *R.*

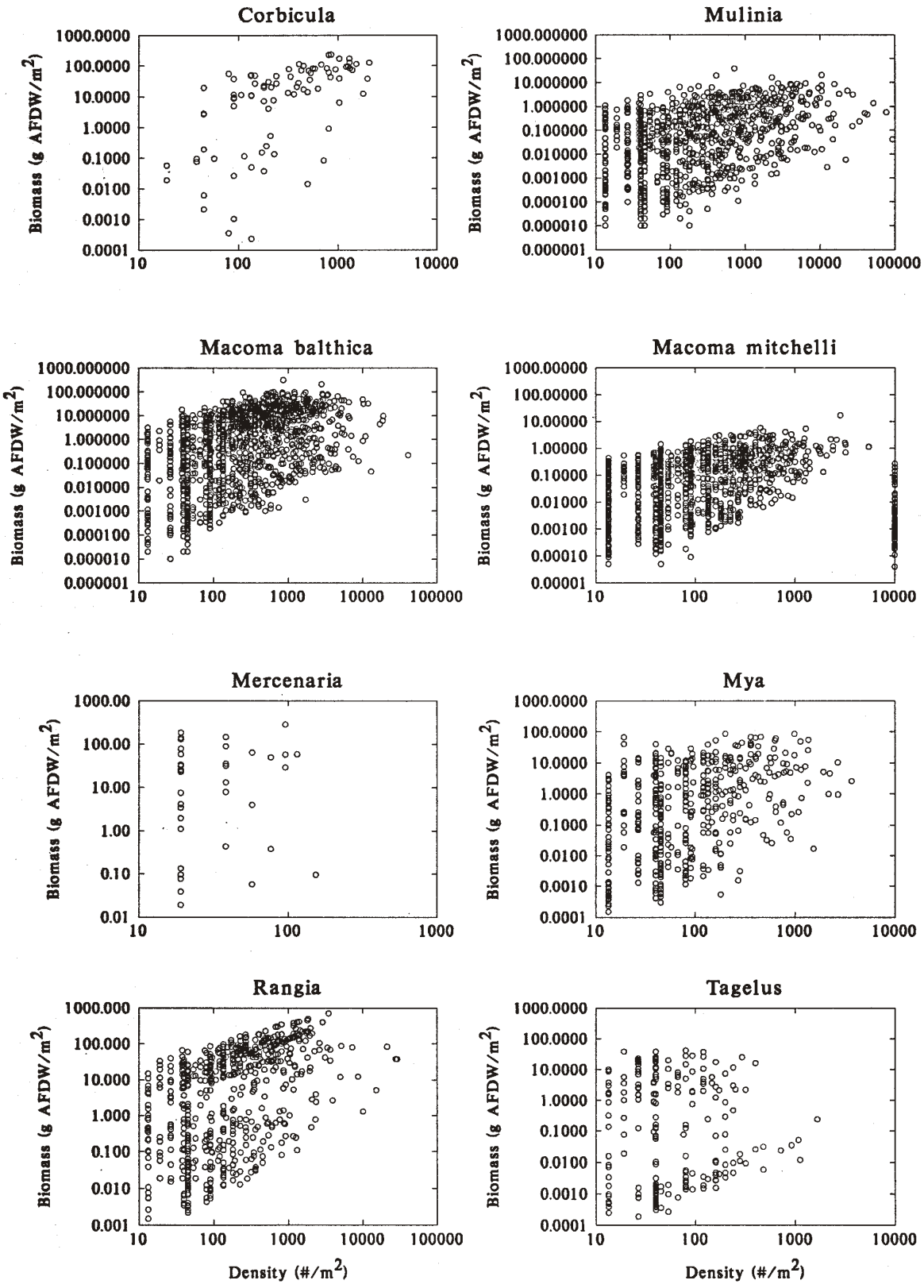

Figure 3-4. Biomass versus abundance for individual species from the Chesapeake Bay Benthic Monitoring Program

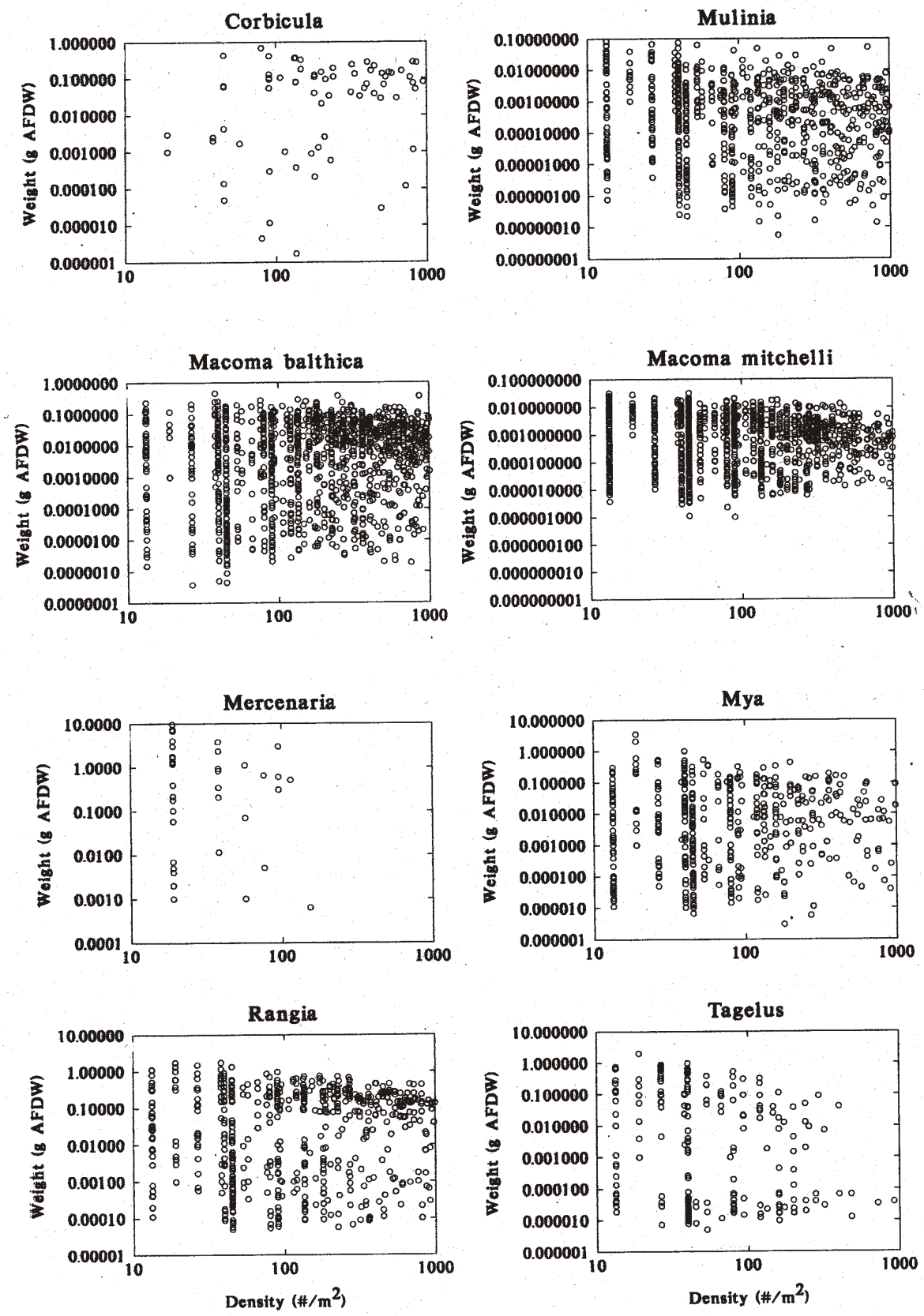

Figure 3-5. Average individual weight versus abundance for individual species from the Chesapeake Bay Benthic Monitoring Program

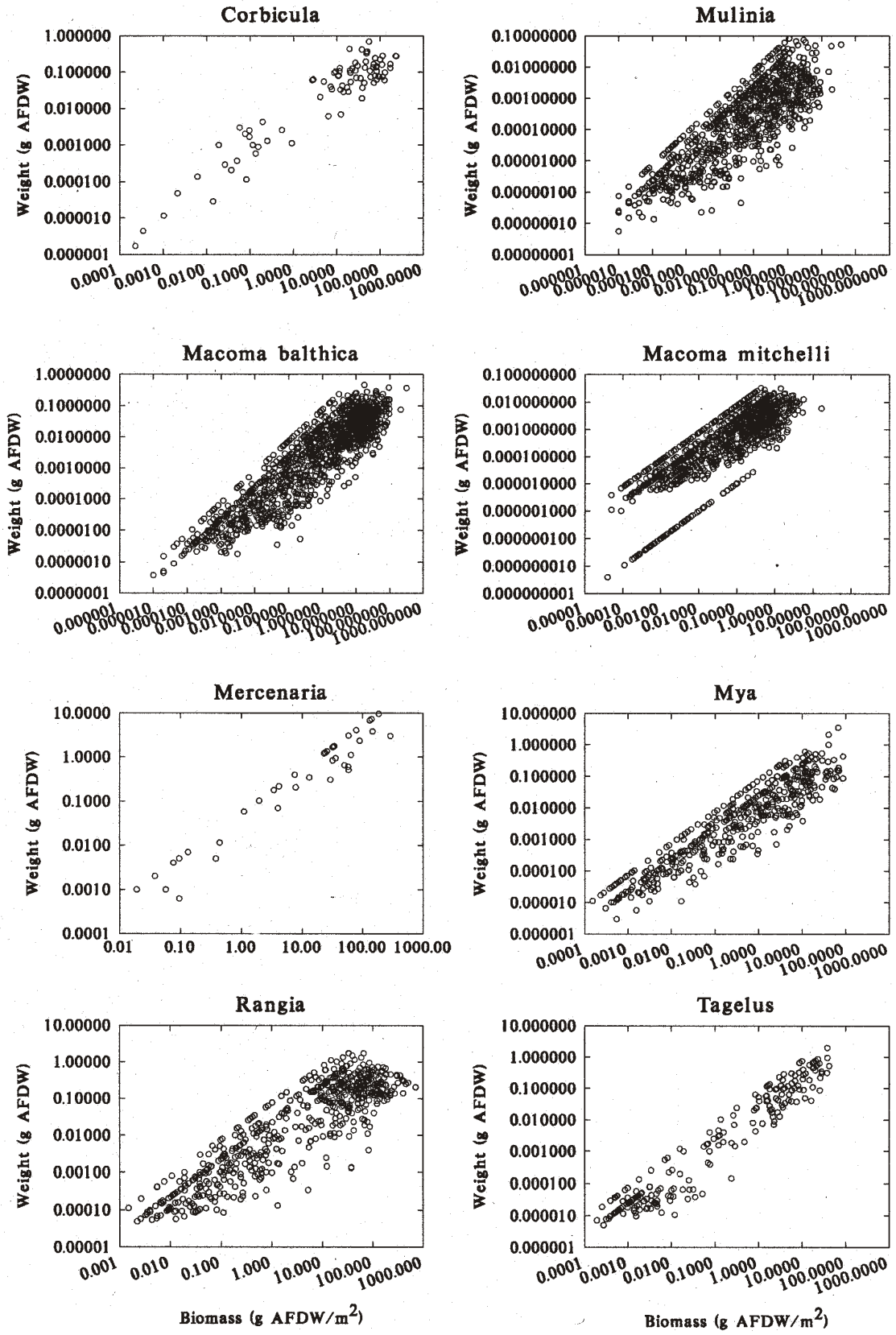

Figure 3-6. Average individual weight versus biomass for individual species from the Chesapeake Bay Benthic Monitoring Program

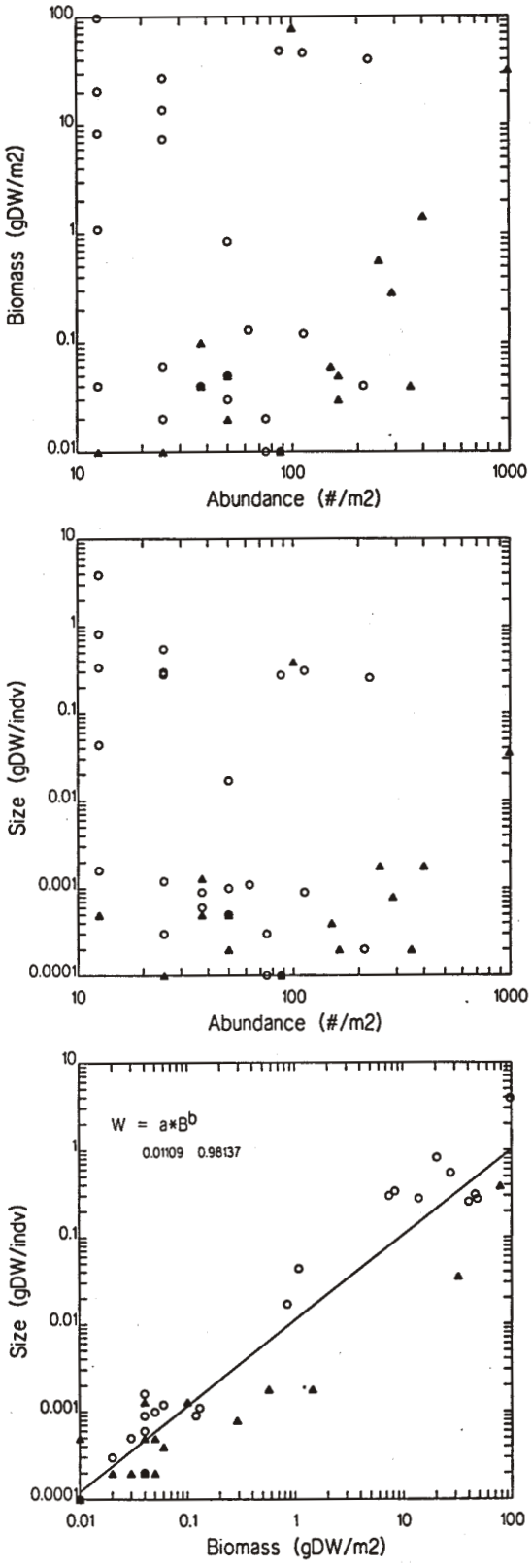

Figure 3-7. Relationship of average individual weight, abundance, and biomass for *Mercenaria mercenaria* from the U.S. EPA New York- New Jersey Harbor REMAP study (1993-1994).

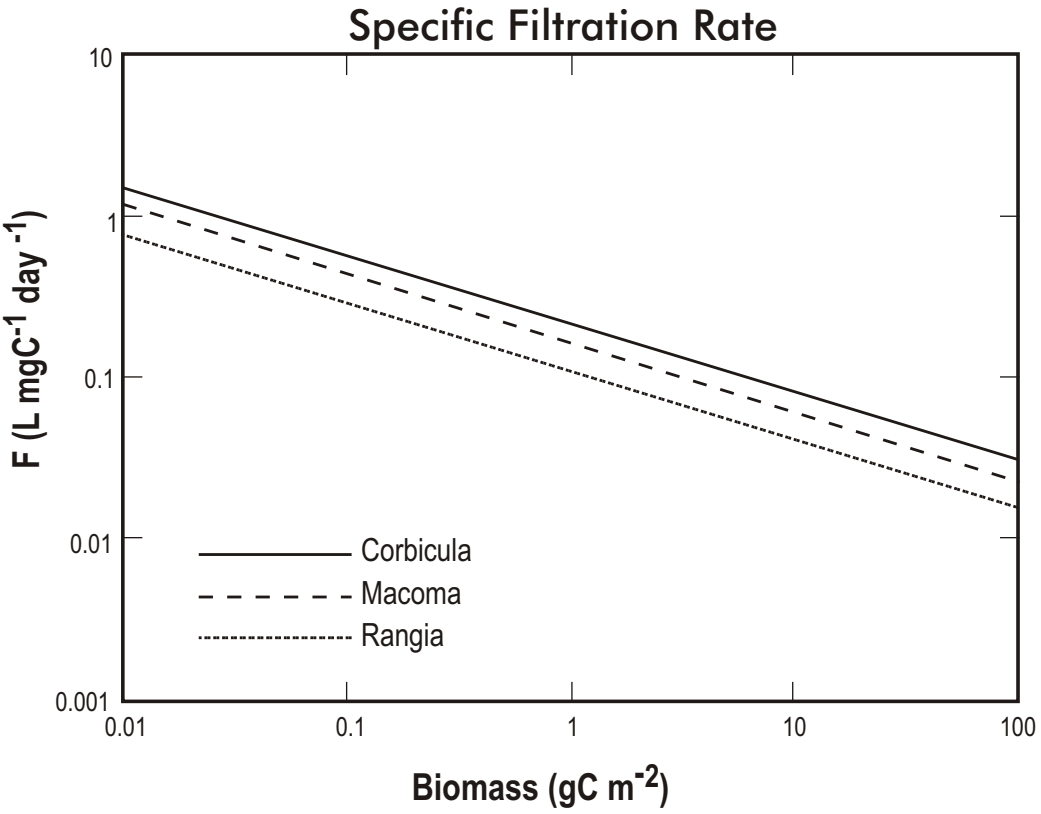

Figure 3-8. Filtration rate-biomass relationships for the three suspension feeder categories used in the model.

cuneata, and a mesohaline-polyhaline class based on *M. baltica* and *M. mercenaria*. In mesohaline reaches of the bay and its tributaries, the latter two classes overlapped.

Based on the size-dependent empiricisms described above, the following biomass dependent filtration rate relation, at a reference temperature of 20°C, was determined. Recall that average individual mass was positively correlated with areal biomass, M. Thus, the relationship of decreasing specific filtration rate with increasing individual mass is maintained by this formulation. Note here that M is in g C m^{-2} to give f in L d^{-1} mg C^{-1}. The instantaneous filtration rate is found by applying the usual Arrhenius temperature function:

$$f = f_{20} \bullet M^{b_f} \bullet \theta_f^{T-20} \qquad \textbf{(3-4)}$$

where b_f is the exponent that relates filtration rate to biomass.

3.2.1.2 Suspended Solids

The concentration of total suspended solids is another factor affecting filtration rates. At high concentrations, filtration rates are reduced as ingestion rates saturate. This is often the case under high inorganic solids loading, which can then lead to nutritional problems for bivalves. In Chesapeake Bay, inorganic solids loads can be very high, reaching hundred of milligrams or more of dry weight solids per liter within the tidal fresh and transitional (turbidity maximum) zones in the major tributaries, during the spring freshet period. A recast version of the turbidity function used in Powell's oyster model (Powell et al., 1992) was employed to represent the reduction in filtration rate due to suspended solids, f_{tss}:

$$f_{tss} = 1 - 0.01\,(a_{tss} + b_{tss} \log_{10} TSS) \qquad \textbf{(3-5)}$$

where TSS is total suspended solids (g DW L^{-1}). The effect is shown in Figure 3-9.

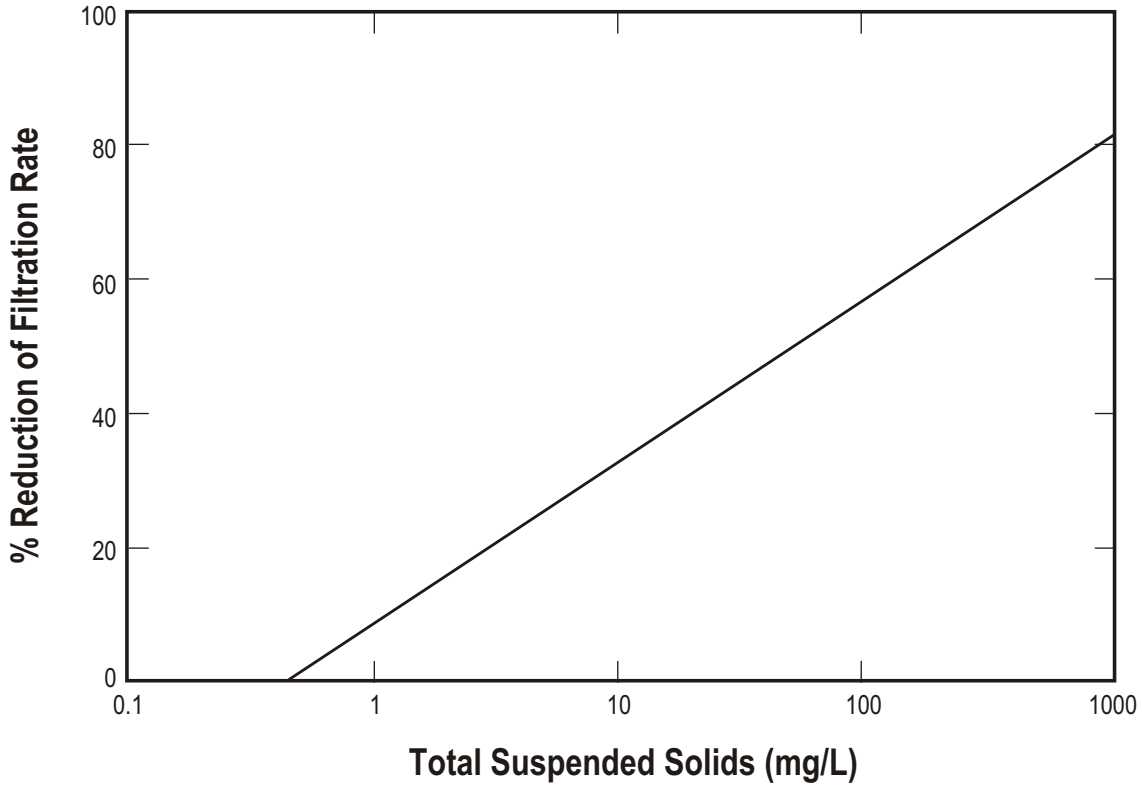

Figure 3-9. The reduction in filtration rate as a function of total suspended solids.

In summary, filtration on particles is assumed to be 100% efficient. That is, the clearance of particulate matter from the overlying water is merely a function of filtration rate and particle concentration, without sorting or rejection of components of the modeled suspended matter. Ingestion is also efficient, in that the filtration of inorganic solids from the water column does not impact assimilation efficiency (though, as shown below, total suspended solids does impact filtration rate). Although the growth rate expression shown above is based on carbon, water column organic matter pools also include particulate organic nitrogen and phosphorus (PON and POP, respectively). Algal nutrient content is also tracked by the water quality model. The suspension feeder model filters out PON and POP at the same rate as it removes POC. From the available ingested carbon, nitrogen and phosphorus, the organism assimilates what it needs for growth in a specified constant stoichiometric proportion. The computations for this are shown in Appendix A. Everything else (unassimilated organic matter) is deposited as feces. In addition to feces formation, pseudofeces is also formed when the maximum ingestion rate is achieved. Pseudofeces represents filtered but uningested matter. Together, these two components of filtered, processed material are referred to as bio-deposits. Computations for the fluxes of particulate matter to the sediments as a result of filtering activity are also shown in Appendix A.

The filtering process, moving water through the bivalve's mantel cavity, also provides for gas exchange and the removal of respiratory byproducts, so filtering is approximately a continuous behavior. While diel patterns in filtering rate may be observed in nature, the model does not adjust filtration rate as a function of the time of day. The model assumes that suspension feeders only feed on particulate matter; there is no uptake of dissolved organic matter. Also, suspension feeders do not directly feed on or affect zooplankton biomass, which is represented in the present version of the water quality model by both micro- and mesozooplankton size fractions. With respect to the water quality model, the following specific water quality constituents are filtered:

Carbon:	algal C (all three modeled groups), labile and refractory POC
Nitrogen:	algal N (all three modeled groups), labile and refractory PON
Phosphorus:	algal P (all three modeled groups), labile and refractory POP, inorganic solids-sorbed P

Silica: algal Si, unavailable (particulate detrital) Si

Solids: suspended inorganic solids (ISS)

3.2.2. Loss Terms: Respiration, Hypoxic/Anoxic Mortality, and Predation

As in filtration rates, respiration is a strong function of size (Figure 3-10). Again, applying the same empirically derived functions, the following biomass dependent respiration relation at a reference temperature of 20°C was determined. The same logic follows here as for the filtration rate--increases in areal biomass were indicative of populations of larger individuals with lower specific respiration rates. Again note here that M is in mg C m^{-2} to give r as d^{-1}. Instantaneous rates were temperature-corrected using a similar Arrhenius function:

$$r = r_{20} \bullet M^{-b_r} \bullet \theta_r^{T-20} \qquad \textbf{(3-6)}$$

Salinity can have a strong effect on respiration rates of individual species. However, salinity is effectively removed as a factor, as bivalve populations are assumed to exist within salinity regimes to which they are already adapted.

Predator-prey interactions are functions of the numbers or often equivalently assumed biomass, of both species. As predators are not modeled here, the suspension feeder state variable is effectively closed by assuming that predation loss is a function of the square of prey biomass. Unlike the vital rate functions described above, the quadratic predation loss rate is not a function of individual prey (suspension feeder) size, but is merely a function of temperature:

$$\beta = \beta_{20}\ \theta_\beta^{T-20} \qquad \textbf{(3-7)}$$

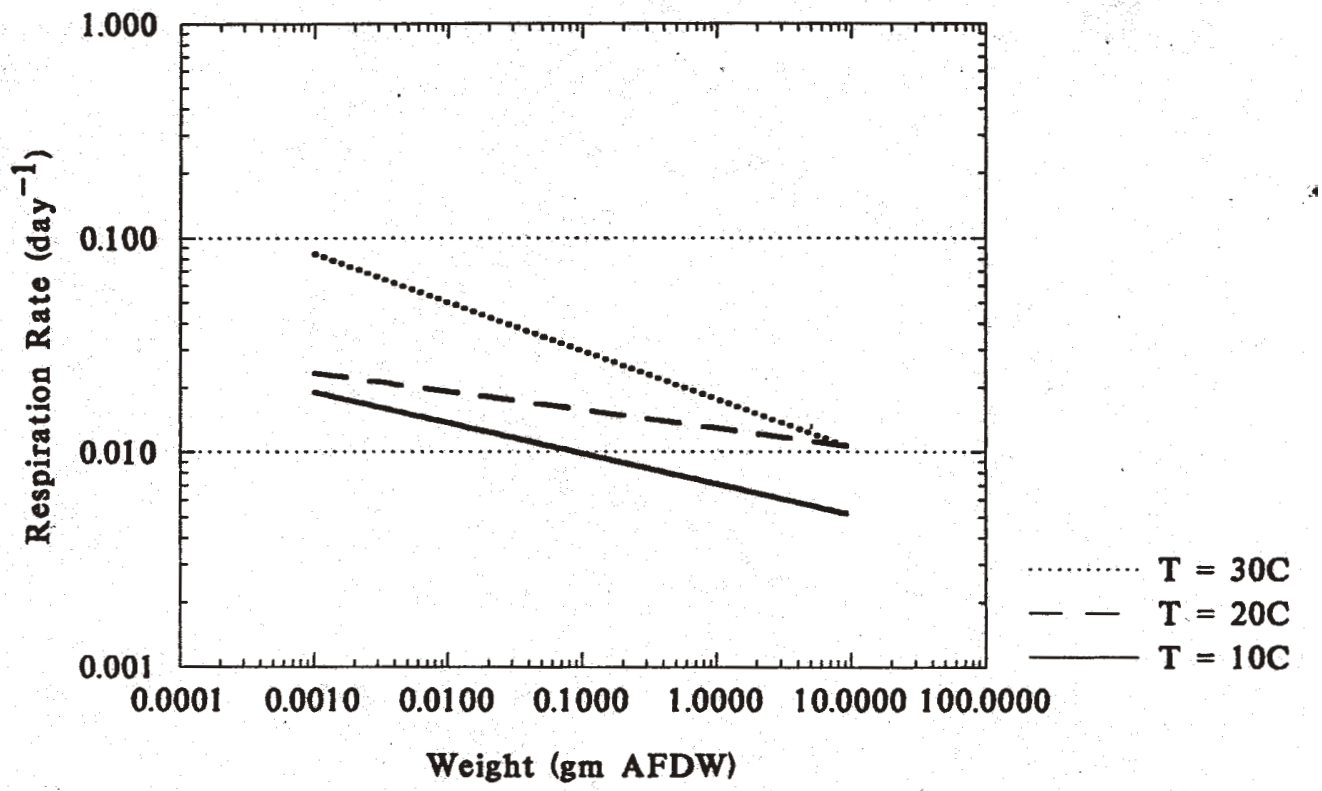

Figure 3-10. Respiration rate relationship at three temperatures for bivalve individual mass.

The temperature dependency assumes that predators (e.g., benthivorous fish and crabs) are mostly feeding during warm summer months. Species-specific rates were established through calibration. Predation in this version of the model has no other spatial or temporal dependencies.

Bivalve mortality caused by sustained hypoxia or anoxia has been discussed above. Mortality occurs below rather sharply defined oxygen concentrations. A logistic function (Figure 3-11) is used to model this behavior.

$$Z = \frac{1}{1 + \exp\left(1.1 \cdot \frac{DO_{hx} - DO}{DO_{hx} - DO_{qx}}\right)} \quad \textbf{(3-8)}$$

where:

DO_{hx} = DO at which the function is 50% of its maximum

DO_{qx} = DO at which the function is 25% of its maximum.

The exponential constant 1.1 is a shaping parameter required for the function to be reduced to 50% or 25% at DO values equal to DO_{hx} or DO_{qx}, respectively.

The mortality rate, m, is a function of an intrinsic rate under anoxic conditions and the logistic dependency under low oxygen conditions (Z).

$$m = r_d \cdot (1 - Z) \quad \textbf{(3-9)}$$

The anoxic mortality rate, r_d is defined by estimating the time to death for 99% of the individuals present:

$$r_d = \frac{\ln(1/100)}{t_d} \quad \textbf{(3-10)}$$

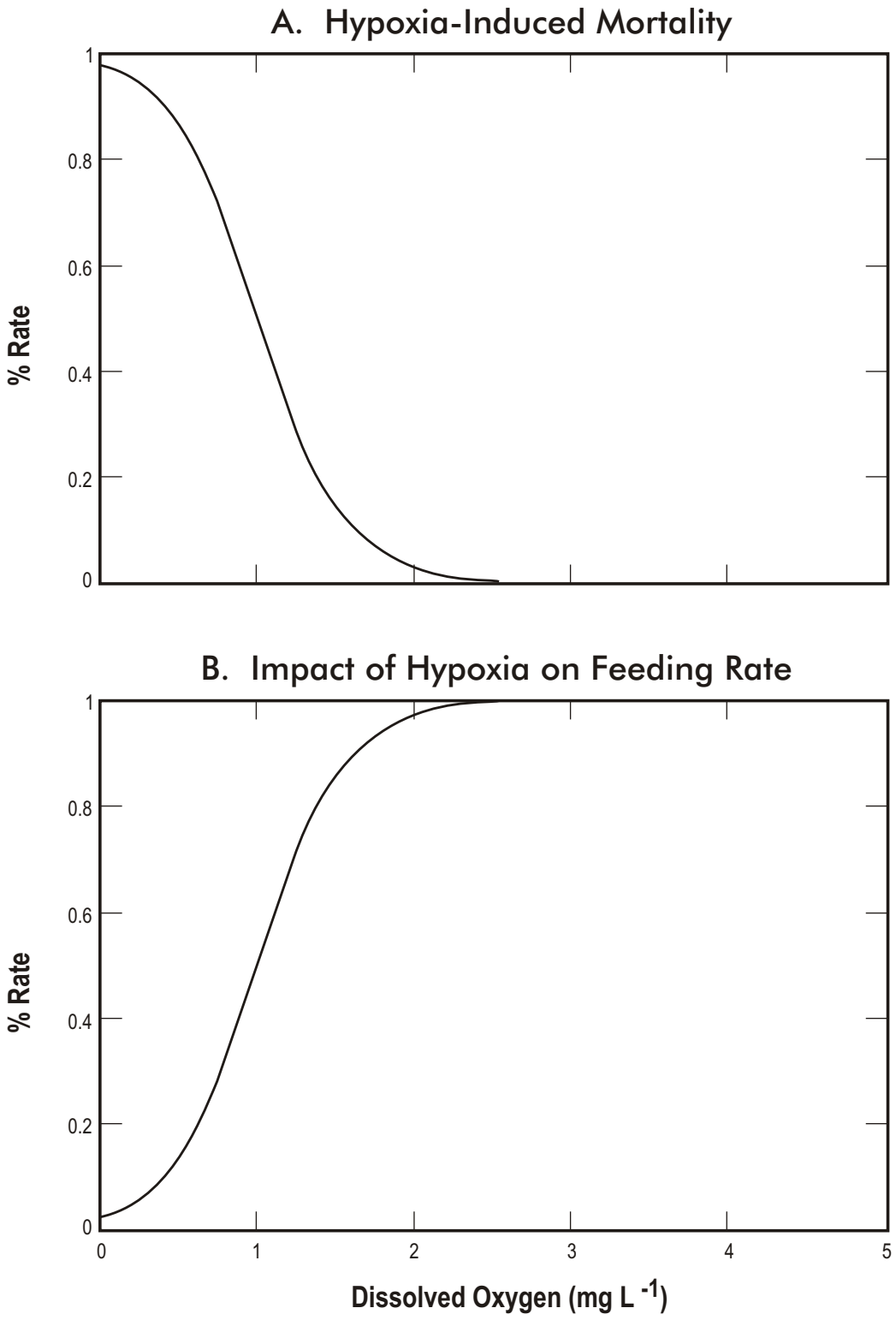

Figure 3-11. Logistic functional response of A. mortality rate, and B.feeding rate to bottom water dissolved oxygen for modeled suspension feeding bivalves.

where:

r_d = hypoxia mortality pressure rate, d^{-1}

t_d = time for 99% mortality, d

In addition to directly affecting mortality, hypoxia impacts other processes. Hypoxia in general slows aerobic respiration and filtration rates in bivalves. At some level of hypoxia, bivalve individuals close their shells and cease filtration altogether. Bivalve species can be fairly efficient anaerobes and can withstand varying lengths of time under anoxic conditions. Thus, in the model, filtration and aerobic respiration rates decline under hypoxia:

$$f = f' \cdot Z \;, \quad r = r' \cdot Z \qquad \textbf{(3-11)}$$

where f' and r' are the filtration and respiration rates before considering hypoxic effects.

Predatory animals are also affected by hypoxia. Generally, predation on the benthos declines dramatically at dissolved oxygen concentrations below approximately 2 mg L^{-1} as mobile predators (fish, crabs) leave the affected area (Nestlerode and Diaz, 1997). There may be a hysterisis response, however, following periodic hypoxia, as predators return and easily feed upon weakened benthos prey, lying on or near the sediment surface. The model does not contain such a functional description. Instead, predation is attenuated at reduced bottom water oxygen concentrations using a relatively smoothly-varying rectangular hyperbolic formulation:

$$\beta = \beta' \frac{DO}{DO + K_{DO}} \qquad \textbf{(3-12)}$$

where β' is the predation rate before considering hypoxic effects and K_{DO} is the bottom water dissolved oxygen concentration at which the predation rate, β is reduced to half its maximum value.

Note that in the model, biomass in a given model grid cell is never permitted to reach zero, as this would preclude regrowth after the hypoxia/anoxia event had passed. A lower limit of 0.10 mg m^{-2} was used to maintain a refuge of biomass. This refuge concentration is in lieu of a simulation for recruitment to the benthos.

Table 3-1. Constants Table for the Tidal-Fresh (TF), Oligohaline (OH), and Mesohaline (MH) Suspension Feeder Functional Groups

Constant	Value			Units
	TF	OH	MH	
f_{20} - base filtration rate	0.216	0.109	0.163	L d^{-1} mg C^{-1}
b_f - filtration factor	0.422	0.422	0.431	-
θ_f - filtration temperature coefficient	1.08	1.08	1.08	-
a_{tss}	81	81	81	-
b_{tss}	24	24	24	-
r_{20} - base respiration rate	0.013	0.0065	0.0065	d^{-1}
b_r - respiration factor	0.119	0.119	0.119	-
θ_r - respiration temperature coefficient	1.08	1.08	1.08	-
β_{20} - 20ºC predation rate	2.0E-7	1.0E-5	2.0E-5	m^2 mg C^{-1} d^{-1}
θ_β - predation temperature coefficient	1.12	1.12	1.12	-
DO_{hx} - logistic DO constant	1.0	1.0	1.0	mg L^{-1}
DO_{qx} - logistic DO constant	0.7	0.7	0.7	mg L^{-1}
K_{DO} - hypoxic half-saturation effect on predation	1.0	1.0	1.0	mg L^{-1}
t_d - time in days for 99% anoxic mortality	14.0	14.0	14.0	days
$\alpha_{1,2,3}$ algal C assimilation efficiencies	0.80	0.80	0.80	-
$\alpha_{4,5}$ LPOC, RPOC assimilation efficiencies	0.80, 0.00	0.80, 0.00	0.80, 0.00	-
Imax - max. ingestion rate	0.24	0.24	0.24	d^{-1}
SFCN - carbon to nitrogen ratio	5.67	5.67	5.67	mg C mg N^{-1}
SFCP - carbon to phosphorus ratio	45.0	45.0	45.0	mg C mg P^{-1}

SECTION 4

DEPOSIT FEEDER MODEL

4.1 INTRODUCTION

In estuarine and marine sediments, deposit feeders are a diverse collection of organisms, which include polychaete and oligochaete worms, crustacean arthropods, and bivalve mollusks. In addition to these diverse taxa, there are distinct feeding niches, often generalized as surface deposit feeders and deep deposit feeders. In this model framework, however, the natural diversity of deposit feeding has been collapsed into a single mode, simulating an infaunal, deposit feeding polychaete worm.

The suite of processes of a deposit feeder couples with the sediment diagenesis model essentially by reworking sediments, ingesting organic matter, creating biomass, and excreting respiratory endproducts into the pore water (Figure 4-1). Given this, there is no direct connection of deposit feeding activity with the water column or water quality model. Deposit feeding processes represent an additional pathway for processing sediment organic matter and as an additional source of pore water nutrients and of sediment oxygen demand (SOD). These variables, in turn, couple sediment diagenetic processes with the water column through fluxes across the sediment-water interface. Deposit feeder survival, however, is distinctly related to the food supply from the water column (represented as downward organic matter fluxes) and the near-bottom water column oxygen content (the source of respiratory oxygen). Thus, predictions of deposit feeder biomass are directly dependent upon the coupling of the sediment model with a water quality model. Described in this section is the development of a deposit feeder model as one aspect of a practical application of benthic-pelagic coupling employed in the CE-QUAL-ICM water quality model of the Chesapeake Bay.

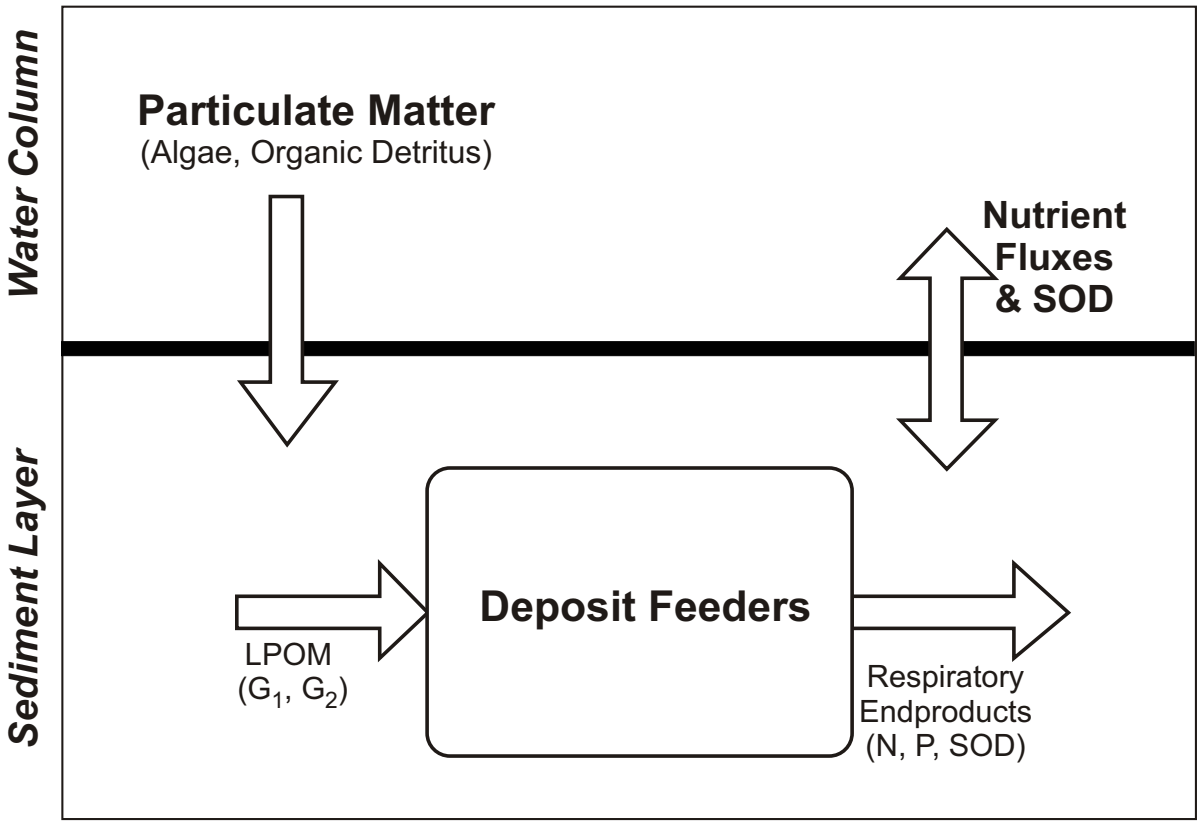

Figure 4-1. Schematic of deposit feeding polychaete submodel interactions with the water quality and sediment diagenesis models.

4.1.1 A Steady-State Analysis of Benthic Biomass and Organic Matter Flux

The roots of the present, time-dependent deposit feeder model can be found in the work of Thomann (1994) and of Kemp and Bartleson (1991; 1994). Motivating their efforts was a need to understand the quantitative relationships between water column primary production, particulate organic carbon flux to the sediments, sediment mixing and diagenesis, and benthic production. For the model of deposit-feeding macroinfaunal biomass, the starting point was Thomann's (1994) steady state analysis of biomass, sediment mixing, and particulate organic matter flux. The model contains two compartments, detrital organic carbon (C) and macrobenthic biomass (M) (Figure 4-2). The latter is assumed to be comprised of only deposit feeders. The processes represented are organic flux to the sediments (J_{POC}), deposit feeder ingestion (I) and assimilation (αI) (the difference between the two equaling the egestion of feces, which is recycled directly back into the detrital organic carbon pool, C), respiration and mortality, and loss of C via burial and diagenesis. The equations are as follows.

$$h\frac{dC}{dt} = J_{POC} - w_s C - hkC - \alpha IMC \qquad \textbf{(4-1)}$$

$$\frac{dM}{dt} = \alpha ICM - rM \qquad \textbf{(4-2)}$$

where

h = sediment mixed layer depth (m)

C = sediment organic carbon (g m^{-3})

J_{POC} = particulate organic carbon (POC) flux from overlying water (mg C m^{-2} d^{-1})

w_s = burial (or sedimentation) rate (m d^{-1})

k = diagenesis rate (d^{-1})

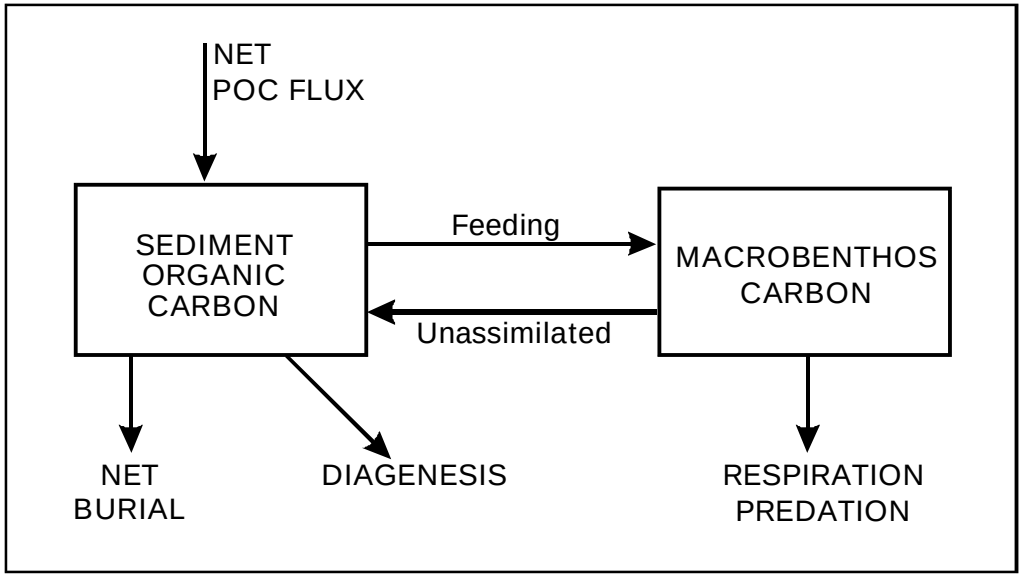

Figure 4-2. Two-compartment, steady-state macrobenthic biomass model (Thomann, 1994).

α = organic carbon assimilation efficiency

I = volumetric ingestion rate (L (mg M)$^{-1}$ d^{-1})

M = macrobenthic biomass (mg C m^{-2})

r = macrobenthic loss (respiration + predation) (d^{-1})

At steady state (dC/dt = dM/dt = 0), the above equations yield

$$C = \frac{r}{\alpha I} = \frac{r}{\alpha}\frac{1}{I} \quad \textbf{(4-3)}$$

and

$$M = \frac{J_{POC} - w_s C - hkC}{\alpha IC} \quad \textbf{(4-4)}$$

At steady state, the detrital sediment carbon fraction represented by C is directly proportional to the macrobenthic (living) carbon loss rate and inversely proportional to macrobenthic assimilation efficiency. This reflects the partitioning of total carbon within the sediments between living and non-living pools of this simplified, two-compartment model (Figure 4-2), under conditions of balanced organic matter influx, diagenesis, and burial.

From Equation 4-3, it can be shown that r = αIC, so that Equation 4-4 becomes

$$M = \frac{J_{POC} - w_s C - hkC}{r} \quad \textbf{(4-5)}$$

At steady state, macrobenthic carbon, M is determined by the net effect of sources and sinks of sediment organic carbon, scaled by the macrobenthic specific loss rate (respiration + predation).

In the context of eutrophication, food web dynamics, or benthic-pelagic coupling, values of J_{POC} can be defined by observations or by water quality model output, or estimated based on overlying water column productivity. To further simplify the model, observations from a variety of

environments suggest that sediment mixed layer depth, h and burial, w_s can be expressed as functions of benthic biomass and carbon flux, respectively (Thomann, 1994):

$$h = bM \quad \text{and} \quad w_s C = \gamma J_{POC} \qquad \textbf{(4-6)}$$

where b and γ are linear regression coefficients.

These state that (i) the sediment mixed layer depth, h is a function of benthic biomass, M, and that (ii) the burial flux of sediment organic carbon, w_sC is a function of the influx of particulate organic carbon from the overlying water column, J_{POC}.

Data from Lake Erie (Robbins et al., 1989) suggest that h is a linear function of M, such that b is a simple linear regression constant with a value of 0.0015 cm (mg macrobenthic C)$^{-1}$ m^{-2} (Thomann, 1994; Figure 4-3). It is a widespread observation that bioturbation is a significant factor in sediment mixing in habitats with moderate deposition rates and minimal physical disturbance, where deep deposit feeders dominate (McCall and Tevesz, 1982; Diaz and Schaffner, 1990).

The simplification for carbon burial is likewise assumed to be a linear function of the flux of particulate organic carbon from the overlying water. Examination of data from lacustrine, estuarine, and oceanic environments suggests that burial is approximately 10% of organic carbon influx; i.e., that γ = 0.1 (Thomann, 1994; Figure 4-4).

Application of the steady-state model, after specifying b and γ as described above, to a suite of data sets with J_{POC} of order 1-100 mg C m^{-2} d^{-1} gave a reasonable fit to observed benthic biomass (dashed line in Figure 4-5). In this range of organic matter input, benthic biomass was never saturated. However, inclusion of additional data with organic carbon fluxes in the range of 1000-10,000 mg C m^{-2} d^{-1} from the Los Angeles County Outfall Study suggested that the rate of increase of benthic biomass declines at high organic matter inputs (Figure 4-5). Competition among individual benthic organisms for space or increased predation loss at high prey biomass are two

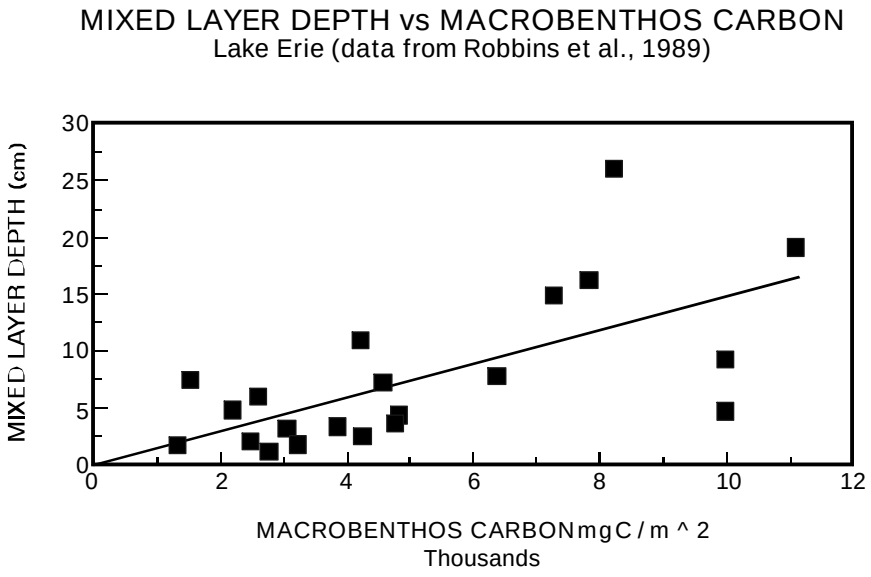

Figure 4-3. The relationship of sediment mixed layer depth to macrobenthos biomass (Thomann, 1994).

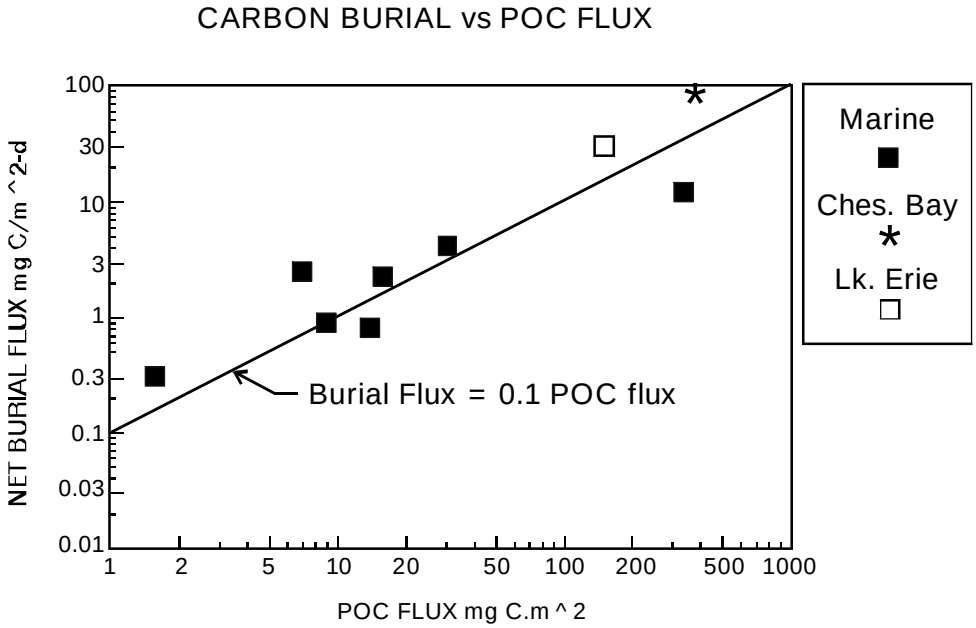

Figure 4-4. The relationship of burial flux to Particulate Organic Carbon (POC)flux(Thomann, 1994).

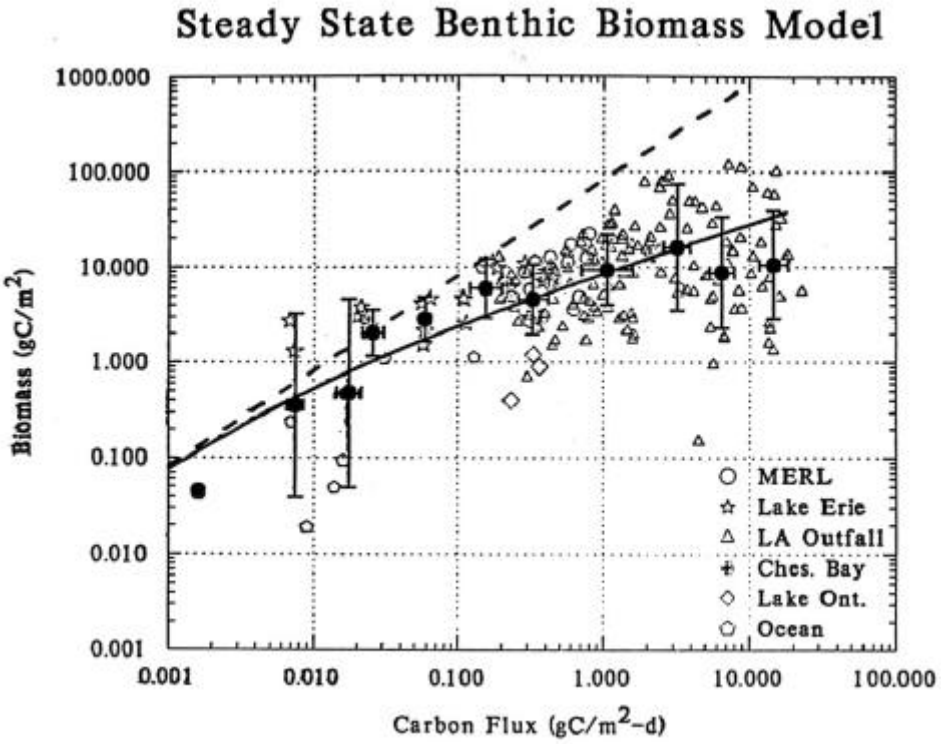

Figure 4-5. Predicted steady-state benthic biomass as a function of Particulate Organic Carbon (POC) flux.

factors that contribute to this relationship. In order to simulate this, a quadratic mortality term, $-\beta M^2$, was introduced to the steady state model of benthic biomass.

$$\frac{dM}{dt} = \alpha ICM - rM - \beta M^2 \qquad \textbf{(4-7)}$$

The separation of benthic losses into linear respiratory and quadratic predation terms has been applied successfully as well to time-dependent models of benthic-pelagic coupling (Kemp and Bartleson, 1991, 1994). The steady-state solution of Equation 4-7, using the simplifying assumptions given above for w_s and h, is

$$M = \sqrt{\frac{(1-\gamma)J_{POC}}{\beta r}\,\frac{\alpha I}{\alpha I + bk}} = \sqrt{\frac{M_{Linear}}{\beta}} \qquad \textbf{(4-8)}$$

where M_{Linear} is the solution of the benthic biomass equation with only the linear loss term (Equation 4-2).

Application of this steady state solution across a broad range of carbon fluxes showed an improved fit at high carbon fluxes (solid line, Figure 4-5), relative to the prediction from the linear-loss model (dashed line; Figure 4-5). Given the spread of the data, shown as standard error bars over binned ranges of carbon fluxes, the mortality rate coefficient controlling the quadratic loss term, specified here as 1×10^{-5} m^2 mg C^{-1} d^{-1}, could easily vary over a factor of 10. The performance of the model at lower carbon fluxes suggests that the intrinsic growth rates (involving ingestion and assimilation functions) were reasonably specified.

4.2 THE MODEL FRAMEWORK

The model simulates the areal biomass of deposit feeders in the sediment. The working units are mg C m^{-2}. To convert from carbon to ash free dry weight (AFDW), a more commonly reported unit for benthic infaunal biomass, multiply by 2, as AFDW is approximately 50% carbon. The state equation for deposit feeder biomass is:

$$\frac{dM}{dt} = \alpha_{G1} \frac{I_0}{m_2 \cdot 10^9} POC_{G1}\, k_{mn1}\, M + \alpha_{G2} \frac{I_0}{m_2 \cdot 10^9} POC_{G2}\, k_{mn2}\, M - rM - \beta M^2 - mM \quad \textbf{(4-9)}$$

where

M	=	areal biomass, mg C m^{-2}
α_{G1}	=	assimilation efficiency for G_1 (most labile) carbon
α_{G2}	=	assimilation efficiency for G_2 (labile) carbon
I_0	=	ingestion rate, mg (sediment ingested) mg C biomass^{-1} day^{-1}
m_2	=	sediment solids concentration, kg L^{-1}
POC_{G1}	=	G_1 sediment particulate organic carbon concentration, mg C m^{-3}
POC_{G2}	=	G_2 sediment particulate organic carbon concentration, mg C m^{-3}
k_{mn1}	=	Michaelis-Menton growth limitation term for G_1 carbon
k_{mn2}	=	Michaelis-Menton growth limitation term for G_2 carbon
r	=	respiration rate, d^{-1}
β	=	predation rate, m^2 mg C d^{-1}
m	=	hypoxia mortality rate, d^{-1}

Note the units conversion 10^9 which takes sediment solids concentration in kg L^{-1} and converts it to mg m^{-3} as follows:

$$\frac{mg}{m^3} = \frac{kg}{L} \bullet \frac{1000g}{1kg} \bullet \frac{1000mg}{1g} \bullet \frac{1000L}{1m^3} = \frac{kg}{L} \bullet 10^9 \quad \textbf{(4-10)}$$

Also note that only the labile organic matter pools are considered available for assimilation. Labile particulate organic nitrogen (PON) and particulate organic phosphorus (POP) are consumed in proportion to their stoichiometric requirements in the deposit feeder model (see below). It is assumed

that refractory organic matter is not available and will pass straight through the organism unaffected. While it is possible that some benthic organisms receive some nutritional value from dissolved organic matter, this is not considered significant to the overall fauna, and is not modeled here. As indicated in Figure 4-1, respiratory endproducts (regenerated inorganic nutrients) are added to sediment pore waters and oxygen demand is added to the sediment diagenesis model's sediment oxygen demand (SOD) term, which couples with bottom water oxygen concentrations predicted by the water quality model. The various terms comprising the state equation are defined below.

4.2.1 Ingestion Rate

Ingestion rate is a function of temperature and of sediment organic content. The temperature dependency uses the classic Arrhenius formulation:

$$I_0 = I_{20}\theta_I^{T-20} \qquad \textbf{(4-11)}$$

Ingestion rate, which is expressed in units of total sediment mass, declines as sediments become richer in organic matter. This is controlled by an reciprocal hyperbolic relationship (a reciprocal Monod function), as follows, for the G1 carbon pool and similarly for the G2 pool:

$$k_{mn1} = \frac{K_1}{K_1 + POC_1} \qquad \textbf{(4-12)}$$

4.2.2 Loss Functions: Respiration, Predation, and Mortality

Both the respiration and predation rates have Arrhenius temperature dependencies:

$$r = r_{20}\theta_r^{T-20} \quad \textbf{(4-13)}$$

$$\beta = \beta_{20}\theta_\beta^{T-20} \quad \textbf{(4-14)}$$

The polychaetes are a diverse group, occupying a variety of feeding guilds, habitats, and even vertical zones within sediment layers, their sensitivity to hypoxia varies. Larger, deeper-dwelling forms are replaced by smaller, near-surface forms under a variety of physical disturbances, including hypoxia. While generally more sensitive to moderate hypoxia than estuarine bivalves, individual taxa can still be found to occupy hypoxic waters, though at reduced biomass. Thus, while the time to death parameterization used here is the same as that for the bivalve suspension feeders, mortality begins to occur at somewhat higher dissolved oxygen levels, while feeding and aerobic respiration rates are depressed. As in the suspension feeder model, a logistic function, Z is used to model the impact on these processes as dissolved oxygen levels decline (Figure 4-6).

$$Z = \frac{1}{1 + \exp(1.1 \cdot \frac{DO_{hx} - DO}{DO_{hx} - DO_{qx}})} \quad \textbf{(4-15)}$$

where

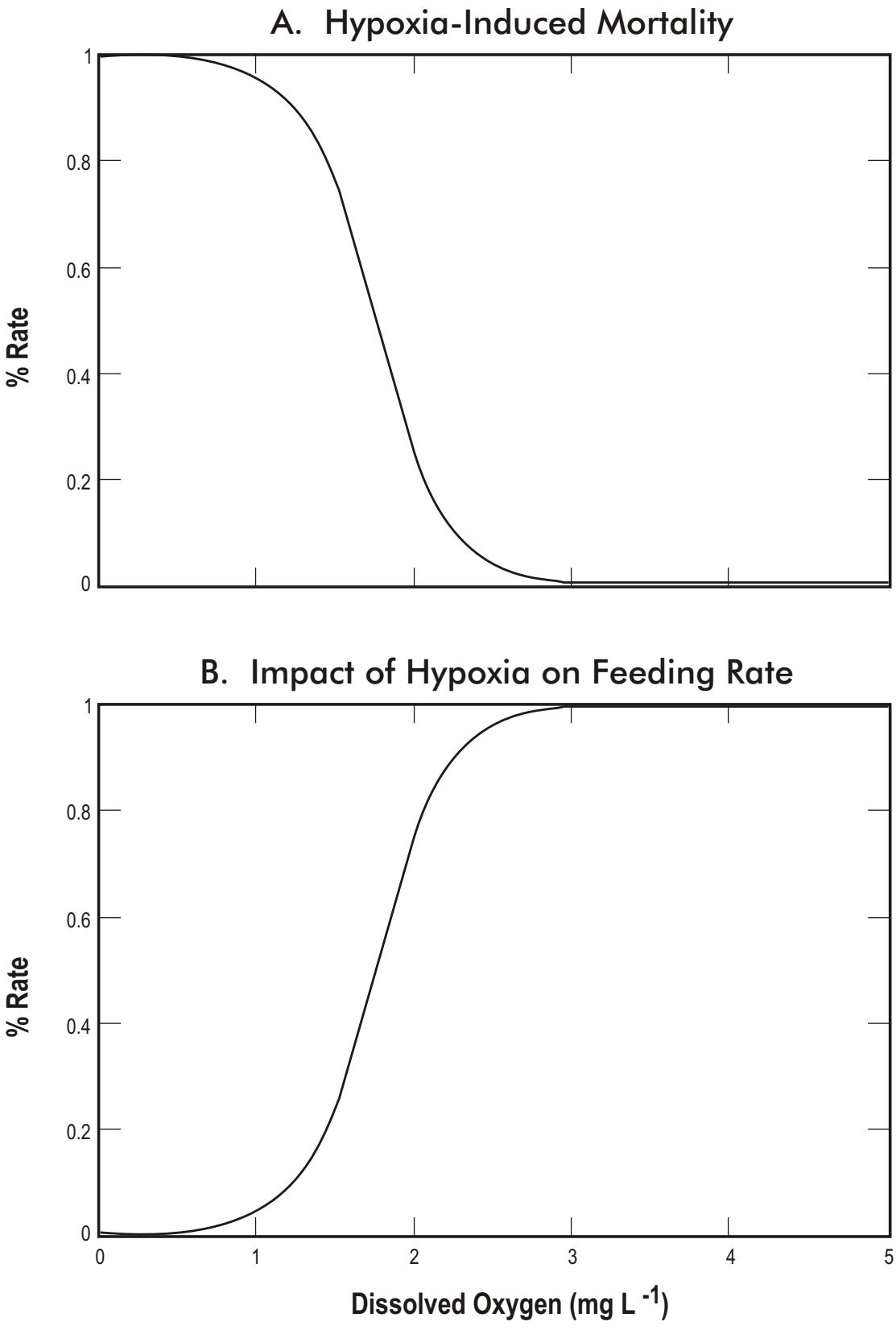

Figure 4-6. Logistic functional response of A. Mortality rate and B. Feeding rate to bottom water dissolved oxygen for modeled deposit feeders.

DO = overlying water dissolved oxygen concentration, mg/L

DO_{hx} = DO at which function is 50% of its maximum

DO_{qx} = DO at which function is 25% of its maximum

The mortality rate, m as a function of DO and the intrinsic mortality rate, r_d (day^{-1}) is computed as:

$$m = r_d \bullet (1 - Z) \quad \textbf{(4-16)}$$

The intrinsic mortality rate is derived assuming a time-to-death, t_d (day) for 99% of the population by:

$$r_d = \frac{\ln(1/100)}{t_d} \quad \textbf{(4-17)}$$

The parameters used are given in Table 4-1. The logistic function is also used to shape the response of ingestion and aerobic respiration rates (Figure 4-6), which both decline with declining DO:

$$I_0 = I'_0 \bullet Z, \quad r = r' \bullet Z \quad \textbf{(4-18)}$$

where I'_o and r' are the injestion and respiration rates before considering hypoxic effects.

Predation by benthivorous fish and crustaceans (e.g., crabs, shrimp) declines under reduced oxygen concentrations as well. This begins to occurs at DO levels above the traditional hypoxic metric of 2.0 mg L^{-1}, as more sensitive fish species move out of low oxygen water. Thus, benthos actually may have a refuge from predation under mildly hypoxic conditions (Nestlerode and Diaz, 1997). A description of this declining predation pressure is achieved using a rectangular hyperbolic formulation:

$$\beta = \beta' \frac{DO}{DO + K_{DO}} \quad \textbf{(4-19)}$$

where β' is the predation rate before considering hypoxic effects.

Note that in the simulation, biomass is never permitted to reach exactly zero, as this would preclude regrowth after the hypoxia/anoxia event has passed. A lower limit of 0.1 mg m^{-2} was used as a refuge level of biomass in the absence of a recruitment model from which to seed new growth once favorable conditions returned.

4.3 ADJUSTMENT OF PARTICULATE POOLS

As mentioned previously, the assimilation of labile organic matter is a loss to the particulate pools and must be accounted for. On the other hand, any predation losses are added back to the particulate pools. Without consideration of deposit feeding processes, (Di Toro and Fitzpatrick, 1993), the mass balance equation for the G_1 particulate organic carbon (POC_1) in the sediment is as follows:

$$H\frac{d(POC_1)}{dt} = J_C - w_s POC_1 - K_{POC_1} POC_1 H \quad \textbf{(4-20)}$$

where

H	=	sediment active layer depth, m
J_C	=	flux of POC_1 to sediment, mg m^{-2} d^{-1}
w_S	=	sedimentation velocity, m d^{-1}
K_{POC1}	=	diagenesis reaction rate, d^{-1}

The modification of the above solution to include deposit feeders results in:

$$H\frac{dPOC_1}{dt} = J_c - W_s\,POC_1 - K_{POC_1}\,POC_1\,H - \alpha_{G1}\frac{I_O}{M_2}POC_1\,M + f_{POC_1}\left(mM + \beta M^2\right) \quad (4\text{-}21)$$

where

f_{POC1} = G_1 fraction of labile carbon, $(G_1/(G_1+G_2))$

For particulate nitrogen and phosphorus, the only modification to the organic matter diagenesis equation is the inclusion of the organism's stoichiometric ratio, carbon:nitrogen or carbon:phosphorus.

4.4 RESPIRATION LOSSES

The organism will respire its organic mass to CO_2 (not modeled), NH_4, and PO_4 via aerobic metabolic pathways which consume oxygen. The oxygen consumption is added to the model's computation of SOD (otherwise, from sediment organic matter diagenesis and chemical oxygen demand) directly:

$$SOD = SOD + 2.667 \cdot r\,M \quad \textbf{(4-22)}$$

The units of SOD are g O_2 m^{-2} d . The conversion factor appears because the oxidation of 1.0 g of carbon requires 2.667 g of oxygen.

Metabolically-generated NH_4 and PO_4 are added to the diagenesis flux of inorganic nitrogen and phosphorus generated by the decay of sediment organic matter. The sediment model then uses

these terms in the computation of solid and pore water phase inorganic nitrogen and phosphorus concentrations. Ultimately, deposit feeder respiratory end-products couple with sediment-water nutrient fluxes, which are driven by the nutrient gradient across the sediment-water interface and the interfacial mass transfer coefficient (Di Toro and Fitzpatrick, 1993; Di Toro, 2000).

Table 4-1. Constants Used on the Deposit Feeder Model

Constant	Value	Units
I_{20} -base ingestion rate	175.0	mg sed (mg C biomass^{-1}) d^{-1}
Θ_I - ingestion temperature coefficient	1.08	-
r_{20} -base respiration rate	0.015	d^{-1}
Θ_{r} - respiration temperature coefficient	1.08	-
β_{20} - base predation rate	2.0e-4	m^2 mg C^{-1} d^{-1}
Θ_β - predation temperature coefficient	1.24	-
CN - carbon/nitrogen ratio	5.67	-
CP - carbon/phosphorus ratio	45.0	-
α_{G1} - G_1 carbon assimilation	0.8	-
α_{G2} - G_2 carbon assimilation	0.5	-
K_1 - G_1 ingestion limitation	1.0e+5	mg C m^{-3}
K_2 - G_2 ingestion limitation	1.0e+6	mg C m^{-3}
K_{DO} - predation DO half-saturation	2.25	mg L^{-1}
t_d - time in days for 99% anoxic mortality	14.0	days
DO_{hx} - logistic DO constant	1.75	mg L^{-1}
DO_{qx} - logistic DO constant	1.50	mg L^{-1}

SECTION 5

CALIBRATION OF THE BENTHOS MODEL

5.1 INTRODUCTION

The benthos model was calibrated using the updated Chesapeake Bay Water Quality Model (CBWQM), which is based on the U.S. Army Corps of Engineers' CE-QUAL-ICM. Improvements in the overall modeling package (hydrodynamics, watershed, and the CBWQM) over the previous version (Cerco and Cole, 1993, 1994) include the following enhancements:

- increased hydrodynamic and water model grid resolution from 4073 cells total, 729 in the horizontal plane (4k grid) to 10,196 total cells and 2100 horizontal cells (10k grid), including explicit hydrodynamic simulation of the adjacent continental shelf,

- improved treatment of turbulence in the hydrodynamic model,

- updated treatment of light attenuation and photosynthesis-light relationships for the algal components of the model,

- improved living resource simulation with the explicit simulation of two size classes of zooplankton, addition of submersed aquatic vegetation (SAV), and

- refined and updated watershed model delivering point source and nonpoint source loads to the water quality model.

Management-based scenarios called for 10-year simulations, covering the period 1985 through 1994. However, in order to tractably handle a problem of this size, preliminary calibration was performed using hydrodynamic and loading information for the simulation year 1987 only. During calibration,

the model was run for three model years, repeating the 1987 information for each year. As conditions within the sediments can take years to reach equilibrium, in some cases, the model was run for six years. Sensitivity analysis based on load inputs was performed by altering loads relative to the 1987 base case. Final calibration was performed with 10-year simulations, using the full 10-year simulations of hydrodynamics and watershed loads based on realistic hydrologic conditions. These simulations were performed by U.S. Army Corps of Engineers' Waterways Experiment Station personnel on a Cray T3E supercomputer. Details of the watershed, hydrodynamic and water quality components of these simulations are reported elsewhere.

Calibration of the benthos model was based on comparisons of computed versus observed biomass of deposit and suspension feeders. Comparisons were made by examination of time series and probability distributions using data primarily from the fixed-station surveys of the Chesapeake Bay benthic monitoring program (discussed in Section 1) with co-located model grid cells (Figure 2-2). Model-data comparison locations are referenced by their Chesapeake Bay Program Segment name (1985 version), which divides the estuarine habitats primarily by their salinity characteristics. The benthic monitoring program database also contains bottom water dissolved oxygen measurements taken at the same time as the benthic samples. These data were plotted against the model-predicted bottom-layer dissolved oxygen in order to clarify responses of both observed and simulated benthic biomass to dissolved oxygen concentrations. Bottom water dissolved oxygen is a complex yet robust indicator of water column productivity, hydrodynamics, and carbon loadings to the benthos. It should be noted that, while similar sampling techniques were used, this oxygen data set is not the same as the water quality monitoring program oxygen data set used in calibration of the water quality model.

5.2 BENTHIC BIOMASS RESPONSE TO WATER QUALITY

Benthic biomass simulation within the mainstem bay is illustrated for the northern bay, by a cross-bay transect in the middle of the bay, and for the southern bay. Monitoring of fixed sites (long-term monitoring at a fixed location) in the far northern bay (Chesapeake Bay Program Segments CB1

and CB2) is very limited; there were no fixed stations on the Susquehanna Flats (CB1). The utility of the data set was further reduced because biomass determinations, which were not performed at all sites and times, were noticeably lacking at locations within CB2.

Figure 5-1 illustrates results at monitoring sites and model cells along a north-south line through CB2, CB3, and the northern portion of CB4. Bottom water dissolved oxygen concentrations in both the model and the benthic monitoring program suggest that there may be some problems associated with periodic summertime hypoxia in CB4. From limited data within CB2, but extensive data at the location within CB3, it is apparent that the benthos model underpredicted suspension feeder biomass by at least ten-fold. In the northern portion of CB4, mean simulated suspension feeder biomass (3.8 g AFDW m^{-2}) was approximately half of the observed mean (8.5 g AFDW m^{-2}). The spatial trend in the data suggests that suspension feeder biomass declines from north to south in this region, though the model predicted that CB3 had greater biomass than either CB2 or CB4. The water quality model, however, predicted higher bottom water POC in CB3, relative to that in either of the CB2 or CB 4 sites, such that suspension feeder growth rates were highest in CB3 (Figure 5-2).

Deposit feeder biomass appears to have been oversimulated in CB3 (Figure 5-1). In CB4, the modeled dissolved oxygen concentration during summers from 1989 through 1992 falls within the range of hypoxic sensitivity for the deposit feeders. Slight increases or decreases in the simulated oxygen concentration near the onset of hypoxia (2 mg L^{-1}) dramatically altered the predicted survival of deposit-feeding biomass through the summer months, which is evident in comparing results for the years 1989-1992 with 1993 and 1994.

The mid-bay transect consisted of three stations from just north of the Patuxent River mouth on the western shore (model grid cell 843), through the middle of the bay (cell 750) and across to the eastern shore (cell 570) (Figure 5-3). The water quality model simulated summer hypoxia in 1989 and later years along the western side and in the middle of the bay. The Benthic Monitoring

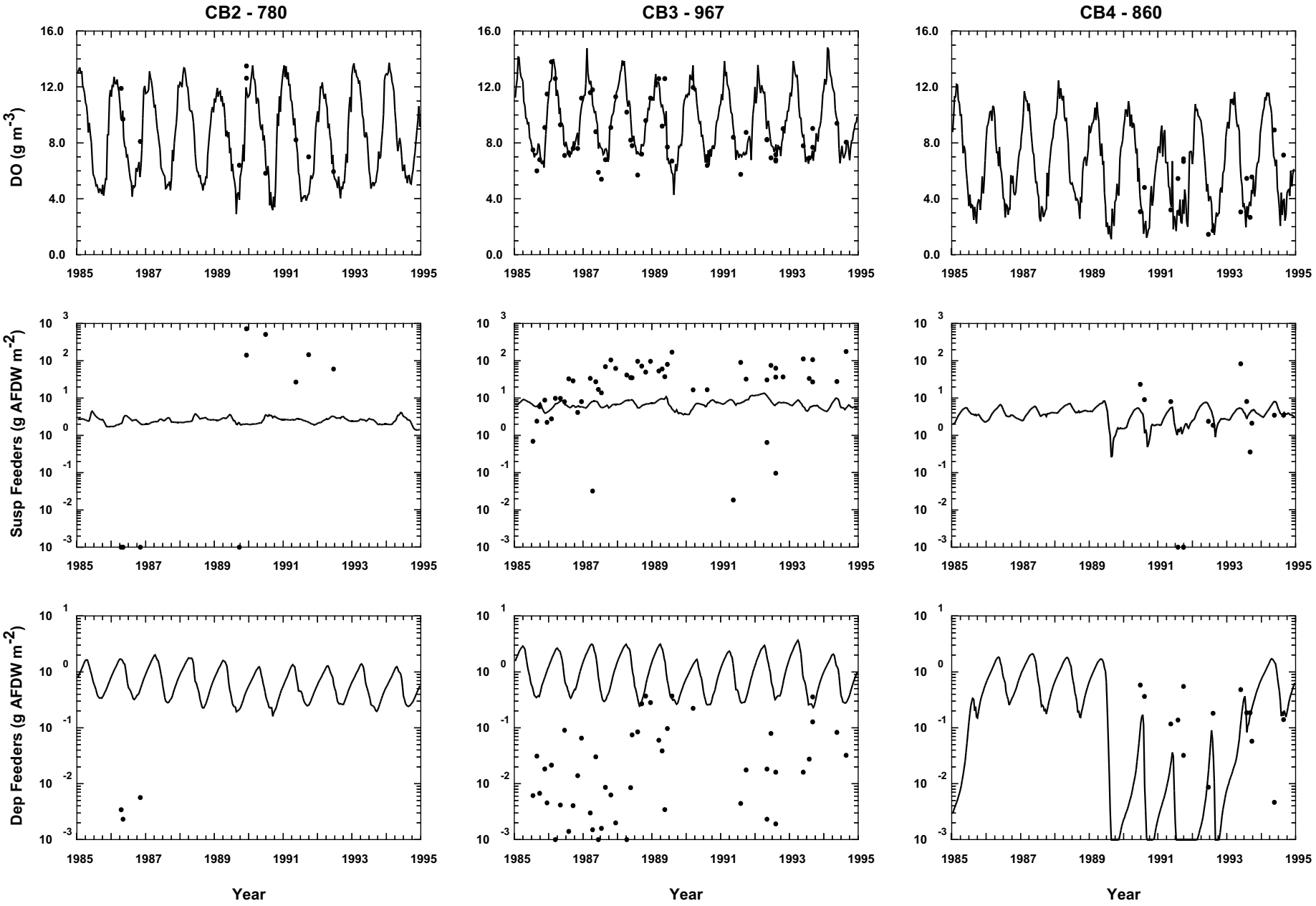

Figure 5-1. Time series of bottom water dissolved oxygen (DO), and of suspension feeder and deposit feeder biomass in the northern Chesapeake Bay. Data are from the Chesapeake Bay Benthic Monitoring Program. Model results are ten-day averages from the 10k-grid Chesapeake Bay Water Quality Model with base case loads.

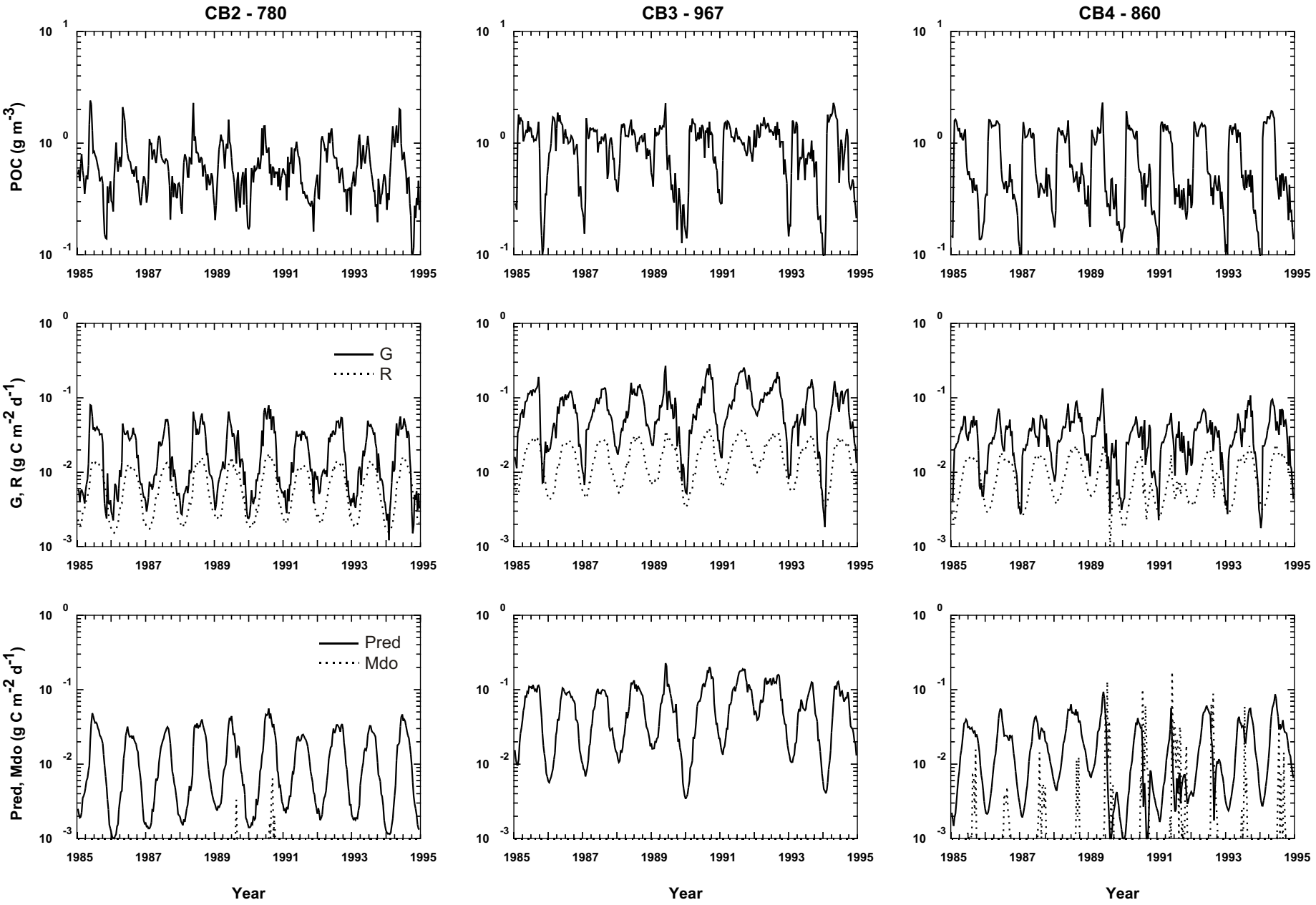

Figure 5-2. Modeled particulate organic carbon flux (Jpoc), labile sediment organic content, and deposit feeder sources and sinks (G-growth, R-respiration, Pred-predation, Mdo-hypoxic mortality) in the northern Chesapeake Bay.

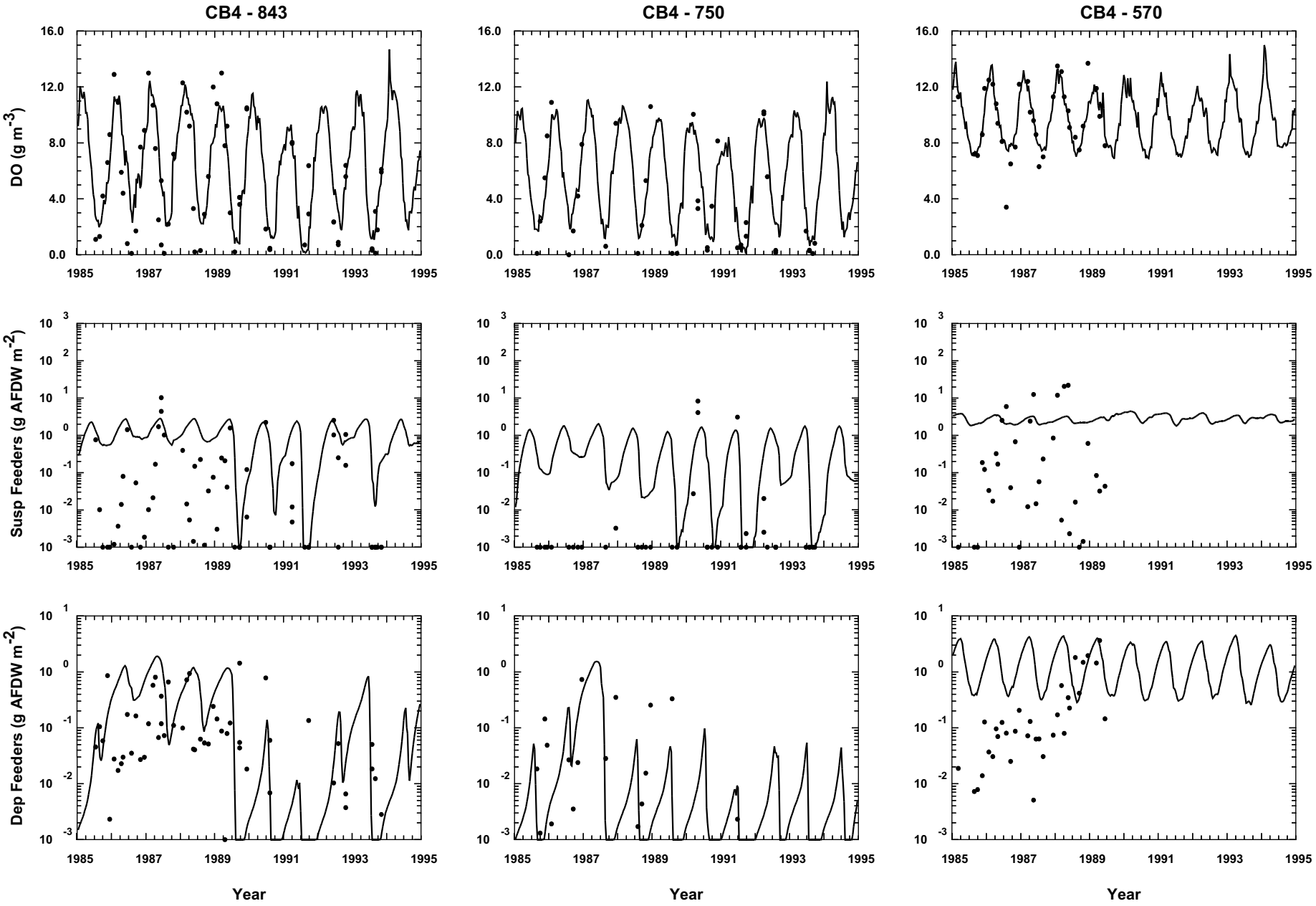

Figure 5-3. Time series of bottom water dissolved oxygen (DO), and of suspension feeder and deposit feeder biomass in the mid Chesapeake Bay. Data are from the Chesapeake Bay Benthic Monitoring Program. Model results are ten-day averages from the 10k-grid Chesapeake Bay Water Quality Model with base case loads.

Program bottom water oxygen data suggest that summer hypoxia and anoxia occurred in the mid-1980s in these regions, as well. Bottom water oxygen conditions, in both the simulation and the observations were much better along the eastern shore in this region. Variability in the observed benthic biomass make it difficult to assess seasonal trends, or perhaps even the magnitude of biomass for comparison with the modeled results. Interannual maximum for suspension feeder and deposit feeder biomass were reasonably simulated along at the western site. Both observed and simulated benthic biomass values were highest at the eastern site. There appeared to be an improving trend in observed deposit feeder biomass while the model simulated relatively consistent seasonal cycles from year to year in the eastern site. At the western site, declining summer oxygen conditions simulated for the period 1989-1992 resulted in depleted deposit feeder biomass. Reduced sampling frequency at this site during this time period, however, make it difficult to assess whether there was a similar trend in the observed values.

In Figure 5-4, three sites are shown for the lower bay. Bottom water dissolved oxygen concentrations were generally favorable for benthic fauna. The water quality model simulated one hypoxic/anoxic period during the late summer of 1991 that led to the demise of both the deposit and suspension feeding fauna, a circumstance not evident in either the dissolved oxygen or the biomass data. Suspension feeding biomass appears to have been overpredicted in the southern bay. It is likely that there are habitat-related factors such as sediment type which were not included in the model which preclude suspension-feeding bivalve growth of the level modeled here. Conversely, while the magnitude of deposit feeder biomass was reasonably simulated at the CB5 site, growth was insufficient to match the observed biomass at sites further south in the polyhaline portion of the bay.

Sample time series of benthic biomass and rates from a ten-year base case simulation are shown for locations in four major tributaries. In Figure 5-5, results from the three major salinity regimes within the Potomac River (TF2--Tidal Fresh; RET2--River-Estuarine Transition; LE2--Lower Estuarine) illustrate the range of benthic responses and the impact of hypoxia. In the upper tidal freshwater (TF2) and oligohaline (RET2) sites examined here, bottom water DO always exceeded 4.0 mg L^{-1}. Suspension feeding bivalve biomass at these sites, as observed and simulated,

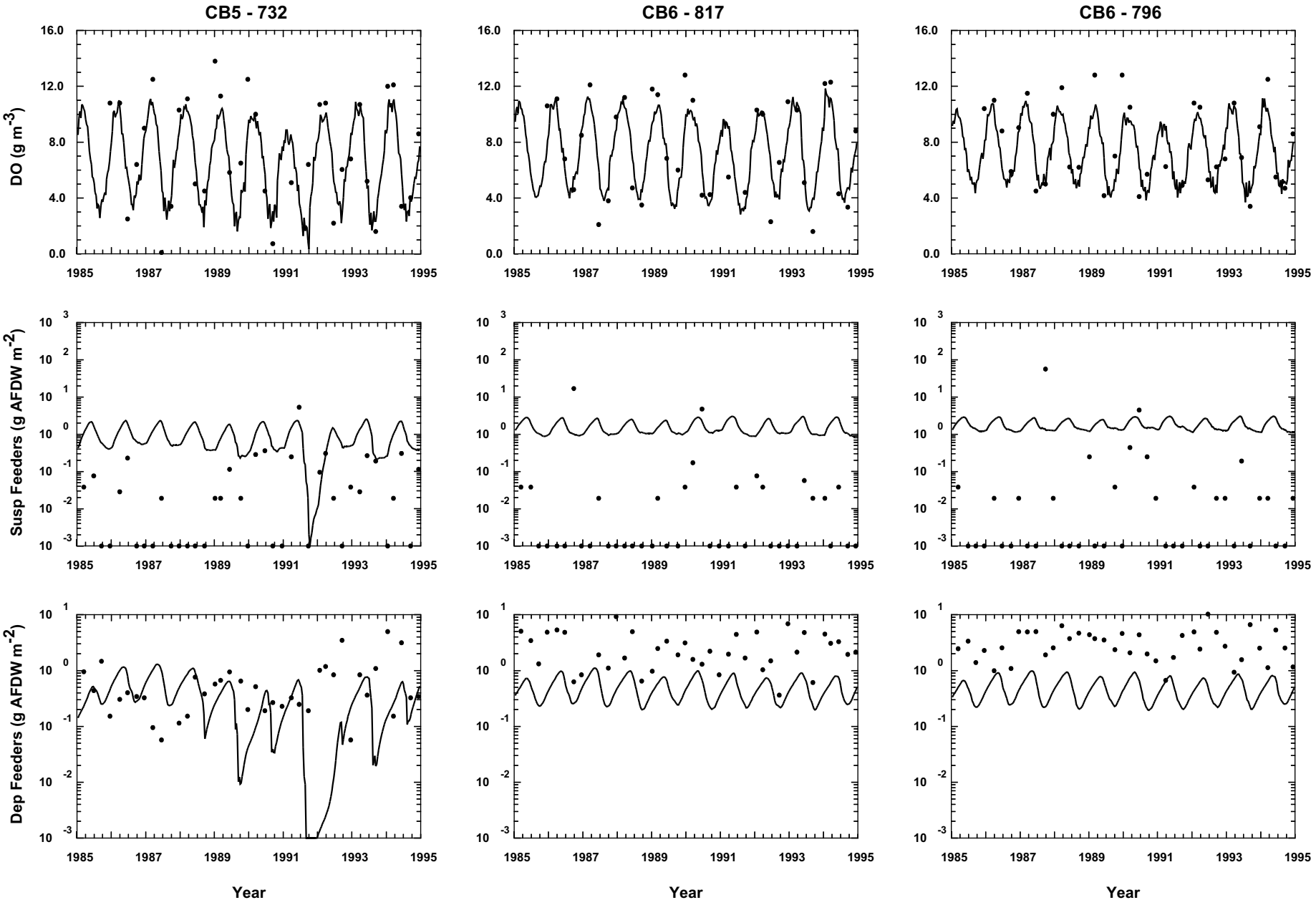

Figure 5-4. Time series of bottom water dissolved oxygen (DO), and of suspension feeder and deposit feeder biomass in the southern Chesapeake Bay. Data are from the Chesapeake Bay Benthic Monitoring Program. Model results are ten-day averages from the 10k-grid Chesapeake Bay Water Quality Model with base case loads.

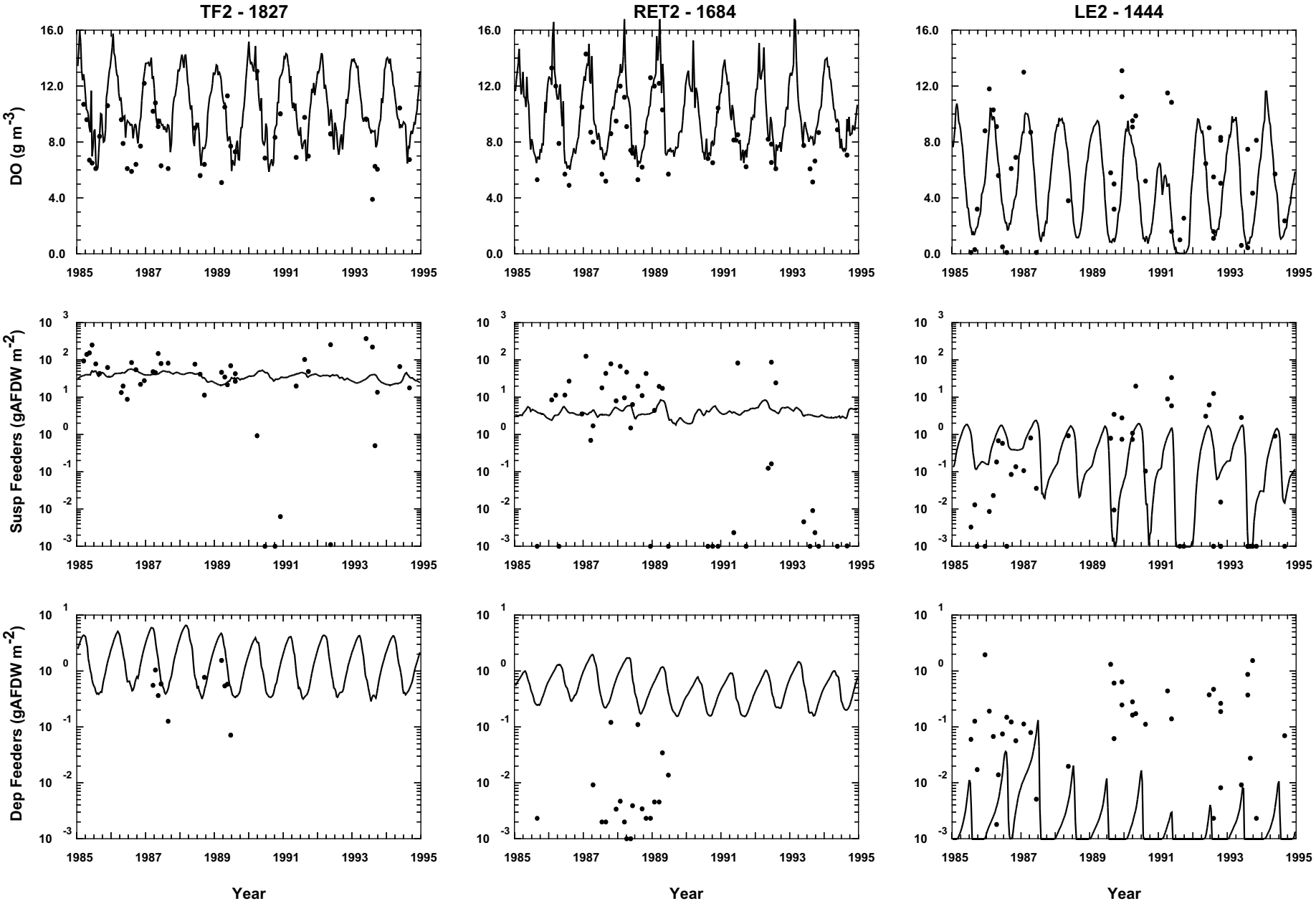

Figure 5-5. Time series of bottom water dissolved oxygen (DO), and of suspension feeder and deposit feeder biomass in the Potomac River. Data are from the Chesapeake Bay Benthic Monitoring Program. Model results are ten-day averages from the 10k-grid Chesapeake Bay Water Quality Model with base case loads.

was both high and stable from year to year. Data from later years (1990+) exhibit greater year to year variability in biomass (but not in oxygen). While the model is capable of simulating broad trends in the range of biomass in both time and space, it cannot match the high bivalve biomass (>100 g AFDW m^{-2}) observed at stations within TF2 and RET2. Simulated deposit feeder biomass at these sites is quite high, ca. 1 and 0.4 g AFDW m^{-2} in TF2 and RET2, respectively, in comparison to the relatively sparse data for this fauna. Oxygen and food (see below) are in relative abundance with regard to modeled processes; this suggests that unresolved phenomena or dynamics, such as sediment characteristics, competition for space with bivalves, and/or site-specific predation may be influencing observed biomass.

In a deep site in the lower reach of the Potomac (LE2), bottom waters experience periodic hypoxia/anoxia during the summer. Summertime simulated bottom water DO was regularly less than 2 mg L^{-1}, often less than 1 mg L^{-1} in the 1990s, and in 1991, anoxia occurred (Figure 5-5). Hypoxic and anoxic events were evident in the benthic monitoring program at these sites as well. In the model, such conditions clearly stressed the more sensitive deposit-feeding fauna as well as the bivalve fauna. In the simulation, the less sensitive suspension feeders were able to persist and recover from seasonal hypoxia in this region. The modeled deposit feeder assemblage, however, was unable to recover from near-collapse during summer hypoxia to the observed biomass levels, especially during the 1990s. The lack of explicit benthic recruitment pulses from pelagic larval pools in the simulation may be one reason why modeled benthic biomass experiencing seasonal hypoxia never recovers to observed levels.

Results from the estuarine transitional zones of the Rappahannock (RET3), York (RET4) and James (RET5) rivers further illustrate the model's ability to capture some of the dynamics observed in benthic biomass (Figure 5-6). With the exception of one modeled hypoxic event at RET3 during summer 1991 (not observed in the data), these sites have favorable bottom water DO conditions (rare apparent anoxic events in the data are "no-observation" data points, rather than reflecting true anoxia). While deposit feeder biomass on the order of 0.1-1.0 g AFDW m^{-2} is well simulated, the

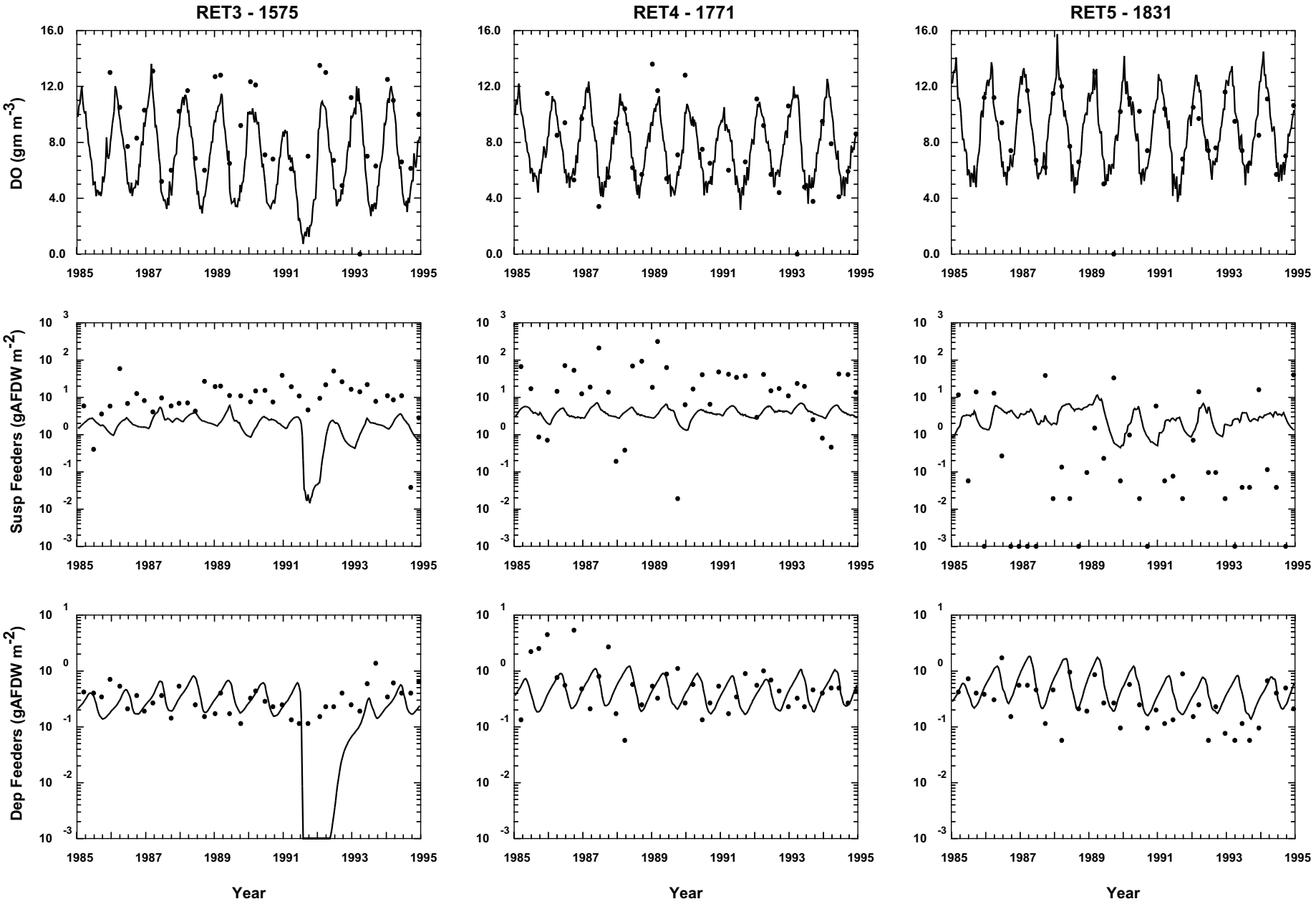

Figure 5-6. Time series of bottom water dissolved oxygen (DO), and of suspension feeder and deposit feeder biomass in the middle reaches of the Rappahannock (RET3), York (RET4) and James (RET5) Rivers. Data are from the Chesapeake Bay Benthic Monitoring Program. Model results are ten-day averages from the 10k-grid Chesapeake Bay Water Quality Model with base case loads.

model underestimates suspension feeder in RET3 and RET4 by a factor of five- to ten-fold. Highly variable data in the mid-James River (RET5) make it difficult to assess model versus observation.

The seasonal hypoxic event simulated in the model at RET3 shows the sensitivity of modeled benthos to bottom water DO. While the less sensitive suspension feeders were able to recover to pre-impact levels by the following summer, the collapse of the deposit feeders required a second year before reaching pre-impact biomass levels. This may suggest that deposit feeder production (net growth) rates are too low in the model. However, the similarity in seasonal ranges in biomass between observations and model during unimpacted years suggests that modeled estimates of production are reasonable. Again, it is likely that recruitment processes involved in post-hypoxia benthic recovery, presently not modeled, will need to be simulated in the future.

5.3 BENTHIC INFAUNAL GROWTH AND LOSS RATES

Further understanding of the dynamics of the coupled, water quality-benthos model can be gleaned by examining time series of growth and loss (respiration, predation, mortality) factors governing deposit and suspension feeder biomass predictions. As noted above in the descriptions of both model frameworks, vital rates (e.g., ingestion/filtration, respiration, predation) have strong temperature dependancies. Typically, biochemical rates approximately vary by a factor of two with a ten degree centigrade change in temperature, all other factors being equal. Intrinsic predation rate was modeled with a much stronger temperature dependency to simulate the general abundance and activity of predators during summer across the entire estuarine system, and conversely, a lack of predation during winter. Also embedded in the seasonal dynamics of the model is the impact of freshwater flows into the estuary. Seasonal and interannual variations in loads affects the delivery of organic matter, inorganic solids, and nutrients, which determine water column primary production and the supply of solids to the sediments and food to the benthos.

The modeled deposit feeding fauna exhibit greater response to such seasonal variability than do the suspension feeders. For example, looking at the same segments within the Potomac River as

before, carbon flux to the sediments, Jpoc has a strong seasonal cycle, while labile organic matter in the sediments exhibits a similar albeit muted signal, representing the dynamics of food available to the deposit feeders (Figure 5-7). Deposit feeder growth and biomass is limited and diminished in summer months by strong predatory control, and to a lesser extent, by increased respiration and decreased food (Figure 5-7). Overall, in the absence of hypoxic impacts within TF2 and RET2, deposit feeder biomass is controlled by the availability of labile sediment carbon, which declines downstream in the illustrated sites along the Potomac (Figure 5-7). Simulated deposit feeder biomass and production is extremely low within the deeper portions of LE2 as a result of strong seasonal hypoxia.

On the other hand, with respect to seasonal cycles, the present simulation of suspension feeding processes yields biomass results which are much less fluctuating, unless impacted by seasonal hypoxia. Modeled suspension feeder biomass within TF2 and RET2 varied annually by less than an order of magnitude (Figure 5-5). Observed suspension-feeding bivalve biomass at these locations similarly varied by five- to ten-fold and occasionally by several orders of magnitude. In the case of suspension feeders, growth mediated by food supply (represented by bottom water POC, which includes algal carbon) and respiratory loss control much of the annual cycle, along with predation loss during summer (Figure 5-8). Ultimately, modeled biomass is sensitive to food supply; peaks in growth and biomass correspond with peaks in POC. There are periods in the simulation where sharp declines in POC brought about by reduced primary production and clearance by suspension feeders resulted in greatly reduced growth rates, often below levels of respiration. Food limitation at various points in time and space is apparent in the model under nominal loading conditions.

The impact on the modeled suspension feeders of food supply from the overlying water column is further apparent when examining results from the Virginia tributaries. Simulated bottom water carbon concentrations are lower in the estuarine transition reaches of the Rappahannock and

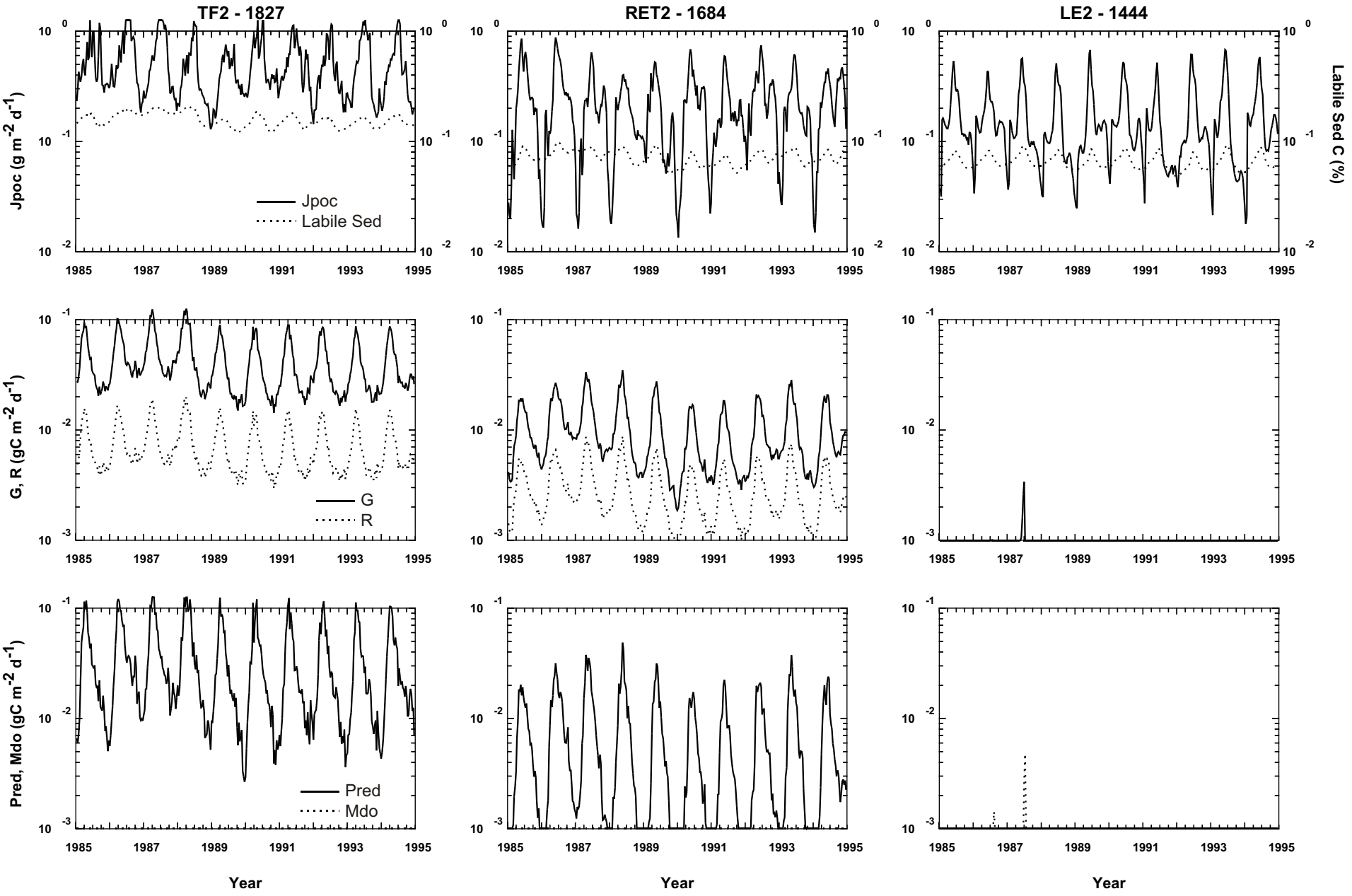

Figure 5-7. Modeled particulate organic carbon flux (Jpoc), labile sediment organic content, and deposit feeder sources and sinks (G-growth, R-respiration, Pred-predation, Mdo-hypoxic mortality) in the Potomac River.

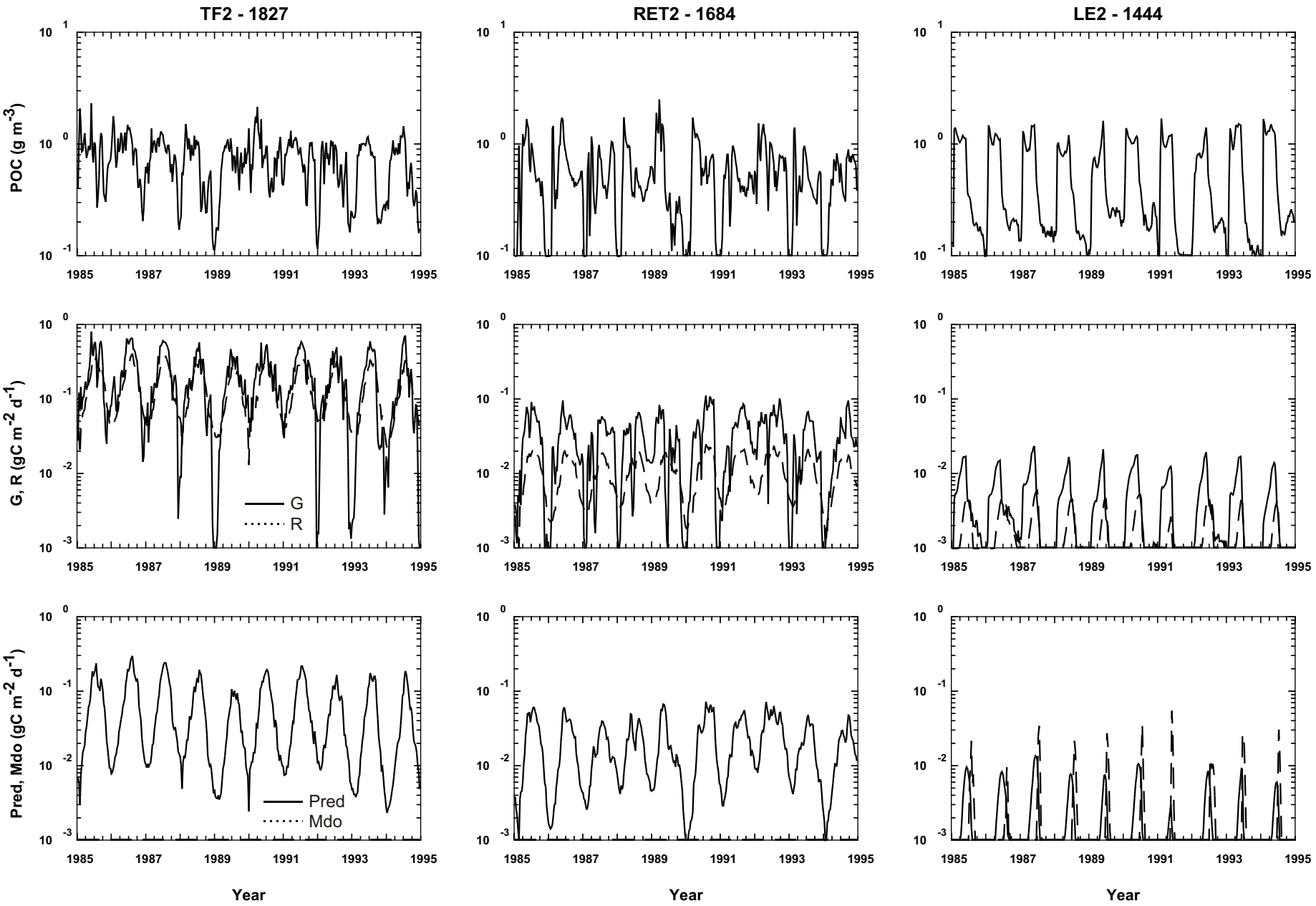

Figure 5-8. Modeled bottom water particulate organic carbon concentration (POC), and suspension feeder sources and sinks (G-growth, R-respiration, Pred-predation, Mdo-hypoxic mortality) in the Potomac River.

York Rivers (RET3 and RET4, respectively) than in the Potomac River (Figures 5-9, 5-8). This applies to both the spring bloom period as well as during the post-bloom early summer, vital periods for bivalve growth. High solids concentrations in RET3 and RET5 also negatively affect suspension growth (Figure 5-10).

Annual maximum deposit feeder biomass in the transitional zones of the Virginia (Figure 5-6) tributaries increased with increasing labile sediment carbon (Figure 5-11). This pattern was seen spatially, with sediment organic carbon content increasing from the Rappahannock to the James and also temporally, with more sustained carbon fluxes reaching the bottom of the James during the late 1980s in the simulation which yielded higher deposit feeder biomass during the same period in comparison with the early 1990s (Figure 5-6). Improving benthic biomass in the simulation between 1986 and 1990 is similar to improving trends within RET5 determined from the monitoring program data set (Dauer and Alden, 1995).

5.4 BENTHIC BIOMASS PROBABILITY DISTRIBUTIONS

The benthos model is sensitive to the water quality model's simulation of spatial and interannual differences in solids concentration, primary production, bottom water dissolved oxygen, and the delivery of food to the benthos as seen in these time series. Nevertheless, variability in the benthic biomass observations appears to be much greater than that of the model. Another way to express this and to assess the model is to compare the distributional properties of modeled and observed biomass in a probability plot. In the following figures, observed and modeled biomass for suspension and deposit feeders were aggregated by season (spring and summer) and the lognormal cumulative frequency distributions of model (open symbols) and data (filled symbols) were compared. Lognormal distributions are common in benthic data sets (Elliot, 1977). As noted in the time series, and evident in the figures which follow, where the water quality model predicted a relatively unimpacted environment with respect to low dissolved oxygen stresses, simulated variability of the benthos was low and benthic biomass was stable. In the simulation, where hypoxic events occurred (summertime hypoxia in LE2 and the one simulated event in RET3 for the sites

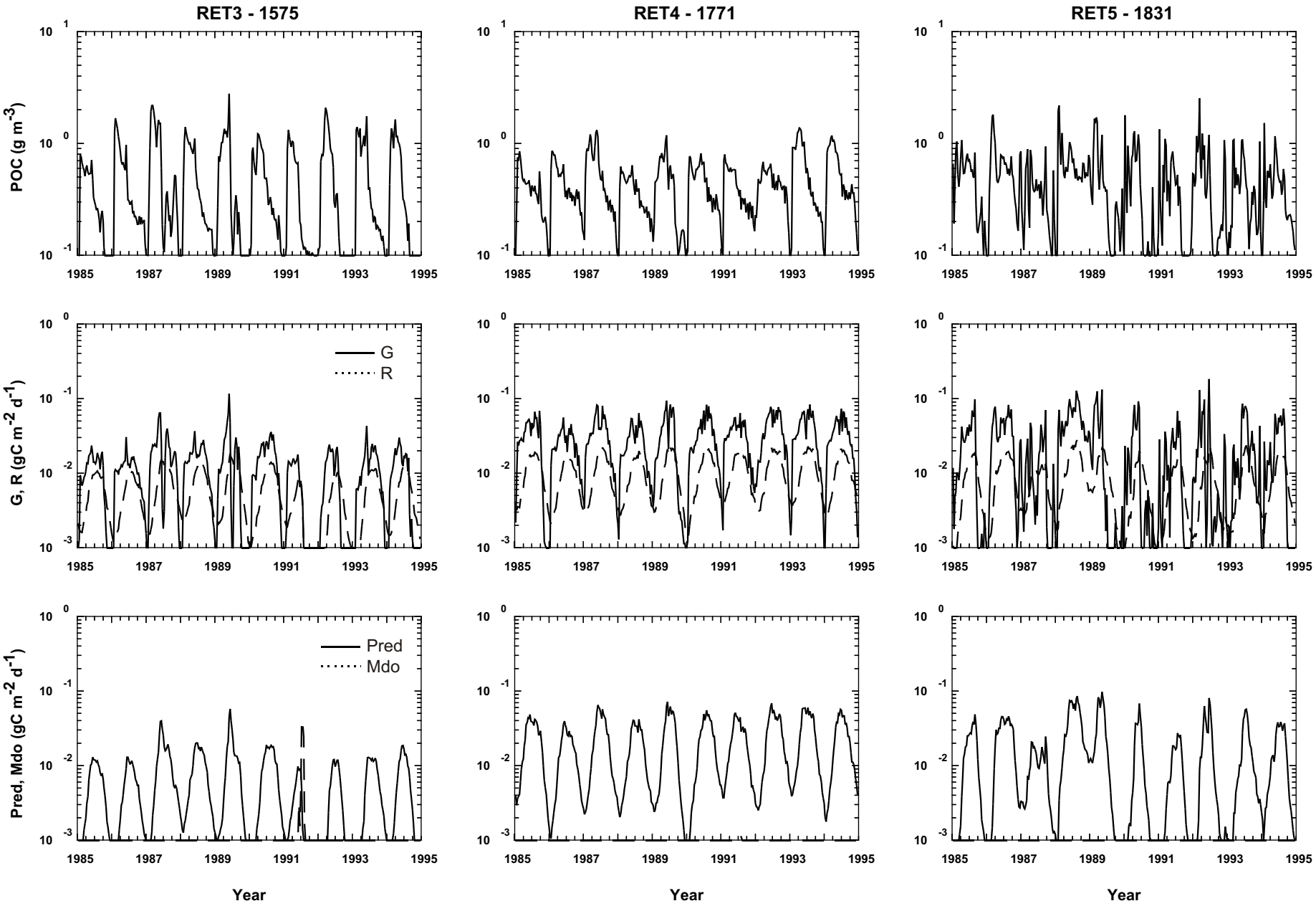

Figure 5-9. Modeled bottom water particulate organic carbon concentration (POC), and suspension feeder sources and sinks (G-growth, R-respiration, Pred-predation, Mdo-hypoxic mortality) in the middle reaches of the Rappahannock (RET3), York (RET4) and James (RET5) Rivers.

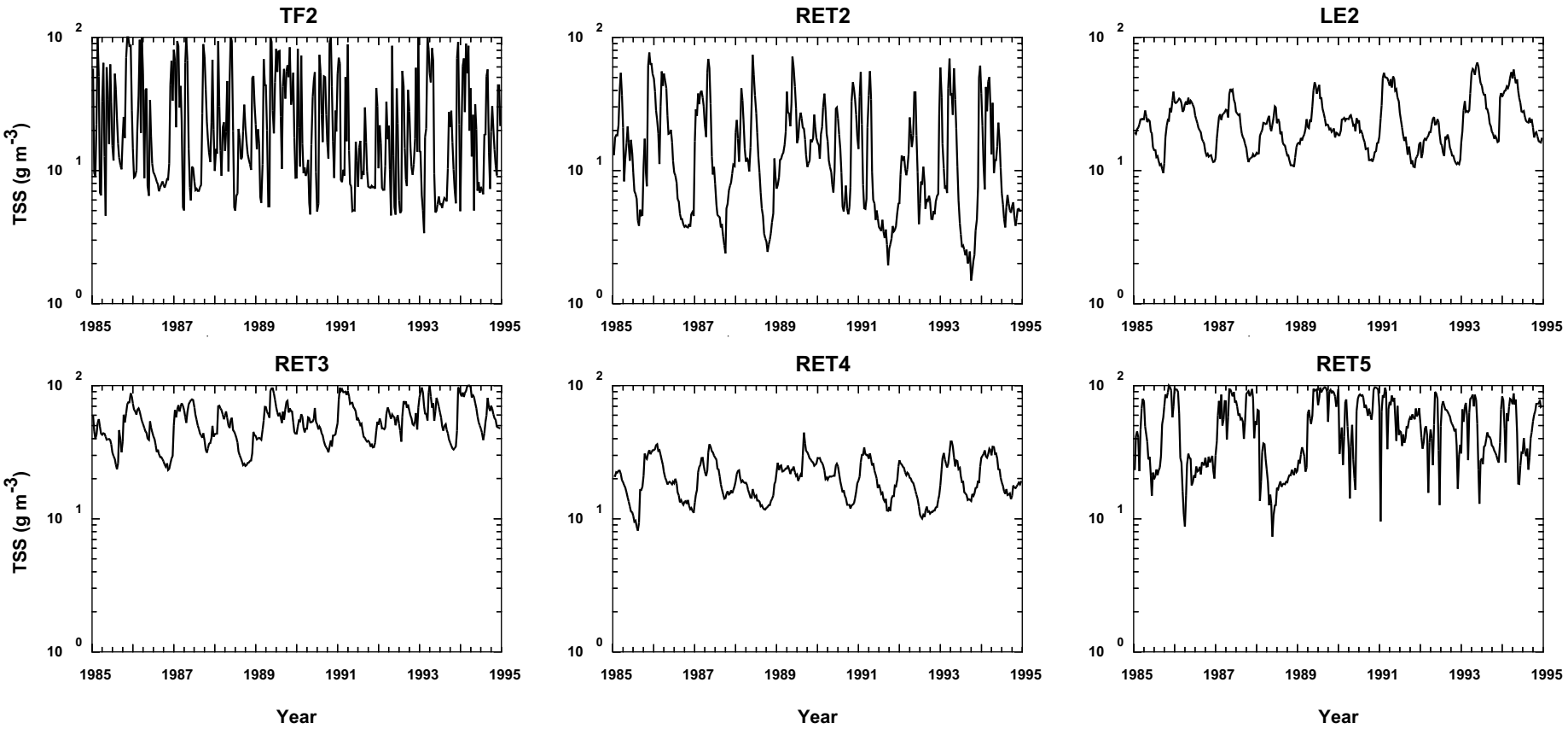

Figure 5-10. Total suspended solids in the Potomac (TF2, RET2, LE2), Rappahannock (RET3), York (RET4) and James (RET5) Rivers.

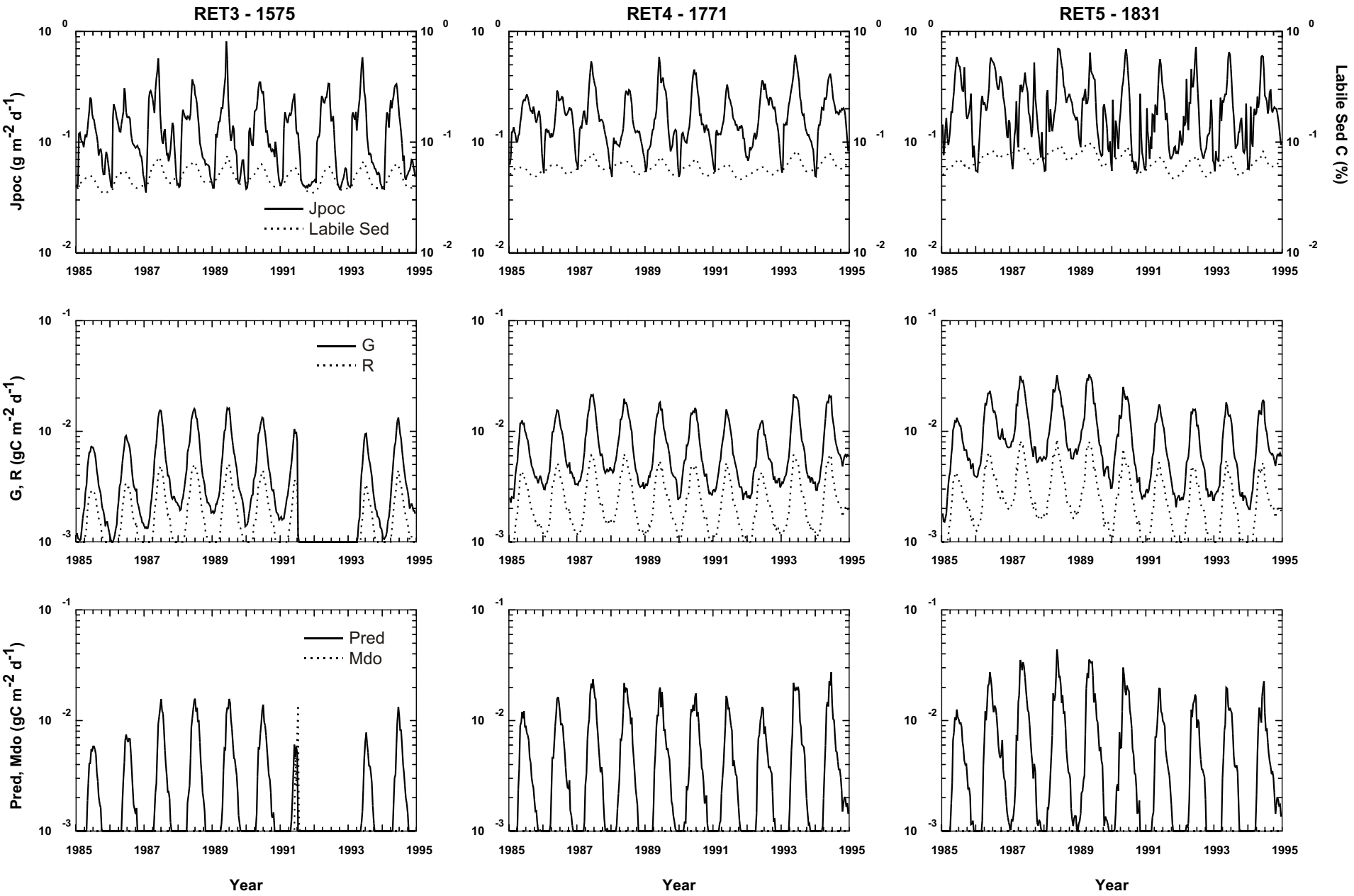

Figure 5-11. Modeled particulate organic carbon flux (Jpoc), labile sediment organic content, and deposit feeder sources and sinks (G-growth, R-respiration, Pred-predation, Mdo-hypoxic mortality) in the middle reaches of the Rappahannock (RET3), York (RET4) and James (RET5) Rivers.

shown here), mass mortality leading to significant loss of biomass is evident in these probability plots as sharp breaks in the lower portion of the modeled distributions (see summer distributions for deposit and suspension feeders in Figures 5-12 through 5-14).

Recalling from above, three different regimes are depicted along the Potomac River. The tidal freshwater zone (TF2) has high food (high algal biomass), but no seasonal hypoxia. The middle Potomac River (RET2) is deeper, wider, has low, but still abundant algal biomass, and limited areas of hypoxia (but not in the cell depicted here). The lower Potomac River (LE2) is highly influenced by the mainstem bay, is much deeper, and bottom waters exhibit seasonal hypoxia. In TF2, deposit and suspension feeding biomass is consistently high for both model results and data (Figures 5-12, 5-13). As noted previously, the suspension feeder model was unable to capture the highest biomass recorded in the data set. In RET2, the model predicted much higher biomass for deposit feeders but somewhat lower suspension feeder biomass than was observed. In the lower Potomac (LE2), deposit feeder biomass was much lower than observed. Despite the reported sensitivity of polychaetes to severe hypoxia, significant polychaete biomass was observed at this site with bottom water dissolved oxygen concentrations of less than 1 mg L^{-1} (Figure 2-7). It is possible that this is a matter of differences in the timing and duration of hypoxia in the lower Potomac between the model and the data. Predicted suspension feeder biomass in the lower Potomac was more similar to observed values, though observed peak spring biomass could not be matched. Both reflect summertime hypoxia (see Figures 2-7, 5-5) impacting the benthos, though the data were more variable.

The benthos in the transitional zones of the Virginia tributaries are not subjected to hypoxic stresses. Periodic hypoxia does occur in the lower Rappahannock and York Rivers. One hypoxic event was simulated in the Rappahannock River during summer 1991 (Figure 5-6) which was not observed in the benthic monitoring program. Suspension feeder biomass in these middle Rappahannock and York River sites (RET3, RET4) was again undersimulated, by about ten-fold (Figure 5-14). In the James River (RET5), springtime suspension feeder biomass values were

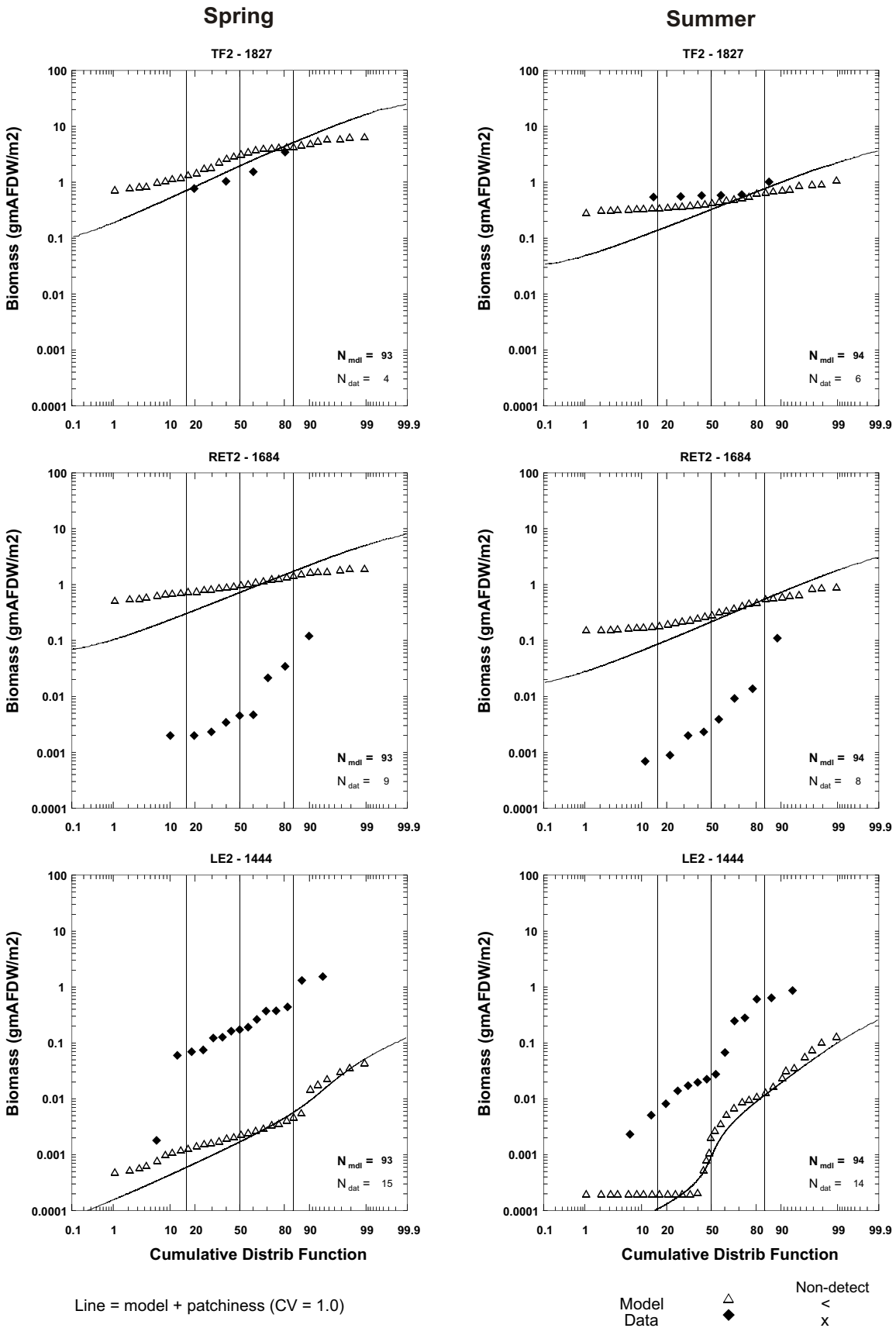

Figure 5-12. Seasonally aggregated deposit feeder biomass probability distributions from the Benthic Monitoring Program and the benthos model in the Potomac River. Spring: Mar, Apr, May; Summer: Jun, Jul, Aug. Data are all observations (1984-1996) within seasons; model are all ten-day averaged results within seasons.

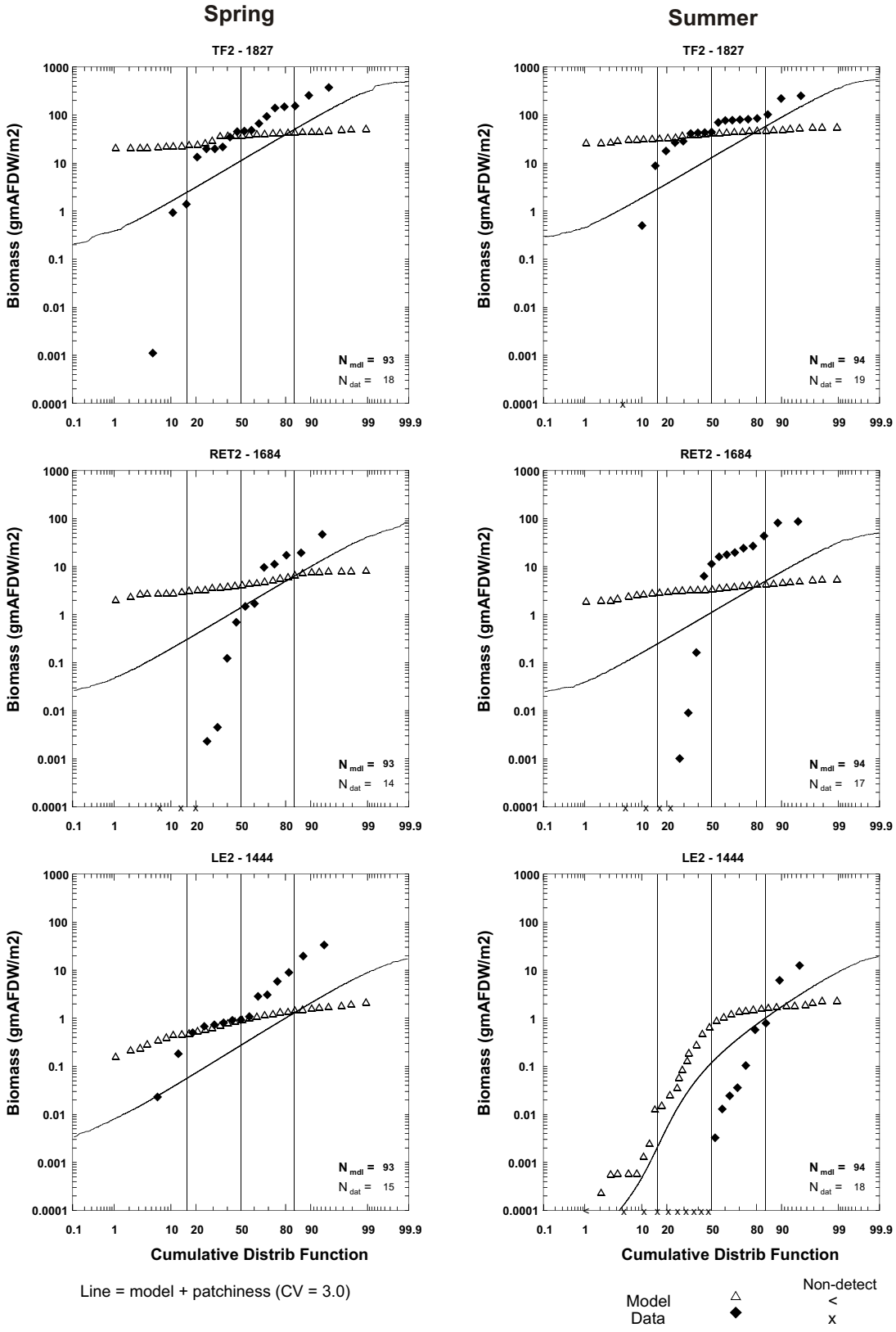

Figure 5-13. Seasonally aggregated suspension feeder biomass probability distributions from the Benthic Monitoring Program and the benthos model in the Potomac River. Spring: Mar, Apr, May; Summer: Jun, Jul, Aug. Data are all observations (1984-1996) within seasons; model are all ten-day averaged results within seasons.

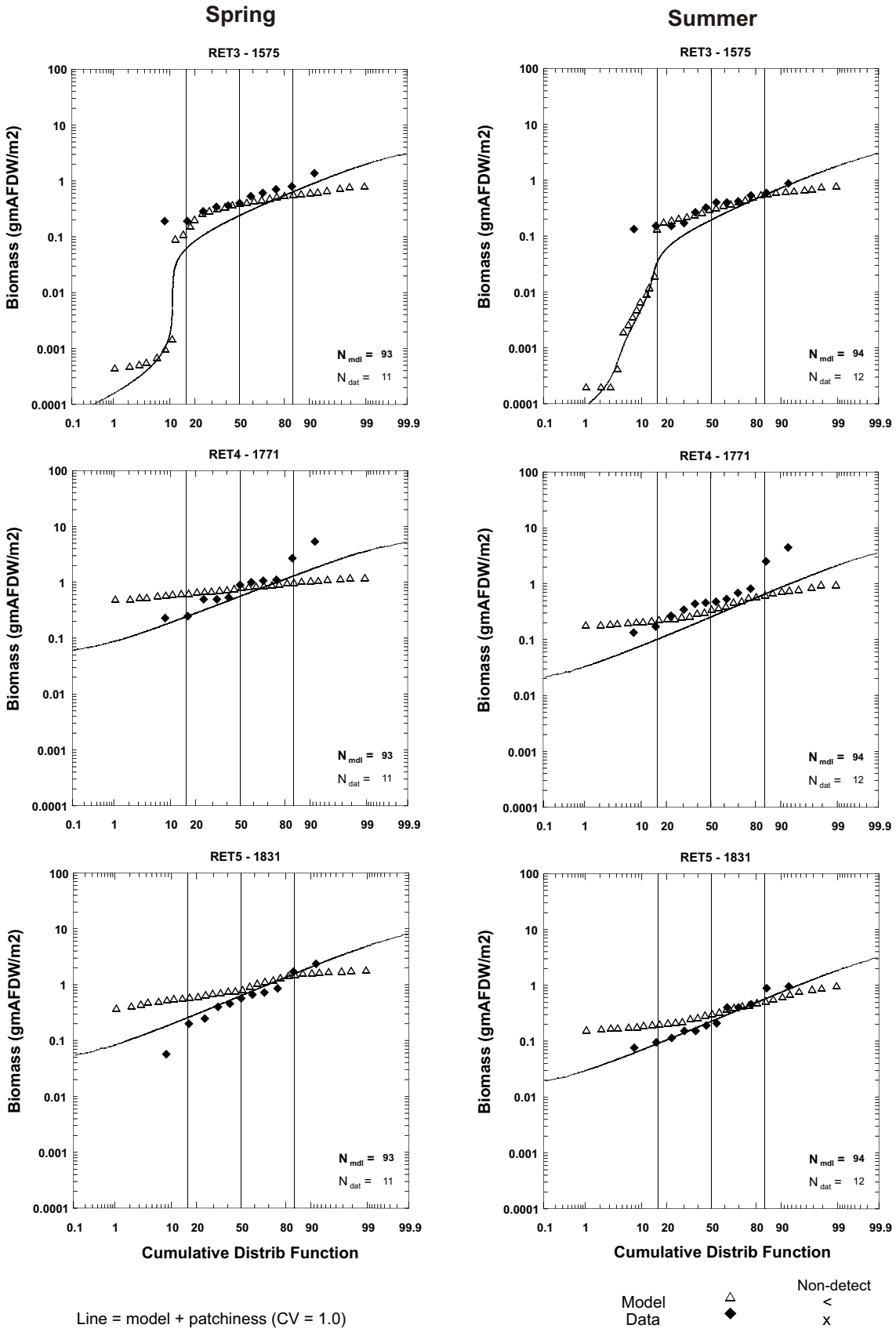

Figure 5-14. Seasonally aggregated deposit feeder biomass probability distributions from the Benthic Monitoring Program and the benthos model in the Rappahannock (RET3), York (RET4) And James (RET5) Rivers. Spring: Mar, Apr, May; Summer: Jun, Jul, Aug. Data are all Observations (1984-1996) within seasons; model are all ten-day averaged results within seasons.

similar to the observations, particularly if patchiness is taken into account. During summer, however, at this site, observed peak biomass was lower by about five-fold. While the model predicted reduced summer biomass, values were consistently higher than observed.

Modeled deposit feeder biomass in these regions was similar to observed values during both spring and summer (Figure 5-15). Impact of the simulated 1991 hypoxic event in the Rappahannock (RET3) can be seen in the lower tail of the model distribution, but since this was an isolated event, it had minimal impact on the overall distribution of summertime deposit feeder biomass.

5.5 BENTHIC BIOMASS VARIABILITY AND SPATIAL PATCHINESS

In additional to hypoxia, however, observed benthos is subjected to processes (recruitment, predation) and features (bathymetry, sediment quality) that either are not incorporated in the model framework or act on scales below which the model can resolve. These environmental factors may create a benthic infauna that is patchy in space on scales of tens to hundreds of square meters. The model, however, computes benthic biomass over a spatial scale of square kilometers. In an attempt to quantify the impact of unresolved sources of variability, statistical "noise" was added to modeled benthic biomass as a post-processing evaluation of patchiness, in a manner that will now be described.

The benthic biomass data within a model segment can be represented as $M_{obs}(x_i,t)$, where x_i is a location within a model segment i, and t is time. The model computes $M_{mdl}(i,t)$ for the segment i. As shown in the preceding sections, modeled biomass is a function of simulated factors (temperature, food, and dissolved oxygen) which are well-resolved on the spatial scale of the model (kilometers-squared). Because in a finite difference model, the mass, M is considered to be well-mixed within a segment on the order 1-10 km^2, the relationship between some observed value and a predicted value $M_{mdl}(i,t)$ at a given time t and model segment i may differ as a function of sub-grid-

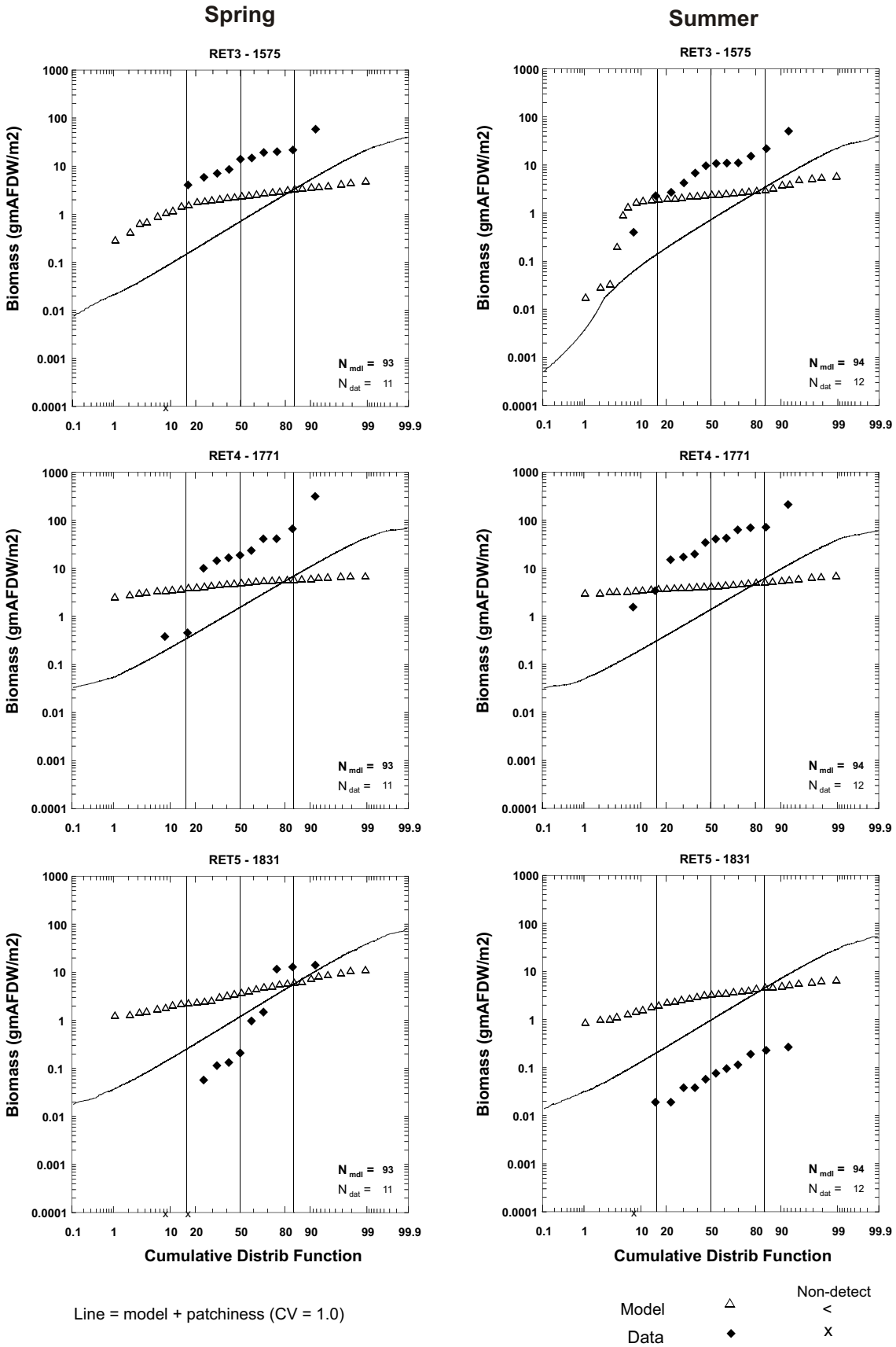

Figure 5-15. Seasonally aggregated suspension feeder biomass probability distributions from the Benthic Monitoring Program and the benthos model in the Rappahannock (RET3), York (RET4) And James (RET5) Rivers. Spring: Mar, Apr, May; Summer: Jun, Jul, Aug. Data are all Observations (1984-1996) within seasons; model are all ten-day averaged results within seasons.

scale, unresolved biological and sampling phenomena. It is assumed that this relationship takes the form

$$M_{obs}(i,t) = M_{mdl}(i,t) \cdot M'(i,t) \quad \textbf{(5-1)}$$

where M′(i,t) is the unresolved spatially and temporally varying component of benthic biomass. The above multiplicative form was chosen because benthic organisms are often lognomally distributed in space (Elliot, 1977). Taking the logarithm of Equation 5-1 yields

$$\log M_{obs} = \log M_{mdl} + \log M' \quad \textbf{(5-2)}$$

In a relatively homogeneous environment on the scale of the model, and in the absence of those ecological forces which the model cannot resolve, a spatial-temporal average (mean) of M_{mdl} should be equal to the average observed biomass:

$$\overline{M_{obs}(x_i,t)} = \overline{M_{mdl}(i,t)} \cdot \overline{M'(x_i,t)} \quad \textbf{(5-3)}$$

Since the model mean should equal the observed mean, the mean of M′ must equal 1. Thus, the properties of M′ are that it is lognormally distributed, with a mean of one (the log of which equals zero) and coefficient of variation, ν_β, to be defined from the data set. Thus, the patchiness variability M′ will not change the mean value of the model result. Rather, the addition of variability to the model results will steepen the slope of the model's probability distribution, simulating sampling from a variable environment.

Based on the above theory, patchiness was included in the model results as follows. The overall observed coefficient of variation (as a metric of patchiness) was used to generate 100 new results from each model result (a ten-day averaged biomass) in the following manner. A set of 100 lognormal deviates with a mean of 1 and a coefficient of variation of $\nu_\beta = 1$ for deposit feeders or ν_β

= 3 for suspension feeders, matching their observed baywide coefficients of variation, was defined. A synthesized data set was then produced by taking the product of each model result and the vector of 100 lognormal deviates (Equation 5-1). This new data set contained the same mean value as the model result, but with the variability characteristics of the (baywide) observed data. That is, the model results were post-processed to include a measure of the observed subgrid variability. The resulting cumulative density function for the post-processed model results with patchiness is shown as a solid line in probability plots (Figures 5-12 through 5-15). The question, then, is, "do the modeled biomass distributions behave similarly to observations when unresolved sources of variability are added?"

The addition of variability to the modeled results in the Potomac River does suggest that when the model correctly simulates the average biomass, differences between model and data may merely reflect spatial patchiness on spatial scales below that of the model (notably, TF2 in Figures 5-12 and 5-13 and for the deposit feeders in the Virginia tributaries, Figure 5-14). Even when the mean biomass is poorly simulated, similar slopes in the distribution of the data and of the patchiness-enhanced model results (e.g., Figure 5-15) suggest that variability in the sparse data record makes traditional ways of comparing eutrophication model results versus data, for example, by examination of time series, difficult to interpret.

5.6 SUMMARY OF THE BENTHIC BIOMASS MODEL AND NEXT STEPS

It is possible for both benthic groups that the lack of a recruitment pulse (typically occurring in late spring) may be responsible for the undersimulation of springtime suspension feeder biomass and the lack of a sufficient seasonal recovery of deposit feeder biomass in regions of seasonal hypoxia. The benthic model is sensitive to the water quality model's simulation of bottom water oxygen concentration as well as the delivery of labile organic carbon (food). The observations, even from fixed location stations, reflect significant spatial variability within the benthic habitats on scales too small to resolve in a eutrophication model. Thus, while the model was able to capture a broad

range of spatial and temporal responses in benthic biomass in response to predicted water quality conditions, additional effort is needed in several areas.

First, additional effort is needed in order to properly define and aggregate the benthos. Given both the observed spatial variability of the benthos and the coarse resolution of the model relative to these scales, it is likely that single station-grid cell comparisons are too severe a test of the model. Such analyses are useful because they show the range of responses of simulated benthic biomass to water quality predictions, but aggregating model results and data over broader spatial scales would mitigate unresolved differences in the environmental heterogeneity of the model and the real estuary. Also, with regard to the deposit feeding polychaetes, species compositional differences in the fauna between disturbed and undisturbed habitats are a significant component in detecting alterations due to eutrophication (Weisberg et al., 1997). Dividing the simulated benthic deposit feeders into pollution-tolerant versus pollution-sensitive species components may provide more insight into the simulation's benthic response to eutrophication and its mitigation.

The inability of the model to simulate the observed peaks in suspension feeding bivalve biomass may suggest that bivalve production is limited by ingestion rate or food supply. Increasing filtration rates resulted in overall lower water column primary production, however, because of reduced algal biomass. Furthermore, the undersimulation of total suspended solids versus observations at higher filtration rates suggested that such rates were not applicable under the observed conditions. It is possible that either the water quality model underestimates primary production or that there are significant additional sources of food that are not included in the model. Presently, it is unlikely that primary productivity is grossly underestimated, given the state of calibration of algal biomass, the various phosphorus and nitrogen pools, and of dissolved oxygen, though this is being investigated. While fall-line inputs of organic matter are well-modeled, below-fall-line inputs such as organic matter from estuarine wetlands are not simulated. Wetlands carbon, however, is not a significant component of bivalve nutrition (Langdon and Newell, 1990; Crosby et al., 1989). It is possible that resuspended labile organic matter, including benthic algae, can be an important component in bivalve diets. Presently, the suspension feeder model does not use benthic

organic matter as a food source. Presumably, this would have a strong spatial signal. In shallow areas, where sufficient light reaches the bottom, modeled benthic algal production could be used to augment water column organic matter as food for suspension feeders.

Lastly, improvements in the model would likely accrue from inclusion of spatial and temporal signals of the source and sink of benthos: recruitment and predation, respectively. Presently, recruitment is not modeled, severely limiting the modeled benthos from recovering from hypoxic events. Recruitment by the dominant benthos of a given region within the bay would have a strong spatial and seasonal signals. Similarly, predation, now distributed evenly around the bay and based solely on temperature, also has strong spatial and seasonal patterns. Now that the basic framework of the benthos model is in place, better resolution of these processes should result in a significant improvement in the coupling of water quality and living resource modeling.

SECTION 6

LITERATURE CITED

Banse, K (1979): On Weight Dependence of Net Growth Efficiency and Specific Respiration Rates Among Field Populations of Invertebrates. Oecologia (Berlin) 38: 111-126.

Banse, K., Mosher, S. (1980): Adult Body Mass and Annual Production/Biomass Relationships of Field Populations. Ecological Monographs 50: 355-379.

Cerco, C.F.; Cole,T.M. (1994): Three-Dimensional Eutrophication Model of Chesapeake Bay. Vol. 1. Main Report (EL-94-4 V. 1). U.S. Army Engineer Waterways Experiment Station, Vicksburg, MS. 658 pages.

Cerco, C.F.; Cole,T.M. (1993): Three-dimensional eutrophication model of Chesapeake Bay. J. Envir. Engrg., ASCE 119, 1006-1025.

Cloern, J.E. (1982): Does the benthos control phytoplankton biomass in South San Francisco Bay? Mar. Ecol.-Prog. Ser. 9, 191-202.

Cohen, R.R.H.; Dresler,P.V.; Phillips,E.J.P.; Cory,R.L. (1984): The effect of the Asiatic clam, *Corbicula fluminea*, on phytoplankton of the Potomac River, Maryland. Limnol. Oceanogr. 29, 170-180.

Coughlan, J. (1969): The estimation of filtering rate from the clearance of suspensions. Marine Biology 2, 356-358.

Crosby, M.P.; Langdon, C.J.; Newell, R.I.E. (1989): Importance of refractory plant material to the carbon budget of the oyster *Crassostrea virginica*. Marine Biology 100, 343-352.

Dame, R.F. (1996): Ecology of Marine Bivalves: An Ecosystem Approach. CRC Press, Boca Raton. 254 pages.

Dauer, D.M.; Alden, R.W., III (1995): Long-term trends in the macrobenthos and water quality of the lower Chesapeake Bay (1985-1991). Mar. Poll. Bull. 30, 840-850.

Dauer, D.M.; Rodi, A.J., Jr; Ranasinghe, J.A. (1992): Effects of low dissolved oxygen events on the macrobenthos of the lower Chesapeake Bay. Estuaries 15, 384-391.

Diaz, R.J.; Rosenberg, R. (1995): Marine benthic hypoxia: a review of its ecological effects and the behavioural responses of benthic macrofauna. Oceanogr. Mar. Biol. Ann. Rev. 33, 245-303.

Diaz, R.J.; Schaffner, L.C. (1990): The functional role of estuarine benthos. In: Perspectives on the Chesapeake Bay, 1990 (CBP/TRS41/90). (Eds: Haire,M; Krome,EC) Chesapeake Research Consortium, Gloucester Point, VA, 25-56.

Di Toro, Dominic M. (2000): Sediment Flux Modeling. John Wiley & Sons, NY. 603 pages.

Di Toro, Dominic M.; Fitzpatrick, James J. (1993): Chesapeake Bay Sediment Flux Model. For U.S. Army Corps of Engineers, Waterways Experiment Station. 201 pages.

Doering, P.H.; Oviatt, C.A. (1986): Application of filtration rate models to field populations of bivalves: an assessment using experimental mesocosms. Mar. Ecol.-Prog. Ser. 31, 265-275.

Elliott, J. M. (1977): Some methods for the statistical analysis of samples of benthic invertebrates. Scientific publication No. 25. Freshwater Biological Association Ambleside, U.K. 160 pages.

Gerritsen, J.; Holland, A.F.; Irvine, D.E. (1994): Suspension-feeding bivalves and the fate of primary production: an estuarine model applied to Chesapeake Bay. Estuaries 17, 403-416.

Griffiths, C.L.; Griffiths, R.J. (1987): Bivalvia. In: Animal Energetics. Vol. 2. (Eds: Pandian,TJ; Vernberg,FJ) Academic Press, San Diego, 1-88.

Hibbert, C.J. (1976): Biomass and production of a bivalve community on an intertidal mud-flat. J. Exp. Mar. Biol. Ecol. 25, 249-261.

Hummel, H. (1985): Food Intake of Macoma Balthica (Mollusca) In Relation to Seasonal Changes In Its Potential Food on a Tidal Flat In the Dutch Wadden Sea. Neatherlands Journal of Sea Research. 19 (1): 52-76.

HydroQual, Inc. (1993): Summary Report Workshops 1-3, Model Interfacing Living Resource and Ecosystem Process Modeling and Suspended Sediments/Light Attenuation Modeling. For U.S. Army Corps of Engineers, Waterways Experiment Station, Vicksburg, Mississippi.

Kemp, Michael W., Bartleson, Richard D. (1991): Preliminary Ecosystem Simulations of Estuarine Planktonic-Benthic Interactions: The Benthic Submodel. New Perspectives in Chesapeake System: A Research and Management Partnership. Proceedings of a Conference. 4-6 December 1990. Baltimore, MD. Chesapeake Research Consortium Publication No. 137.

Kemp, Michael W., Bartleson, Richard D. (1994): Chesapeake Bay Plankton-Benthos Ecosystem Process Model: Feedback Effects On Nutrient-Oxygen Relations. Towards a Sustainable

Coastal Watershed: The Chesapeake Experiment. Proceedings of a Conference. 1-3 June 1994. Norfolk, VA. Chesapeake Research Consortium Publication No. 149.

Kemp, W.M.; Boynton, W.R. (1992): Benthic-pelagic interactions: nutrient and oxygen dynamics. In: Oxygen dynamics in Chesapeake Bay. (Eds: Smith,DE; Leffler,M; Mackiernan,G) Maryland Sea Grant College, College Park, MD, 149-221.

Langdon, C.J.; Newell, R.I.E. (1990): Utilization of detritus and bacteria as food sources by two bivalve suspension-feeders, the oyster *Crassostrea virginica* and the mussel *Geukensia demissa*. Mar. Ecol.-Prog. Ser. 58, 299-310.

McCall, L., Tevesz, J.S. (1982): Animal-Sediment Relations, The Biogenic Alteration of Sediments. Plenum Press, New York, NY. 336 pages.

Nestlerode, J.A.; Diaz, R.J. (1997): Effects of periodic environmental hypoxia on predator utilization of macrobenthic infauna. Mar. Ecol.-Prog. Ser., .

Officer, C.B.; Smayda, T.J.; Mann, R. (1982): Benthic filter feeding: a natural eutrophication control. Mar. Ecol.-Prog. Ser. 9, 203-210.

Ólafsson, E.B. (1986): Density Dependence In Suspension-Feeding and Deposit-Feeding Populations of the Bivalve Macoma Balthica: A Field Experiment. Journal of Animal Ecology. 55: 517-576.

Pearson, T.; Rosenberg, R. (1978): Macrobenthic succession in relation to organic enrichment and pollution of the marine environment. Oceanogr. Mar. Biol. Ann. Rev. 16, 229-311.

Peters, R.H. (1983): The Ecological Implications of Body Size. Cambridge University Press, New York, NY. 329 pages.

Phelps, H.L. (1994): The asiatic clam (*Corbicula fluminea*) invasion and system-level ecological change in the Potomac River estuary near Washington, D.C. Estuaries 17, 614-621.

Powell, E.N.; Hofmann, E.E.; Klink, J.M.; Ray, S.M. (1992): Modeling oyster populations. I. A commentary on filtration rate. Is faster always better? J. Shell. Res. 11, 387-398.

Ranasinghe, J.A., Scott, L.C., and Weisberg, S.B. (1996): Chesapeake Bay Water Quality Monitoring Program Long-Term Benthic Monitoring and Assessment Component - Level 1 Comprehensive Report, Vol. 1. Versar, Inc., Columbus, MD.

Robbins, J.A., Keilty, T.J. et. al. (1989): Relationships Between Tubificid Abundances, Sediment Composition, and Accumulation Rates in Lake Erie. Canadian Journal of Fisheries and Aquatic Sciences. 46: 223-231.

Thomann, R. V. (1994): A Generic Steady State Model of Macrobenthos-Mixing Depth Relationship to Net Carbon Flux to Sediment. Tributary/Ecosystem Modeling Workshop, St. Michael's, MD. July 12 - 13.

Thomann, R.V.; Collier, J.R.; Butt, A.; Casman, E.; Linker, L.C. (1994): Technical analysis of response of Chesapeake Bay Water Quality Model to Loading Scenarios. CBP/TRS 101/94, U.S. EPA Chesapeake Bay Program Office, Annapolis, MD.

Virnstein, R.W. (1977): The Importance of Predation by Crabs and Fishes on Benthic Infauna in Chesapeake Bay. Ecology 58, 1199-1217.

Weisberg, Stephen B.; Ranasinghe, J.A.; Dauer, D.M.; Schaffner, L.C.; Diaz, R.J.; Frithsen, J.B. (1997): An estuarine benthic index of biotic integrity (B-IBI) for Chesapeake Bay. Estuaries 20, 149-158.

APPENDIX A

MODEL COMPUTATIONAL PROCEDURES FOR SUSPENSION FEEDER PROCESSES

CALCULATION PROCEDURE

The model can be run repeatedly for different species types, as different species will have different constants. For a given species the following calculation procedure is followed:

1. Calculate respiration and filtration rates based on existing biomass.

$$f = f_{20} \; M^{-b_f} \bullet \theta_f^{T-20} \bullet Z \bullet [1 - 0.01 \, (a_{TSS} + b_{TSS} \log_{10} TSS)]$$

$$r = r_{20} \; M^{-b_r} \bullet \theta_r^{T-20} \bullet Z$$

$$Z = \left[1 + \exp\left(1.1 \frac{DO_{hx} - DO}{DO_{hx} - DO_{qx}} \right) \right]^{-1}$$

2. Calculate hypoxia mortality term.

$$m = \frac{\mathrm{Log}_e (1/100)}{T_d} \bullet (1 - Z)$$

3. Calculate the carbon ingestion rate, Ic

$$\mathbf{Ic = f \bullet (PC_1 + PC_2 + PC_3 + LPOC + RPOC)}$$

units: $(L \, d^{-1} \, mg \, C^{-1}) \bullet (mg \, C \, L^{-1}) = d^{-1}$

where: PC_1...RPOC are mg C L^{-1} in the water column

4. Calculate maximum carbon growth rate, GCmax.

$$\mathbf{GCmax = S \bullet f \bullet (\alpha_1 \bullet PC_1 + \alpha_2 \bullet PC_2 + \alpha_3 \bullet PC_3 + \alpha_4 \bullet LPOC + \alpha_5 \bullet RPOC)}$$

units: $(mg \, C \, m^{-2}) \bullet (L \, d^{-1} \, mg \, C^{-1}) \bullet mg \, C \, L^{-1}) = mg \, C \, m^{-2} \, d^{-1}$

where: α_1..α_5 are the assimilation efficiencies for the various carbon components.

5. Compare Ic to maximum ingestion rate, a constant, Imax. If Ic < Imax then the rest of the calculation is unaffected. If Ic > Imax then reduce growth rate by Imax/Ic:

$$\mathbf{GC = (Imax\ Ic^{-1})\ \bullet\ GCmax}$$

6. Compute nitrogen and phosphorus growth rates:

$$\mathbf{GN = S\ \bullet f\ \bullet (\alpha_1 \bullet PC_1\ \bullet N{:}C_1 + \alpha_2 \bullet PC_2\ \bullet N{:}C_2 + \alpha_3 \bullet PC_3\ \bullet N{:}C_3 + \alpha_4 \bullet LPON + \alpha_5 \bullet RPON)}$$

$$\mathbf{GP = S\ \bullet f\ \bullet (\alpha_1 \bullet PC_1\ \bullet P{:}C_1 + \alpha_2 \bullet PC_2 \bullet P{:}C_2 + \alpha_3 \bullet PC_3 \bullet P{:}C_3 + \alpha_4 \bullet LPOP + \alpha_5 \bullet RPOP)}$$

units: $mg\ C\ m^{-2}\ \bullet (L\ d^{-1}\ mg\ C^{-1})\ \bullet (mg\ C\ L^{-1})\ \bullet mg\ N\ mg\ C^{-1}) = mg\ N\ m^{-2}\ d^{-1}$

where:

PC_i, $N{:}C_i$, and $P{:}C_i$ are algal carbon, and algal nitrogen to carbon and phosphorus to carbon ratios for each of the algal groups (i = 1, 2, 3).

7. Convert N and P growth rates to carbon equivalents in order to compare:

$$\mathbf{GN = GN\ \bullet SFCN}$$

units: $(mg\ N\ m^{-2}\ d^{-1})\ \bullet (mg\ C\ mg\ N^{-1}) = mg\ C\ m^{-2}\ d^{-1}$

$$\mathbf{GP = GP\ \bullet SFCP}$$

units: $(mg\ P\ m^{-2}\ d^{-1})\ \bullet (mg\ C\ mg\ P^{-1}) = mg\ C\ m^{-2}\ d^{-1}$

where: SFCN is the suspension feeder C:N ratio
SFCP is the suspension feeder C:P ratio

8. Find minimum of nutrient growth rates:
Gmin = min (GN, GP)

9. If Gmin > GC then assimilation rates are unchanged and there is no nutritional limitation.

If Gmin < GC there is a nutritional limitation and the assimilation rates must be scaled so that the organism will only take up nutrients to match its stoichiometry:

If Gmin < GC
$\alpha_i = \alpha_i \bullet$ **Gmin/GC**
$\alpha_{i,N} = \alpha_i \bullet$ **Gmin/GN**
$\alpha_{i,P} = \alpha_i \bullet$ **Gmin/GP**
where i = 1. . .5 for the five organic matter pools (3 algal groups and labile and refractory particulate organic detritus).

10. With the assimilation rates computed, the amount of feces can be calculated:

$$\mathbf{Cfeces = S \bullet f \bullet ((1-\alpha_1) \bullet PC_1 + (1-\alpha_2) \bullet PC_2 + (1-\alpha_3) \bullet LPOC)}$$
$$\mathbf{Nfeces = S \bullet f \bullet ((1-\alpha_{1,N}) \bullet PC_1 \bullet N{:}C_1 + (1-\alpha_{2,N}) \bullet PC_2 \bullet N{:}C_2 + (1-\alpha_{3,N}) \bullet PC_3 \bullet N{:}C_3 + (1-\alpha_{4,N}) \bullet LPON) + (1-\alpha_{5,N}) \bullet RPON)}$$
$$\mathbf{Pfeces = S \bullet f \bullet ((1-\alpha_{1,P}) \bullet PC_1 \bullet P{:}C_1 + (1-\alpha_{2,P}) \bullet PC_2 \bullet P{:}C_2 + (1-\alpha_{3,P}) \bullet PC_3 \bullet P{:}C_3 + (1-\alpha_{4,P}) \bullet LPOP) + (1-\alpha_{5,P}) \bullet RPOP)}$$

11. Assign feces and pseudofeces (filtered but not ingested particles formed when Ic exceeds Imax) to particulate fluxes to sediment. Note that filtered, non-food particles (e.g., inorganic solids) are treated like feces and have suspension-feeder induced fluxes to the sediments. Predation losses are also assumed to be labile particulate fluxes to provide closure for the mass balance of organic matter. Note here that any mortality loss associated with hypoxia is also added to fluxes to sediment. It was decided that closure of mass balance in this manner was more important than allowing the export out of the system of predation losses.

$$\mathbf{FLUX\_LPOC = Cfeces + \beta \bullet S^2 + m \bullet S}$$

note: β here is predation rate
units: m^2 mg C^{-1} d^{-1}

FLUX_LPON = Nfeces + β • S^2 • SFCN + m • S note: β here is predation rate
units: m^2 mg N^{-1} d^{-1}

FLUX_LPOP = Pfeces + β • S^2 • SFCP + m • S note: β here is predation rate
units: m^2 mg P^{-1} d^{-1}

FLUX_RPOC = S • f • RPOC units: (mg C m^2) • (L d^{-1} mg C^{-1}) • mg C L^{-1} = mg C m^{-2} d^{-1}

FLUX_RPON = S • f • RPON units: (mg C m^2) • (L d^{-1} mg C^{-1}) • mg C L^{-1} = mg C m^{-2} d^{-1}

FLUX_RPOP = S • f • RPOP units: (mg C m^2) • (L d^{-1} mg C^{-1}) • mg C L^{-1} = mg C m^{-2} d^{-1}

FLUX_UnSi = S • f • UnSi Unavailable silica

FLUX_Si = S • f • Si Available silica

FLUX_SS = S • f • SS Suspended solids

12. The water column derivatives have to be corrected for the loss due to suspension feeders. Note that total loss is the total amount filtered, as once it is filtered all of that amount is removed from the water column and routed either to the sediment or to the organism.

$$\frac{d(PC_1)}{dt} = \frac{d(PC_1)}{dt} - \frac{S \bullet f \bullet PC_1}{1000}$$

$$\frac{d(PC_2)}{dt} = \frac{d(PC_2)}{dt} - \frac{S \bullet f \bullet PC_2}{1000}$$

$$\frac{d(LPOC)}{dt} = \frac{d(LPOC)}{dt} - \frac{S \bullet f \bullet LPOC}{1000}$$

$$\frac{d(PC_3)}{dt} = \frac{d(PC_3)}{dt} - \frac{S \bullet f \bullet PC_3}{1000}$$

$$\frac{d(LPON)}{dt} = \frac{d(LPON)}{dt} - \frac{S \bullet f \bullet LPON}{1000}$$

$$\frac{d(LPOP)}{dt} = \frac{d(LPOP)}{dt} - \frac{S \bullet f \bullet LPOP}{1000}$$

$$\frac{d(RPOC)}{dt} = \frac{d(RPOC)}{dt} - \frac{S \bullet f \bullet RPOC}{1000}$$

$$\frac{d(RPON)}{dt} = \frac{d(RPON)}{dt} - \frac{S \bullet f \bullet RPON}{1000}$$

$$\frac{d(RPOP)}{dt} = \frac{d(RPOP)}{dt} - \frac{S \bullet f \bullet RPOP}{1000}$$

$$\frac{d(UnSi)}{dt} = \frac{d(UnSi)}{dt} - \frac{S \bullet f \bullet UnSi}{1000}$$

$$\frac{d(Si)}{dt} = \frac{d(Si)}{dt} - \frac{S \bullet f \bullet Si}{1000}$$

$$\frac{d(SS)}{dt} = \frac{d(SS)}{dt} - \frac{S \bullet f \bullet SS}{1000}$$

units: $(mg\ C\ m^{-2})\ \bullet\ (L\ d^{-1}\ mg\ C^{-1})\ \bullet\ (mg\ L^{-1})\ \bullet\ (1g\ 1000\ mg^{-1}) = g\ C\ d^{-1}$

13. Calculate respiration fluxes. These are ultimately added to fluxes computed in the sediment model.

Jnh4 = r S / SFCN

units: $d^{-1}\ \bullet\ mg\ C\ m^{-2}\ (mg\ C\ mg\ N^{-1})^{-1} = mg\ N\ m^{-2}\ d^{-1}$

Jpo4 = r S / SFCP

units: $d^{-1}\ \bullet\ mg\ C\ m^{-2}\ (mg\ C\ mg\ P^{-1})^{-1} = mg\ P\ m^{-2}\ d^{-1}$

SOD = r S • 2.67 / 1000.

units: $d^{-1} \bullet (mg\ C\ m^{-2}) \bullet (mg\ O_2\ mg\ C^{-1}) \bullet (1g\ 1000\ mg^{-1}) = g\ O_2\ d^{-1}$

14. Take integration step

$S = S + DT \bullet (GC - rS - \beta S^2 - mS)$